Microporous and Mesoporous Materials 332 (2022) 111703

Contents lists available at ScienceDirect

Microporous and Mesoporous Materials

journal homepage: www.elsevier.com/locate/micromeso

Composites of porous materials with ionic liquids: Synthesis, characterization, applications, and beyond

Ozce Durak [a,b], Muhammad Zeeshan [a,b,1], Nitasha Habib [a,b,1], Hasan Can Gulbalkan [a,1], Ala Abdulalem Abdo Moqbel Alsuhile [a,b,1], Hatice Pelin Caglayan [a,b,1], Samira F. Kurtoğlu-Öztulum [a,b,1], Yuxin Zhao [a,b,1], Zeynep Pinar Haslak [a,1], Alper Uzun [a,b,c,**], Seda Keskin [a,b,*]

[a] Department of Chemical and Biological Engineering, Koç University, Rumelifeneri Yolu, 34450, Sariyer, Istanbul, Turkey
[b] Koç University TÜPRAŞ Energy Center (KUTEM), Koç University, Rumelifeneri Yolu, 34450, Sariyer, Istanbul, Turkey
[c] Koç University Surface Science and Technology Center (KUYTAM), Koç University, Rumelifeneri Yolu, 34450, Sariyer, Istanbul, Turkey

ARTICLE INFO

Keywords:
Porous materials
Ionic liquid
Hybrid materials
Adsorption
Catalysis
Ionic conductivity

ABSTRACT

Modification of the physicochemical properties of porous materials by using ionic liquids (ILs) has been widely studied for various applications. The combined advantages of ILs and porous materials provide great potential in gas adsorption and separation, catalysis, liquid-phase adsorption and separation, and ionic conductivity owing to the superior performances of the hybrid composites. In this review, we aimed to provide a perspective on the evolution of IL/porous material composites as a research field by discussing several different types of porous materials, including metal organic frameworks (MOFs), covalent organic frameworks (COFs), zeolites, and carbonaceous-materials. The main challenges and opportunities in synthesis methods, characterization techniques, applications, and future opportunities of IL/porous materials are discussed in detail to create a road map for the area. Future advances of the field addressed in this review will provide in-depth insights into the design and development of these novel hybrid materials and their replacement with conventional materials.

1. Introduction

Post-synthesis modification of a porous material offers the opportunity to design a composite material with task-specific properties desirable for any targeted application. In this regard, hybrid composites that can be synthesized by combining two or more materials with different physicochemical properties provide various advantages. Such hybrid composites exhibit almost limitless possibilities for superior performance in any target application with enhanced structural characteristics that offer improved chemical and thermal properties and novel functionalities. Among different guest molecules, ionic liquids (ILs) provide a high degree of flexibility due to the availability of a theoretically unlimited number of cation-anion combinations, high thermal/chemical stabilities, and low vapor pressures. ILs are molten salts in the liquid phase at room temperature and are commonly used as solvents. Most of ILs have more environmentally-friendly production pathways compared to conventional solvents, and thus can be considered as alternative "green solvents" to the volatile organic compounds (VOCs) [1].

Over the last two decades, a myriad of porous materials has been utilized and modified with ILs for hybrid composite generation [2–8]. Among them, metal organic frameworks (MOFs), covalent organic frameworks (COFs), zeolites, and carbonaceous-materials have become the focus for engineering processes owing to their unique and versatile physicochemical properties, such as high surface area and porosity, structural tunability, and flexibility [9]. For these materials, ILs can be used as different types of modifying agents, such as a functional ligand for structural modifications or a solvent for the synthesis of a composite material. In addition, ILs are directly used to prepare membranes with IL/porous material composites and are introduced as a third component to improve the interface adhesion between polymer and inorganic fillers for the preparation of mixed matrix membranes (MMMs).

The fast-growing field of hybridization with ILs generated several different types of composite materials, such as IL/MOFs [2,5,10–13], IL/COFs [14,15], IL/zeolites [16,17], and IL/carbonaceous-materials

* Corresponding author. Department of Chemical and Biological Engineering, Koç University, Rumelifeneri Yolu, 34450, Sariyer, Istanbul, Turkey.
** Corresponding author. Department of Chemical and Biological Engineering, Koç University, Rumelifeneri Yolu, 34450, Sariyer, Istanbul, Turkey.
E-mail addresses: auzun@ku.edu.tr (A. Uzun), skeskin@ku.edu.tr (S. Keskin).
[1] Equal contribution.

https://doi.org/10.1016/j.micromeso.2022.111703
Received 27 September 2021; Received in revised form 10 January 2022; Accepted 12 January 2022
Available online 16 January 2022
1387-1811/© 2022 The Authors. Published by Elsevier Inc. This is an open access article under the CC BY-NC-ND license (http://creativecommons.org/licenses/by-nc-nd/4.0/).

[4,18,19], for potential applications in adsorption-based separation processes [5,10]. On the other hand, various types of membranes with IL/porous material composites, including supported IL membranes (SILMs) [20], IL polymer membranes (ILPMs) [21], IL/MOF mixed matrix membranes (IL/MOF MMMs) [22], and poly(ionic liquid) membranes (PILMs) [23,24] have shown promising improvements in gas separation applications as well [25]. These hybrid materials also provide cost-efficiency, superior performances, and new possibilities for other applications, such as catalysis [26,27], liquid-phase adsorption and separation [8,28], and ionic conductivity [29–31] as shown in Fig. 1.

The historical evolution of IL/porous material composites starting from the investigation of the first protic IL in 1914 is illustrated in Fig. 2. To the best of our knowledge, the field of IL/porous material composites started in 1997 with the IL-incorporated composite membranes to enhance the stability of membrane structure for ionic conductivity studies [32]. Then, in 2002, the solvothermal synthesis of a MOF was conducted by utilizing an IL as the solvent and structure-directing agent, which was eventually named as ionothermal synthesis [33,34]. Later in 2004 and 2010, IL usage was extended to other types of porous materials covering the synthesis of zeolites and functionalized graphene, respectively [35,36]. Thereafter, in 2008, an IL/carbonaceous-material composite was used for catalysis applications [26].

With increasing experimental research studies in the field, the need for more extensive screening methods has become a critical issue. Thus, computational screening methods were developed to screen thousands of different IL/porous material composites to address the future directions in experimental research [6,37]. In 2014, the first experimental study on IL-impregnated MOF composite was performed for the case of liquid-phase adsorptive desulfurization [38]. After that point, the scope of application for IL/porous material composites was extended to various fields from gas adsorption to catalysis with many types of IL/porous material composites [2,4,10,14,23]. There exists a large number of promising studies in the literature for each application field, and the scale of screening is enhanced to a level where the best-performing combinations of materials can be determined among more than thousands of candidates before experimental testing [8,13,39–41].

In this review, we aim to present a comprehensive overview of the recent advances in the synthesis methods, characterization techniques, and applications of IL/porous material composites covering state-of-the-art experimental and computational studies, mostly focusing on the last five years. Applications of IL/porous material composites, such as adsorption-based and membrane-based gas separation, adsorption-based liquid separation, catalysis, and ionic conductivity, are discussed by providing illustrative studies. We highlighted the role of high-throughput computational screening (HTCS) and density functional theory (DFT) calculations that are critical to identify the promising composites and quantify the interactions between ILs and porous materials. Current challenges and opportunities in various applications of IL/porous material composites, including the rational design of composites, stability of materials, elucidation of the structural factors that control various performance measures, applicability into real-life processes, cost, and combination of experiments with computational studies are highlighted to shed light on the prospective studies.

2. Preparation of IL-based hybrid materials

In-situ techniques, such as ionothermal synthesis, and post-synthesis modification techniques, such as capillary action, wet impregnation, ship-in-a-bottle, and grafting, are widely used to prepare new hybrid materials with the help of ILs. These techniques provide a wide range of possibilities for higher performance and create opportunities to tune the porous structure accordingly. In this review, IL/porous material composites, which emerged as a result of post-synthesis modification with IL, will be highlighted after a brief discussion on the *in-situ* synthesis of IL-based hybrid materials via ionothermal synthesis or different chemical procedures.

2.1. In-situ synthesis of IL-based hybrid materials

Hybrid materials can be defined as the mixture of two different constituents combined at a molecular- level. Throughout this section, solid porous materials with ILs as a constituent in their structure will be discussed as IL-based hybrid materials. During the *in-situ* synthesis of solid porous materials, ILs can be used as a multi-functional green solvent by acting as both solvent and structure-directing agents. This method, called ionothermal synthesis, directly parallels the well-known hydrothermal synthesis with the only difference being the usage of IL as the solvent [34]. Moreover, ionothermal synthesis eliminates the possibility of any competition between the ions of solvent and ions of structure-directing agent during the growth of the porous solid by using one species simultaneously for both purposes.

Several *in-situ* synthesis techniques have been reported in literature

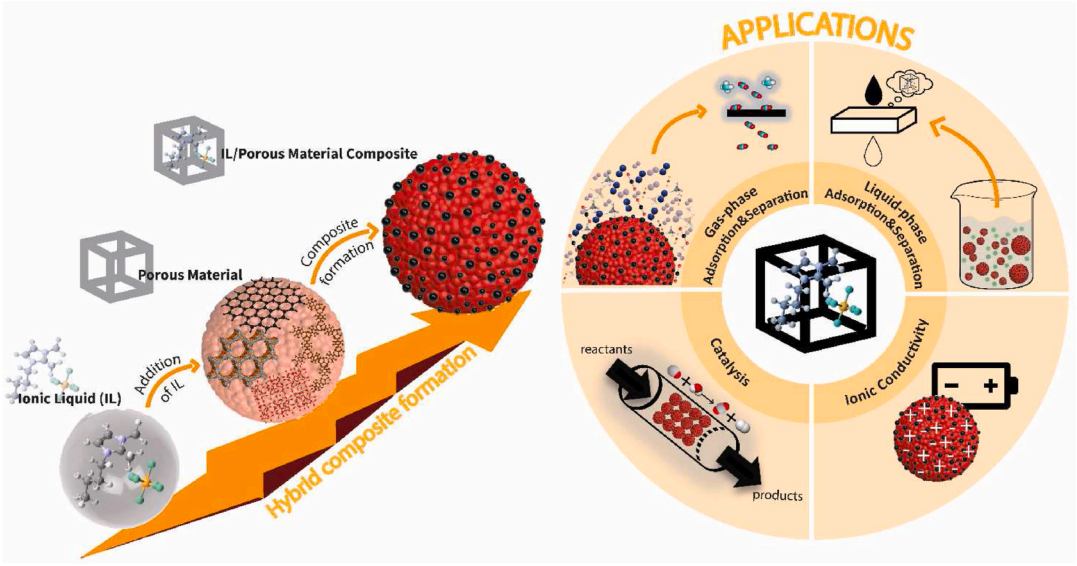


Fig. 1. Representative illustration for composite formation and the scope of application for IL/porous material composites.

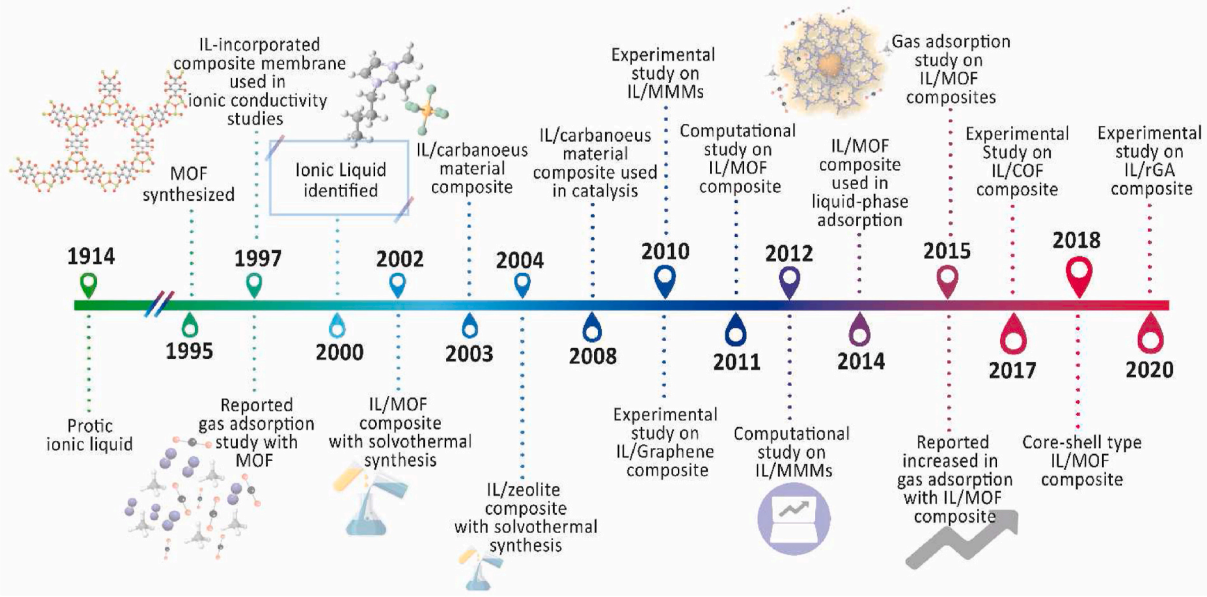


Fig. 2. The progress in the historical evolution of IL/porous material composites.

with ionothermal synthesis to obtain different porous materials, starting from zeolite analogues [36], zeolites [42], MOFs [33], COFs [43], and carbonaceous-materials [44]. Detailed review articles are also available on ionothermal synthesis of organic/inorganic porous materials [42,45,46]. However, there are certain limitations for this method in terms of matching IL and desired final porous material structure. The similarity between the common organic templates of zeolites and the cation part of IL significantly benefits the synthesis of zeolite-like structures. However, there is also an anion part present in the structure of IL and it should be carefully selected according to the desired final structure. Anion part of the IL plays an important role in controlling the chemical and electronic nature of the IL; therefore, it directly affects the synthesized porous solid during the synthesis [47]. Similarly, for IL/carbonaceous-material, the IL should have a high affinity towards carbonaceous-material to maintain the structural integrity, whereas, in the case of IL/MOF or IL/COF composites, organic linkers and metal salts should have sufficient solubility in ILs for *in-situ* synthesis. Moreover, for IL/MOF or IL/COF combinations, the organic linker's reactivity with the IL and the resulting charge neutrality of the surface can be listed as the other limitations. For instance, cation-templating and anion-templating synthesis routes of ionothermal synthesis result in charged structure where the size and the electronic structure of both constituents create an important impact on the final product. While the main goal of templating-based synthesis is to have a precise control over the final architecture, changing the size and electronic structure of the constituents does not produce very specific outcomes for precise structural architecture of the final porous material.

In the first attempt for ionothermal synthesis of the coordination polymer, [Cu(I)(bpp)][BF_4], [BMIM][BF_4] (*please see the abbreviations section*) was used as a solvent, and the IL-based hybrid material contained only the anion of the IL, whereas cations remained in the solution to maintain the surface neutrality [33,48]. Similarly, there are studies where the structure contains only the cationic part of the IL acting as a structure directing agent [42]; and the IL is multifunctionalized through various templating routes with both constituents [49]. Consequently, the resulting structure, in which only one component is present, cannot reproduce the desired properties of the IL in the composite, and the precise control over the architectural design of final porous material cannot be maintained due to the possible multifunctionality of ILs.

Besides ionothermal synthesis, ILs are also used in different reaction routes to synthesize the IL-based hybrid materials. In the synthesis of a graphene-like carbonaceous-material, IL/graphene layered films were synthesized in the presence of IL, which played a crucial role in controlling the spacing between graphene layers during the direct reduction of graphene oxide [35]. Resulting IL-based hybrid materials, generally called graphene IL layered films, contained IL molecules in-between graphene layers. Similarly, in another study, an IL was used as a stabilizing agent during the exfoliation of graphite to obtain IL/graphene hybrid material [50]. Surfactant-like property of ILs makes them suitable for usage as a stabilizing agent during exfoliation of graphite. Moreover, synthesis techniques, such as the sol-gel method, is also used to confine the IL molecules inside the pores of the porous materials to obtain IL-based hybrid materials [51,52].

2.2. *Post-synthesis modification techniques to prepare IL/porous material composites*

To overcome the challenges mentioned in the previous section and to provide a more straightforward methodology compared to the *in-situ* synthesis routes, post-synthesis modification strategies have been developed, as presented in Fig. 3. ILs are incorporated into the pores or deposited on the external surfaces of the porous material supports by taking advantage of the IL's liquid nature, extremely low vapor pressure, and the capability of creating interactions with the pores or surface of the porous material. Post-synthesis modifications can be achieved by applying various methods, such as wet impregnation [53], incipient wetness [54], capillary action [14], ship-in-a-bottle [9], and grafting [55]. Among these methods, wet impregnation is the most commonly applied one to the porous materials to prepare their composites with ILs. In this method, the IL is first dissolved in an excess amount of solvent, such as acetone, dichloromethane, ethanol etc. Then, the pristine porous material is added to the mixture solution to reach a homogenous dispersion of the IL. The resulting mixture is stirred at mild temperatures followed by solvent evaporation, and then the homogeneous composite is further dried to remove the solvent completely and to form the final sample in powder form. Various studies on different applications use this post-synthesis modification method to successfully prepare IL-impregnated composites [2,4,5,8,10–13,24,28,38,41,53,56–66]. Similar to the wet impregnation, incipient wetness technique includes the same experimental steps; however, the only difference is the amount of solvent that is used to dissolve the IL. In the incipient wetness method, the amount of the IL/solvent mixture is adjusted to have enough volume

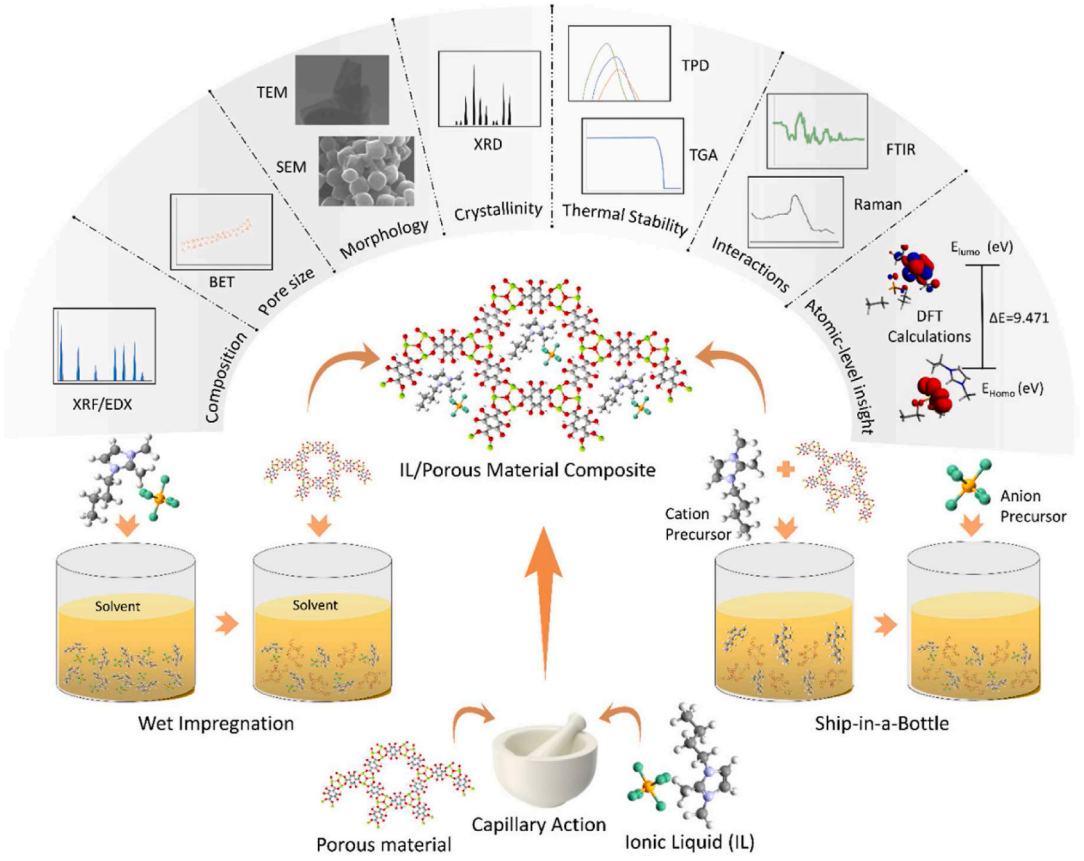


Fig. 3. Synthesis and characterization methods of IL/porous material composite.

to fill the pores of the desired porous material [54,67]. The capillary action method is another technique for post-synthesis modifications, where IL and pristine porous material are directly mixed using pestle and mortar. The amount of IL and porous material are determined by using a certain volumetric occupancy ratio. The resulting mixture is then placed inside an oven for overnight heat treatment to facilitate the diffusion of IL molecules into the pores [14,29,66,68,69].

Unlike the impregnation techniques described above, the "ship-in-a-bottle" method consists of cation and anion precursors of IL (ship) and pores of a porous material (bottle). In this technique, the precursors of the IL are dissolved in a solvent, and then they are impregnated onto the porous material to allow diffusion inside the pores (bottle), where they react to form the IL molecules (ships). Then, the remaining non-reacted IL molecules are removed by washing the material with a solvent, and the obtained wet composite is then dried. The advantage of this method is that the IL molecules larger than the pore openings of the porous material can be trapped inside the cavities successfully [9,70–72].

Composite preparation with the grafting method can be mainly defined as the incorporation of the IL molecules onto the surface of the pores. There are two different grafting methods called grafting-from and grafting-to. For the grafting-from method, the modification agents, ILs, grow *in-situ* on the surface of the porous support with the help of a previously anchored initiator [73]. For the grafting-to method, a reaction is induced between the IL molecules and the surface of porous support to attach IL molecules onto the surface [74–77]. In the case of IL/porous material composites, the grafting-to method is widely preferred due to its highly controllable nature for locating IL molecules and high stability of deposited molecules on the surface of the porous support. Especially in the field of catalysis, the grafting-to method enables the immobilization of catalytically active metal sites and stabilizes these catalytically active complexes or metal nanoparticles formed on the interface, which improve the stability and recyclability of these composites [78].

To select a post-synthesis modification, desired IL loading can be considered as a subject of interest. In the case of impregnation method, a variety of ILs with different chemical and physical properties can be incorporated into the porous adsorbents up to their wetness point. For instance, 30 wt.% was reported as the wetness limit of IL for an IL/MOF composite, [BMIM][BF_4]/CuBTC [5], whereas 50 wt.% was reported for an IL/rGA composite, [BMIM][PF_6]/rGA [4]. However, beyond a certain loading point, leaching issues due to weak molecular interactions or formation of a muddy composite can be observed. Alternatively, more stable composites can be formed with the grafting method considering stronger molecular bonding interactions. However, a limited number of ILs can be loaded due to the chemistry restrictions which makes it difficult to control ILs on the surface [74]. Overall, for higher IL loadings up to wetness point, the use of the impregnation method will be more beneficial, while for lower IL loadings, the use of grafting will be more appropriate in terms of structural stability.

3. Characterization of IL/porous material composites

To characterize the resulting IL/porous material composites, investigations on their morphology, crystal structure, surface area and pore size distribution, surface interactions, elemental composition, and molecular-level investigations are conducted by different techniques. In this section, characterization techniques of IL/porous material composites will be highlighted.

Rational design of new IL/porous material composites is only possible with an understanding of (i) the individual amounts of IL and porous material in the composite; (ii) interactions between the IL molecules and the porous materials; (iii) dependency of these interactions to the structures of the individual components; and (iv) their consequences on different performance measures [53,79]. The presence of ILs can

modify many properties of the host material, such as morphology, crystal structure, surface area and pore volume, thermal and chemical stability, and surface interactions. Various characterization techniques have been used to provide an understanding of what is physically/chemically happening in the host material upon IL incorporation, as illustrated in Fig. 3. Among these techniques, X-ray fluorescence (XRF) spectroscopy and inductively coupled plasma mass spectroscopy (ICP-MS) are powerful in determining the IL loading as in the cases of [BMIM][PF_6]/ZIF-8 [11] and [BMIM][BF_4]/ZIF-8 [12]. In these studies, actual IL loading of the composites was mostly determined by XRF and ICP-MS using the obtained quantification of distinctive elemental species, like phosphorus, and boron (together with zinc).

To determine the IL loading, it is necessary for both host and guest materials to have at least one distinct elemental species due to limitations of these characterization techniques, such as the inability to measure lighter elements and matrix definition for quantitative analysis [80]. For instance, it will not be possible to back-calculate IL loading of a non-functionalized carbonaceous-material, such as activated carbon, graphene, carbon black etc., due to the lack of distinctive elemental species of the porous material. For those cases, other characterization methods, such as thermogravimetric analysis (TGA) [81] or quantitative washing experiments [2], can be referred. Besides, thermal analysis, TGA, can also be utilized to prove the formation of a newly synthesized hybrid material [53]. Generally, newly synthesized IL/porous material composites provide a two-step decomposition curve, representing IL and porous material, during thermal analysis different than their one-step pristine and bulk counterparts. In a study of investigating the thermal stability of different IL/porous material composites of CuBTC and ZIF-8, lower and higher thermal stability limits were obtained compared to those of pristine ILs used to prepare the composites, demonstrating newly formed hybrid materials with different thermal stabilities [79]. Data illustrated that thermal stability limits of ILs in IL/MOF composites were generally decreased with increasing alkyl chain length and functionalization of imidazolium ring, whereas increased with fluorination of the anion. In the study of Kinik et al. [11] such a decrease in the decomposition temperature was discussed based on the newly formed strong interactions between IL and MOF identified with the help of Fourier transform infrared (FTIR) spectroscopy complemented by DFT calculations. Deconvolution of the FTIR spectra provides detailed information on the newly formed intermolecular weak interactions, such as van der Waals interactions, π-π interactions, dipole-dipole interactions, or hydrogen bonding interactions, through red- or blue-shifts of designated characteristic IR fingerprints.

To gain further insights on the composites, scanning electron microscopy (SEM), energy-dispersive X-ray spectroscopy (EDX), transmission electron microscopy (TEM), and X-ray diffraction (XRD) spectroscopy can be used to analyze the changes in the morphology and crystal structure upon the addition of IL. In some cases, such as core-shell type composites, IL layer formation on the surface of supports can be directly observed by TEM imaging. Furthermore, for IL/reduced graphene aerogel (rGA) composites, the uniformly distributed presence of IL molecules were proven with SEM/EDX images, where it was reported that the wrinkled-sheet-like structure of rGA stayed intact [4]. Moreover, the images were combined with XRD results to analyze the crystal structures of prepared composites [3,13,17,41]. Due to the nature of post-synthesis modification strategies, crystal structure is generally expected to be unchanged without any disturbance on the skeleton after the deposition of IL molecules. However, having a significant change in XRD spectra demonstrates the change in structure for a porous material, which can yield an unwanted decrease in the porosity or the surface area. Moreover, Raman spectra holds great importance, especially for carbonaceous-materials, in terms of detecting changes in the surface defects upon IL incorporation, which control the performance measures [4,18]. Nevertheless, investigation of the surface defects can be quite challenging, especially for the composites with IL layer formation and evaluation should be conducted with regards to obtained XRD data.

To complement the interface analysis conducted on the surface of the composites, newly formed surface interactions are defined by X-ray photoelectron (XP) spectroscopy to understand the nature of the interactions. Also, the addition of advanced techniques, such as layer-by-layer etching with XP spectroscopy, is possible for the identification of IL accumulation sites, if present any, or for the identification of IL layer formation on the surface. Similarly, the presence of IL in the porous structure is confirmed by applying Brunauer–Emmett–Teller (BET) analysis. However, in most cases, BET does not provide reliable results due to the poor nitrogen solubility in ILs, especially at the measurement conditions of liquid nitrogen temperature. Thus, (i) the solubility of probing gas molecule inside the bulk IL and (ii) the location of IL molecules in the composite holds significant importance for BET analysis. Determination of gas solubility for ILs can be obtained through experimental studies or computational tools, such as conductor-like screening model for real solvents (COSMO-RS) calculations [82,83]. Quantitative precision of COSMO-RS calculations can be debatable due to the different phenomena observed during the dissolution of gas molecules inside the bulk IL, such as chemisorption through reacting IL's anion or cation [84]. However, COSMO-RS calculations provide a quick rough estimate of the gas solubilities in ILs.

Location of the IL molecules becomes the other main consideration because when the IL molecules are located at the pore openings, they might block the passage of the probing molecule, which leads to considerably lower BET surface area results compared to the real case [5,53,79]. Washing experiments complemented by spectroscopy can be used to identify the exact position of IL molecules whether they are located inside the micro-pores or on the external surface of the porous material. For example, in the case of a core-shell type [HEMIM][DCA]/ZIF-8 composite (Fig. 4(a)), the location of the IL was confirmed by washing experiments and complemented with TEM images, given in Fig. 4(b), providing the direct evidence [2]. [HEMIM][DCA]/ZIF-8 composite was washed with a solvent, dimethylformamide (DMF), which cannot fit into the pores of ZIF-8, and results illustrated that the IL molecules were deposited on the external surface of MOF creating a shell-layer consistent with TEM images.

In the light of mentioned characterization techniques, it is appropriate to state that the characteristic spectra of IL-incorporated porous composites, such as crystal structure and morphology, are closer to the characteristics of porous materials rather than bulk ILs due to the employment of the post-synthesis modification techniques. For composite materials, the IL remains as the component with a lower quantity compared to that of host porous material. Thus, the focus of this study was mostly on the consequences of IL incorporation on the properties of the porous host material. For these hybrid materials, IL only acts as a modifying agent to tune the properties of porous material, such as porosity, affinity, catalytic activity, ion mobility, by locating on the walls/surface. Therefore, the effect of IL after incorporation can be detected by the deviations from the characteristics of porous material. Moreover, ideally, evaluation of each characterization technique mentioned is equally required for each application area to reach a fundamental-level of understanding on the structure-performance relationships.

4. Applications of IL/porous material composites

4.1. Gas storage and separation

Various types of IL/porous material composites, such as IL-incorporated MOF [5,10], IL-deposited MOF [2], IL/COF [15,43], IL/zeolite [85,86], and IL/carbonaceous-material composites [4,35], have been used for gas adsorption and separation owing to their high surface area, tunable characteristics, and high affinity towards desired gas molecules. Likewise, IL-incorporated composite membranes including SILMs [87], ILPMs [88], IL/MOF MMMs [23], and PILMs [89]

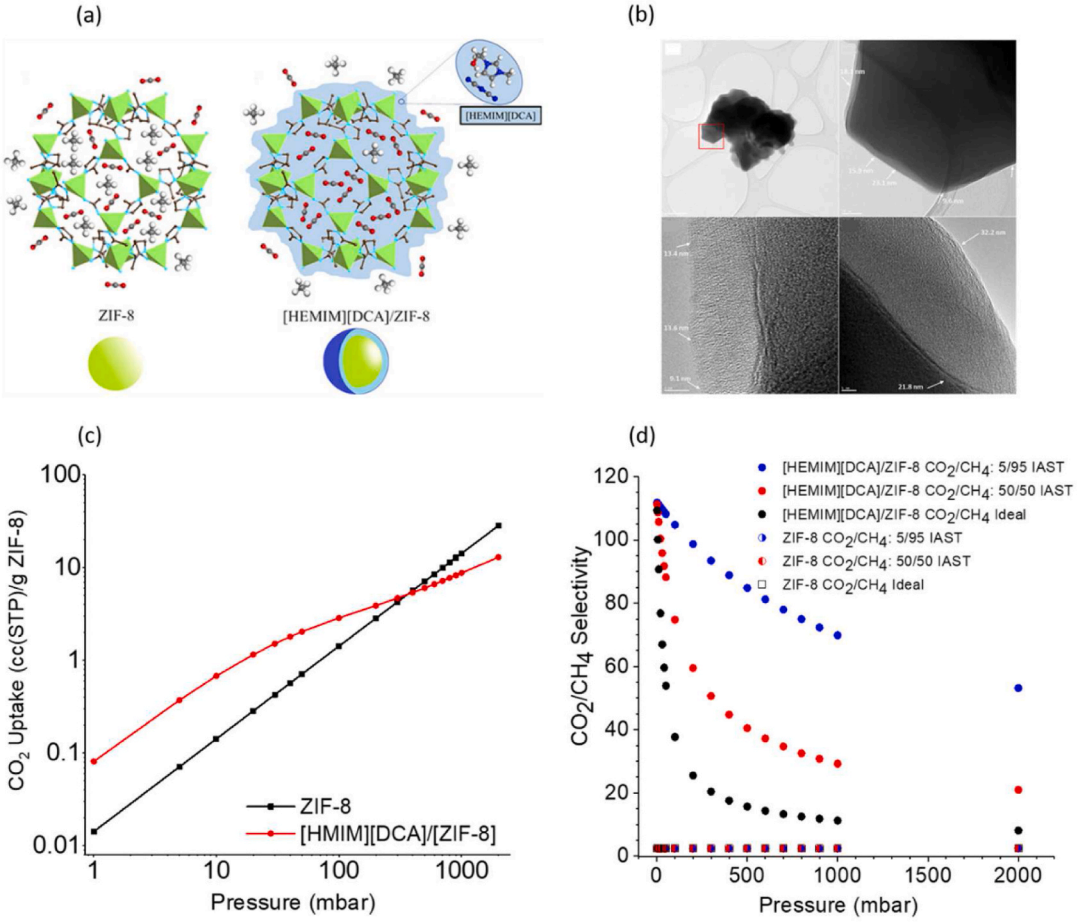


Fig. 4. (a) Schematic representation of the proposed Core−Shell Type IL/MOF structure (b) TEM images of [HEMIM][DCA]/ZIF-8 composite, (c) CO_2 uptake of pristine ZIF-8 and IL/ZIF-8 composite at 25 °C, and (d) Ideal and IAST-predicted selectivities of pristine ZIF-8 and IL/ZIF-8 composite at 25 °C. Reproduced with permission [2]. Copyright 2018, American Chemical Society.

are generally studied for gas separation due to their selective CO_2 separation performance. Almost all of these materials show significant improvements in the gas separation performance compared to their pristine counterparts. In the following sections, recent progress in IL-incorporated composites for gas adsorption and separation applications is discussed.

4.1.1. Adsorption-based gas storage and separation

IL/MOFs and IL/COFs. Combining ILs with MOFs to prepare hybrid materials has gained growing attention in adsorption-based gas separation processes [31,90–94]. One of the earliest studies on IL-incorporated MOFs was reported by our group in 2016 [5]. In this study, [BMIM][BF_4] was incorporated into CuBTC, and the resulting composite showed approximately 1.5-times improved ideal selectivities for CH_4 over H_2 and N_2 compared to the pristine MOF at low pressures (Fig. 5(a) and (b)). These enhancements were attributed to the modifications in the pore environments, the formation of new adsorption sites, and enhanced interactions of guest molecules with IL-MOF interfaces. Likewise, another earliest contribution to this field was reported by Yang's group showed an increase in the CO_2 adsorption capacity by incorporating [BMIM][NTf_2] into the nanocages of ZIF-8 to tune its molecular sieving property (Fig. 5(c) and (d)) [23]. The high CO_2 solubility and its affinity towards the IL molecules allow CO_2 to have more preferential adsorption sites leading to its preferred adsorption more than the other gases.

To further understand the influence of IL incorporation on the selective gas adsorption and separation performance of IL/MOF composites, [BMIM][PF_6] was incorporated into a different MOF, ZIF-8 [11]. Since the incorporation of [BMIM][PF_6] created additional adsorption sites within the ZIF-8 and $[PF_6]^-$ has a higher affinity towards CO_2 compared to other gases, ideal CO_2/CH_4 and CO_2/N_2 selectivities of IL-incorporated ZIF-8 were improved by more than two-times at low pressure. Following this, Henni and coworkers reported that the CO_2 uptake of ZIF-8 increased seven-times by the incorporation of [BMIM][Ac], and 18-times higher CO_2/N_2 selectivity was obtained by incorporating [EMIM][Ac] into ZIF-8 at 0.1 bar [91]. These improvements in CO_2 adsorption and separation performance were attributed to the introduction of IL molecules into ZIF-8 cages as energetically favorable CO_2 adsorption sites, which ultimately improve CO_2 adsorption and separation performance [95]. However, we also note that when the IL is present as multiple layers especially at high IL loadings, it is possible to have multiple sorption mechanisms, where absorption of the gas molecules inside the IL layer may exist in addition to their adsorption on the surface. Furthermore, the key observation is that ILs with acetate anions have the potential to enhance the CO_2 uptake capacity of a composite material due to the presence of acetate ion, which acts as a strong Lewis base that creates additional CO_2 adsorption sites [96,97]. In short, these findings demonstrate that changing the anion type of IL has a significant impact on CO_2 capture and separation performance of IL/MOF composite.

In an attempt to further analyze the effect of structural differences of ILs on the gas separation performances of IL/MOF composites, Isabel and coworkers studied the effect of ten different imidazolium-based ILs on the adsorption and CO_2/CH_4 separation performances of IL-impregnated ZIF-8 composites [81]. Results showed that imidazolium-based cations with small alkyl side chains and $[NTf_2]^-$

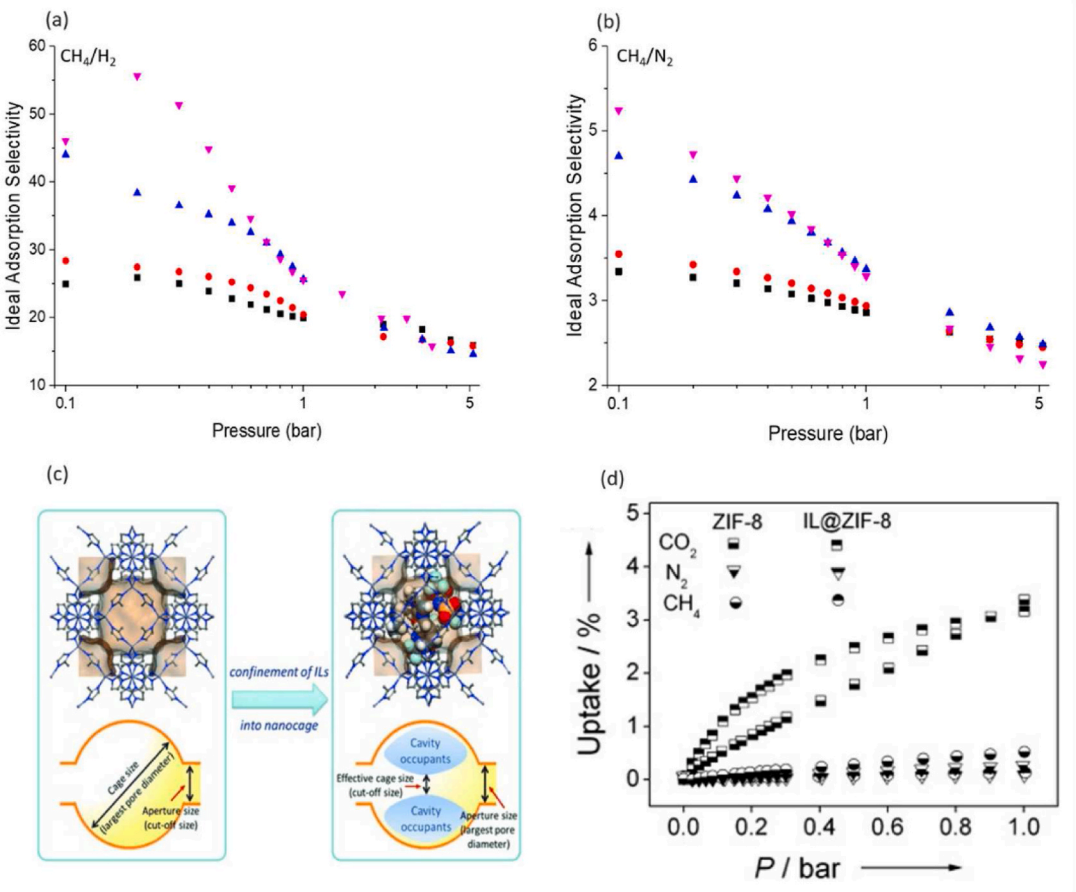


Fig. 5. Ideal selectivities of CuBTC and [BMIM][BF_4]-incorporated CuBTC composites (a) CH_4/H_2 and (b) CH_4/N_2 selectivity in the pressure range 0.1–5 bar and 25 °C. Reproduced with permission [5]. Copyright 2016, American Chemical Society. (c) Schematic illustration of RTIL incorporation into the ZIF-8 pores for modifying molecular sieving properties by shifting its cut-off size from aperture to effective cage size. (d) CO_2, N_2, and CH_4 adsorption isotherms of pristine ZIF-8 and IL@ZIF- 8 composite in the pressure range 0.1–1 bar and 25 °C. Reproduced with permission [23]. Copyright 2015, Wiley-VCH.

anion tend to provide a higher adsorption capacity in IL/ZIF-8 composites at high pressures. Moreover, an IL/MOF composite prepared by impregnating a non-polar IL ([C_2MIM][NTf_2]) into the MOF exhibited a better adsorption capacity than the IL/MOF composite with a polar IL, [C_2OHMIM][NTf_2]. Recently, four different imidazolium-based ILs were incorporated into ZIF-8 [41]. Results illustrated that when the IL contained a fluorinated anion, the resulting IL/ZIF-8 composite demonstrated three-times improved CO_2/CH_4 separation performance compared to the non-fluorinated IL/ZIF-8 composite. This improvement was associated with a highly polar C–F bond in the fluorinated anion. When the incorporated IL has a relatively small anion, the gas separation performance of the composite sample was superior compared to the one which has a bulky anion.

In 2019, our group suggested that when IL and MOF with similar hydrophilic/hydrophobic characters are combined, the resulting IL/MOF composite has the potential of superior gas separation performance than that of a parent MOF. For instance, when a hydrophilic IL ([BMIM][$MeSO_4$]) was incorporated into a hydrophilic MIL-53(Al) and a hydrophobic IL ([BMIM][PF_6]) was impregnated into a hydrophobic ZIF-8, for each case, the resulting composite showed enhanced gas separation performance than that of a parent MOF [98]. Due to the hydrophilicity of MIL-53(Al), water loss was observed in TGA analysis at 100 °C for the composite and parent MOF [98]. Thus, these composites should be prepared in dried conditions to reduce the moisture effect. Moreover, a single adsorption experiment for CuBTC, a hydrophilic MOF, showed that vapor water uptake was higher than CO_2 by one order of magnitude. For this reason, to maximize CO_2 uptake, the water content in the feed gas should be minimized as much as possible [99]. We also illustrated the influence of interionic interaction energy between the cation and anion of the bulk ILs on the gas adsorption and separation performance of seven [BMIM]$^+$-based IL-incorporated CuBTC composites [94]. Probing the interionic interaction energies in ILs by the ν(C2H) band position in the IR spectrum of the bulk ILs, it was illustrated that both CO_2 and CH_4 uptakes in the IL-incorporated CuBTC composites decrease as ν(C2H) of the corresponding IL presents a red shift, indicating an increase in the interionic interaction energy.

Apart from the common ILs, amine-functionalized ILs and polymerized ILs (polyILs) were also incorporated into MOFs to prepare hybrid composites. For instance, an amine-functionalized IL, [C_3NH_2bim][Tf_2N], was incorporated into NH_2-MIL-101(Cr), which resulted in a doubling of the CO_2/N_2 separation performance, because of the excellent affinity of CO_2 towards amine-functionalized IL [24]. This is expected because of the strong Lewis acid-base and dipole-dipole interactions between the amine functional group and CO_2 molecules [100]. Similarly, an imidazolium-based IL was confined in the pores of MIL-101 via *in-situ* polymerization of IL [101]. Introducing Lewis base active sites by the confinement of polyILs in MOF pores resulted in a better CO_2 uptake (62 cm^3/g) compared to that of the pristine MIL-101 (57 cm^3/g) at 1 bar.

Although IL-incorporated MOFs are one of the promising composite materials among various adsorbents for gas separation, there are limitations, such as when an IL is incorporated into pores of the MOF, lower gas adsorption is observed in IL-incorporated composites compared to the gas uptakes of the parent MOF. Thus, the new emerging concepts, such as core-shell type IL/MOF and porous liquid-IL/MOF composites, gain more attention due to their excellent adsorption and separation

performances. For instance, to prevent the inevitable reduction of gas uptake arising from the occupation of MOF pores by the confinement of IL molecules, our group demonstrated a new class of core-shell type IL/MOF composite by depositing [HEMIM][DCA] (hydrophilic) on the external surface of ZIF-8 (hydrophobic) to retain the original pore volume of the parent MOF [2]. The prepared core (MOF)-shell (IL) type composite showed 5.7-times improved CO_2 uptake compared to parent MOF at low pressures providing a record-high CO_2/CH_4 selectivity of 110, an almost 45-times better selectivity compared to that of the parent MOF at similar operating conditions (Fig. 4(c) and (d)) [2].

Compared with MOFs, IL confinement of COFs has been a relatively new field with ongoing research since 2016. While we were writing this review article, a minireview was published on IL-based COF composite materials, which discusses the details of these emerging composite materials [102]. Therefore, in this manuscript, we only highlight the pioneering studies demonstrating the gas adsorption ability of IL/COF composites. In 2018, Shilun's group experimentally demonstrated a fast ionothermal synthesis method using IL as a solvent for the preparation of 3D IL-containing COFs (3D-IL-COFs) (Fig. 6(a) and (b)) [43]. Ideal CO_2/N_2 and CO_2/CH_4 selectivities obtained from the ratio of the initial slopes in Henry's region of the isotherms were 24.6 and 23.1 in IL-incorporated COF compared to the corresponding ideal CO_2/N_2 (7.1) and CO_2/CH_4 (5.3) selectivities of the parent COF at room temperature. This enhancement in gas separation performance in the synthesized 3D-IL-COFs was attributed to the stronger interactions of CO_2 molecules towards dicyanamide-based IL. Following this study, Dong and co-workers reported an acylhydrazone-linked COF decorated with an allyl-imidazolium-based IL (Fig. 6(c)). The data suggested that the prepared IL/COF material has ideal CO_2/CH_4, CO_2/H_2, and CO_2/N_2 selectivities of 4.9, 76.1, and 11.3 at 1 bar and room temperature, respectively (Fig. 6(d)) [15].

The adsorption performances mentioned in this section are obtained by either gravimetric or volumetric adsorption methods. For the gravimetric method, the change in weight of the adsorbent material is measured continuously as a function of applied temperature and pressure, whereas, for the volumetric method, the difference in the volume of the injected gas is used to measure adsorbed quantities [103]. In detailed comparison, the gravimetric method can be considered inherently more accurate than the volumetric method due to its lower dependence on temperature/pressure change during the analysis. The volumetric method suffers from several drawbacks related to errors in volume determination, gas leakage, and pressure control over constant

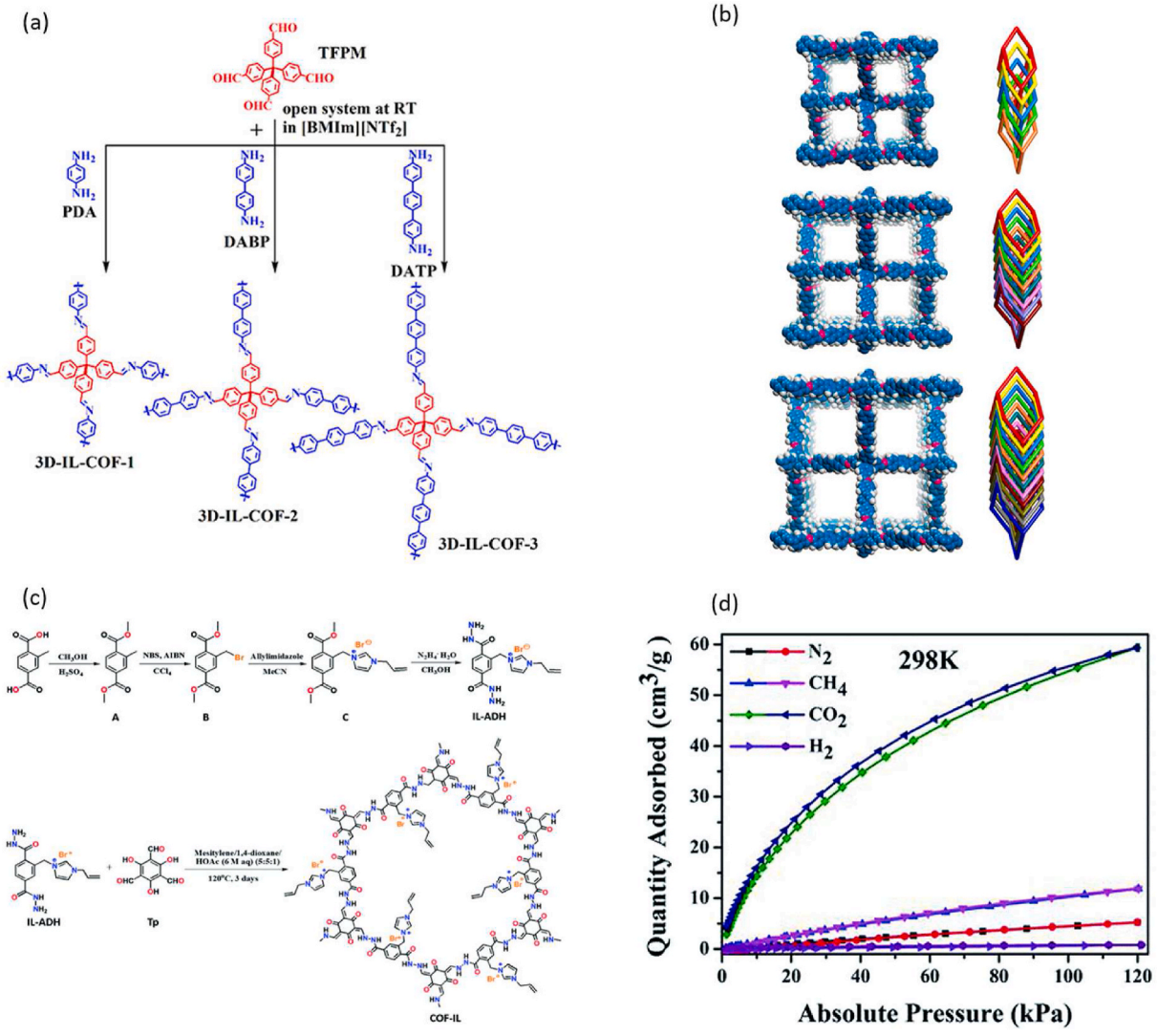


Fig. 6. (a) Preparation strategy for 3D IL-Containing COFs (3D-IL-COFs) and (b) Structural representations of the synthesized 3D-IL-COFs. Color code: C, blue; H, gray; N, red. Reproduced with permission [43]. Copyright 2018, American Chemical Society. (c) Design strategy of IL-ADH and COF-IL and (d) Adsorption isotherms of CH_4, CO_2, N_2, and H_2 on COF-IL. Reproduced with permission [15]. Copyright 2019, The Royal Society of Chemistry. (For interpretation of the references to colour in this figure legend, the reader is referred to the Web version of this article.)

pressure points [104–106]. For the volumetric method, uncertainty in the measurement of adsorbed quantities is primarily induced by systematic and accumulated errors in pressure determination during helium expansion. On the other hand, while the gravimetric method yields more reliable results with the direct measurement of adsorbed quantities, it requires higher accuracy for buoyancy corrections to reach the exact adsorbed quantity amount [107,108]. Therefore, it can be stated that there are different concerns surrounding these methods.

In summary, the studies reported in the literature demonstrate that incorporation of ILs into MOFs and COFs significantly enhances the gas adsorption and separation performance of the parent material. Furthermore, the gas separation performances of the IL-incorporated MOFs are summarized in Table 1. Considering that both ILs and MOFs are highly tunable and have a theoretically unlimited number of possible structures, further studies are required to reach a fundamental level understanding of the structural factors controlling the performance towards the rational design of novel composites that can achieve even higher separation performances.

IL/zeolites. Zeolites are natural or synthetic porous crystalline structures with rigid frameworks, providing superior structural properties, such as high surface areas and tunable porosities. They also created the inspiration for MOF-like structures owing to their well-defined rigid framework and flexible architectural design. Their structure can be tuned with ILs through both *in-situ* synthesis routes and post-synthesis techniques. However, it was observed that the studies on gas adsorption and separation performance of this particular composite type are limited compared to that of other porous materials, such as MOFs and carbonaceous-materials. Thereby, the majority of the studies on gas adsorption and separation performance of IL/zeolite composites will be covered in this section.

The similarity between the cation of IL and the common organic templates of zeolite provides a significant opportunity for the direct *in-situ* synthesis of zeolite porous material. Moreover, the chemically and thermally stable nature of zeolites enables their usage for other *in-situ* synthesis techniques without disrupting the zeolite porous framework. A different type of composite, containing polymerized IL and zeolite, was *in-situ* synthesized by conventional free-radical polymerization [110]. Results revealed that the obtained poly[Veim][Tf_2N]/zeolite polymer composite has approximately 5-times higher capability for adsorbing CO_2. The choice of polymerized IL was made according to the desired application measures, particularly, by considering its superior CO_2 sorption capacity.

Besides their great potential for *in-situ* techniques, high porosity and high surface area can also qualify zeolites as promising support material for post-synthesis modification methods. Various studies showed that IL molecules can be trapped in the pores of zeolites for enhanced selective adsorption of different types of gas molecules. Different types of ILs, [CnMIM][Br] and [APMIM][Br], were encapsulated in the cages of NaY zeolite by using the ship-in-a-bottle technique to overcome the steric effect arising from the large molecule sizes of ILs [16,111]. Therefore, the selection of ILs was made considering the cage size of zeolite and the molecular sizes of IL precursors. Results demonstrated that the CO_2 adsorption capacity of pristine zeolites could be enhanced with encapsulation. Enhanced results by deposition of IL were obtained with different IL/zeolite composites for various cases of selective gas adsorption as well [112]. In the case of MCM-36 zeolite, an acidic IL, [BTPIm][HSO_4], was immobilized into the pores to increase the surface acidity with the help of anionic [HSO_4] moieties [17]. The resulting composite has tuned the adsorption of isobutane over 1-butene due to enhanced interactions between the acidic surface of the composite and isobutane. Similarly, the same composite was tested for adsorption/-desorption of 2,2,4-trimethylpentane, where an enhanced desorption mechanism was achieved [86]. In the case of MCM-22 zeolite, the effect of IL immobilization on selective paraffin adsorption was investigated by using a dual acidic ionic liquid yet again to improve surface acidity of the zeolite [113]. It was reported that the adsorption of ethane over

Table 1
An overview of the IL-incorporated MOFs composites (prepared by wet impregnation method) reported in the literature for adsorption-based gas separation applications.

IL/MOF composites	Pressure (bar)	Ideal Selectivities					
		CO_2/CH_4	CO_2/N_2	CH_4/N_2	CO_2/CH_4	CO_2/N_2	CH_4/N_2
Pristine ZIF-8 [11]	0.001	2.7	7.2	2.8	–	–	–
	0.1	2.2	6.5	2.7	–	–	–
	1	–	–		2.5	7.3	2.7
[BMIM][PF_6]/ZIF-8 [11]	0.1	8.9	24.2	2.8	–	–	–
	1	–	–	–	5.1	13.2	2.5
[BMIM][BF_4]/ZIF-8 [12]	0.1	4.3	14.6	3.4	–	–	–
	1	–	–	–	3.5	11.6	3.3
[HEMIM][DCA]/ZIF-8 [2]	0.001	110	–	–	–	–	–
	1	–	–	–	11.3	–	–
[BMIM][Ac]/ZIF-8 [91]	0.1	–	92	–	–	–	–
[EMIM][Ac]/ZIF-8 [91]	0.1	–	105	–	–	–	–
[BMIM][SCN]/ZIF-8 [92]	0.01	6.5	21.2	2.2	–	–	–
	1	–	–	–	5.1	10.5	2.1
[BMIM][$MeSO_3$]/ZIF-8 [41]	0.01	1.7	19.1	11.3	4.6	9.5	2.0
	1	–	–	–	4.6	9.5	2.0
[BMIM][CF_3SO_3]/ZIF-8 [41]	0.01	6.6	3.4	0.52	–	–	–
	1				6.3	5.5	0.87
[BMIM][$MeSO_4$]/ZIF-8 [41]	0.01	2.2	9.2	4.4	–	–	–
	1				4.5	23.1	5.1
[BMIM][$OcSO_4$]/ZIF-8 [41]	0.01	4.7	2.6	0.53	–	–	–
	1	–	–	–	3.6	6.7	1.9
[C_2MIM][Ac]/ZIF-8 [81]	0.5	–	–	–	3.3	–	–
[C_{10}MIM][NTf_2]/ZIF-8 [81]	0.5	–	–	–	3.1	–	–
[C_6MIM][NTf_2]/ZIF-8 [81]	0.5	–	–	–	2.6	–	–
[BzMIM][NTf_2]/ZIF-8 [81]	0.5	–	–	–	2.4	–	–
[P_{66614}][NTf_2]/ZIF-8 [81]	0.5	–	–	–	2.4	–	–
[C_6MIM][DCA]/ZIF-8 [81]	0.5	–	–	–	3.1	–	–
[C_6MIM][$C(CN)_3$]/ZIF-8 [81]	0.5	–	–	–	2.6	–	–
[C_6MIM][Cl]/ZIF-8 [81]	0.5	–	–	–	3	–	–
Pristine MIL53(Al) [98]	1	–	–	–	3.5	10.1	–
[BMIM][BF_4]/MIL-53(Al) [98]	1	–	–	–	7.7	16.8	–
[BMIM][PF_6]/MIL-53(Al) [98]	1	–	–	–	9.1	17.3	–
[BMIM][CF_3SO_3]/MIL-53(Al) [98]	1	–	–	–	3.8	12.1	–
[BMIM][SbF_6]/	1	–	–	–	3.1	9.5	–

(*continued on next page*)

Table 1 (*continued*)

IL/MOF composites	Pressure (bar)	Ideal Selectivities					
		CO_2/CH_4	CO_2/N_2	CH_4/N_2	CO_2/CH_4	CO_2/N_2	CH_4/N_2
MIL-53(Al) [98]							
[BMIM][$MeSO_4$]/MIL-53(Al) [98]	1	–	–	–	7.7	24	–
[BMIM][NTf_2]/MIL-53(Al) [98]	1	–	–		3.4	11.1	–
Pristine CuBTC [93]	0.01	4.6	17.6	3.7	–	–	–
	1	–	–	–	5.4	15.7	2.9
[BMIM][PF_6]/CuBTC [93]	0.01	4.3	26.2	5.1	–	–	–
[BMMIM][PF_6]/CuBTC [93]	0.01	5.2	23.1	4.4	–	–	–
[EMIM][DEP]/CuBTC [109]	0.01	7.27	42.3	5.8	–	–	–
[BMIM][NTF_2]/CuBTC [94]	0.01	3.2	13.1	3.8	–	–	–
[BMIM][CF_3SO_3]/CuBTC [94]	0.01	4.14	19.4	4.5	–	–	–
[BMIM][BF_4]/CuBTC [94]	0.01	4.6	21.1	4.7	–	–	–
[BMIM][$MESO_4$]/CuBTC [94]	0.01	4.4	21.8	4.9	–	–	–
[BMIM][SBF_6]/CuBTC [94]	0.01	5.5	25.7	4.4	–	–	–
[BMIM][$OCSO_4$]/CuBTC [94]	0.01	5.4	26.7	5.0	–	–	–
[BMIM][$MESO_3$]/CuBTC [94]	0.01	5.6	27.1	4.8	–	–	–
[BMIM][SCN]/CuBTC [94]	0.01	5.7	29.6	5.2	–	–	–

ethylene was increased by more than 30% upon IL immobilization due to task-specific selection of an acidic IL. Moreover, the same zeolite was also used with four different types of ILs for the selective adsorption of isobutane over 1-butene. Results demonstrated that enhanced surface density of acidic groups led to an increase in the adsorbed molar ratio of isobutane over 1-butene [85].

Overall, hybrid IL/zeolite composites enhanced the selective gas adsorption performance for different gases and improved the stability of bulk ILs by forming comparably stable hybrid structures. In this respect, the requirements of the desired separation and the cage characteristics of zeolites play an important role in the selection of task-specific IL. Therefore, reviewed literature studies illustrated that zeolites can be utilized as an efficient porous material option for IL-containing hybrid composites, and the intensity of the studies conducted on this area can be increased.

IL/porous carbonaceous-materials. Carbon-based porous materials create many opportunities for extended modifications with their tunable porosity and structural diversity as a promising branch among adsorbent materials. However, extremely harsh and high-temperature conditions of carbonization reactions make IL utilization quite difficult during *in-situ* synthesis of randomly oriented carbon-based structures, such as activated carbon, porous carbon etc., due to the relatively low thermal stabilities of most ILs. On the other hand, sophisticated new techniques can be introduced for carbon-based structures with higher complexity, as in the case of the layer-by-layer reassembly technique for IL/graphene films where the nanospace formed between sp^2-hybridized carbon nanosheets enhanced the affinity towards toxic aromatic hydrocarbons [35]. Yet, IL usage through post-synthesis methods constitutes the majority of the research conducted on the field.

In the case of selection, there are a variety of options for IL-incorporation starting from complex 3D-structured carbonaceous materials to commercially abundant and cost-effective ones. For instance, in the study of Erto et al., different commercial activated carbons (ACs), Filtrasolb 400, and Nuchar RGC30 were modified with amino acid-based ILs, [HMIM][BF_4] and [EMIM][Gly], through impregnation and their CO_2 capture performances were investigated accordingly [114]. The study highlighted that sterically hindered IL molecules, [HMIM][BF_4] in this case, can create a blockage in the pores of AC, leading to a decrease in CO_2 adsorption. Even though [HMIM][BF_4] is classified as a physical solvent for CO_2, less sterically hindered [EMIM][Gly] increases the adsorption capacity while a decrease is observed for the composite with [HMIM][BF_4]. Similarly, the same pore blockage phenomenon was observed in the cases of both amine-functionalized ILs [115], and phosphonium-based ILs [116]. Enhanced CO_2 adsorption capacity can also be attributed to the newly formed interactions between the IL and AC where new adsorption sites became available, similar to the study where Lewis-acidic IL (choline chloride-zinc chloride) was used to change the CO_2 adsorption mechanism of pristine AC [3]. Besides CO_2 adsorption, IL/AC composite materials were also used for selective removal of other gaseous species such as mercury capture from natural gas [117] and SO_2 capture from the atmosphere [118].

Among all the possible strategies for enhanced performance measures, functionalization of IL for higher molecular affinity towards the desired molecules has created another possibility for gas storage enhancement through post-synthesis techniques. Tamilarasan et al. modified graphene [18,75] and carbon nanotubes [119] by using non-functionalized IL, functionalized IL, polymerized IL (PIL), and amine-rich IL (ARIL) to obtain higher CO_2 adsorption capacities by increasing the CO_2 affinity of used IL. They obtained an enhancement in CO_2 gas adsorption capacity for all composites. However, composites with functionalized-IL, PIL, and ARIL, showed a higher increase compared to non-functionalized counterparts [18,75,119]. Yet, it is better to mention the main drawback of impregnation methods, especially for carbon nanotube bundles, where the impregnation solvent causes aggregation of the bundles, which can lead to insufficient impregnation due to lack of homogeneity of the support material.

Likewise, the functionalization of porous materials before IL-impregnation has become a new research field to explore the desired molecular affinities as in IL-modified graphitic carbon nitride nanosheets and rGAs [4,120]. In recent years, an IL/rGA composite was introduced for the first time by modifying a GA first through a thermal reduction treatment followed by the deposition of [BMIM][PF_6] on its surface. The data showed a remarkable increase with more than 20-times enhancement in the CO_2/CH_4 selectivity upon the deposition of the IL, attributing to the newly formed interactions between impregnated [BMIM][PF_6] and rGA [4]. Consequently, IL/carbonaceous-material composites provide an extended possibility of functionalization and constitute a promising class of IL-incorporated composites for further research studies.

4.1.2. Membrane-based gas separation

Traditional polymeric membranes suffer from the trade-off between permeability and selectivity for gas separation, hindering their commercialization. The performance of these membranes is evaluated with respect to the Robeson upper bound [121], the trade-off relationship between the gas permeability and the selectivity, which is empirically defined from experimental results for different gas pairs. The combination of ILs with polymeric membranes is an interesting

approach to intensify their performance. This section describes the properties of IL-incorporated composite membranes for gas separation, specifically SILMs, ILPMs, IL/MOF MMMs, and PILMs. Fig. 7 visualizes the schematics of IL-based membranes and illustrates their structural morphology.

SILMs are porous membranes impregnated with ILs, which have shown great potential in gas separations due to their attractive properties, such as low solvent loading and high selectivity [20]. For instance, "commercially attractive" SILMs based on [EMIM][CF_3SO_3], [EMIM][Tf_2N], [C_6MIM][Tf_2N], and [EMIM][BF_4] with polyether sulfone (PES) support yield better CO_2/CH_4 and CO_2/N_2 selectivities than pure polymeric membranes [122]. However, the membranes tend to swell over time as determined by optical methods. In the case of swelling, the thickness of membrane is changed, which affects the gas diffusion path as well as the mechanical stability of the membranes, and thus, their efficiency diminishes [123,124]. To overcome this issue, stability studies were carried out by varying the types of membrane support, ILs, and synthesis procedures [125]. The utilization of nanofiltration (NF) supports to strengthen the capillary forces between the IL and the membrane pores enhances the stability of SILMs. Hence, polyimide (PI) was used as a support for [Benz][Ac] to fabricate SILMs, which showed superior separation performances for CO_2/CH_4 and CO_2/N_2 with selectivities of approximately 38 and 41, respectively [126].

Leaching of ILs from the pores of the membranes due to high-pressure operation is identified as a drawback of SILMs [127]. To prevent the loss of ILs, synthesis of ILPMs is a possible solution, in which instead of immersing IL in membrane pores, the physical blending of IL and the polymer is done. ILPM based on a polymer of intrinsic property (PIM-1) and [C_6MIM][Tf_2N] showed a 58% increase in CO_2/N_2 selectivity and a 36% increase in CO_2/CH_4 selectivity compared to pure PIM-1 at low IL loading of 10 wt.% [21]. To have further insights into the effect of IL loadings on the gas permeabilities, the IL content was increased up to 81 wt.% in the PI matrix, which induced an increase in CO_2 permeability from 84 to 500 Barrer at 35 °C [128]. These high permeabilities were attributed to the increased gas diffusivity due to the presence of IL and the plasticization effect of the polymer. However, by increasing the IL content, the mechanical strength of ILPMs, including tensile strength and extension to break decreased.

To enhance the mechanical properties without compromising the separation performances, combining ILs with inorganic filler in the polymer matrix to form three-component mixed matrix membranes (IL/MOF MMMs) has been investigated [129]. Hudiono and coworkers [130] pioneered the IL/MOF MMMs by demonstrating that incorporation of ILs in MMMs resulted in enhanced compatibility between the polymer and the filler, along with an increase in the gas separation performance due to synergistic effects, for instance, permeability and selectivity [131]. The high sorption capacity of IL improves the permeability, while the shape-selective nature of the filler enhances the selectivity [131]. IL/MOF composites comprised of ZIF-67 coated with different ILs including [BMIM][BF_4], [EMIM][Tf_2N], and [BMIM][Tf_2N] were prepared to explore the effect of IL loading on filler-polymer interactions. MMMs were synthesized by incorporating the prepared composites in 6FDA-durene. Selectivity increased for both CO_2/N_2 and CO_2/CH_4, as shown in Fig. 8(a–b). By increasing the filler loading, CO_2 permeability enhanced by 35%, which is attributed to better compatibility between polymer/filler interface due to the formation of a thin IL layer around ZIF-67 particles [22]. A similar trend in terms of performance was identified for [BMIM][NTf_2]/ZIF-8 incorporated in Pebax, which is a widely used block co-polymer, and the resulted MMMs showed an improvement in the mechanical strength with improved gas separation [132].

Inorganic materials that possess superior selectivities but demonstrate poor compatibility with a polymer can be used for MMM fabrication by utilizing ILs as wetting agents [133]. For instance, an

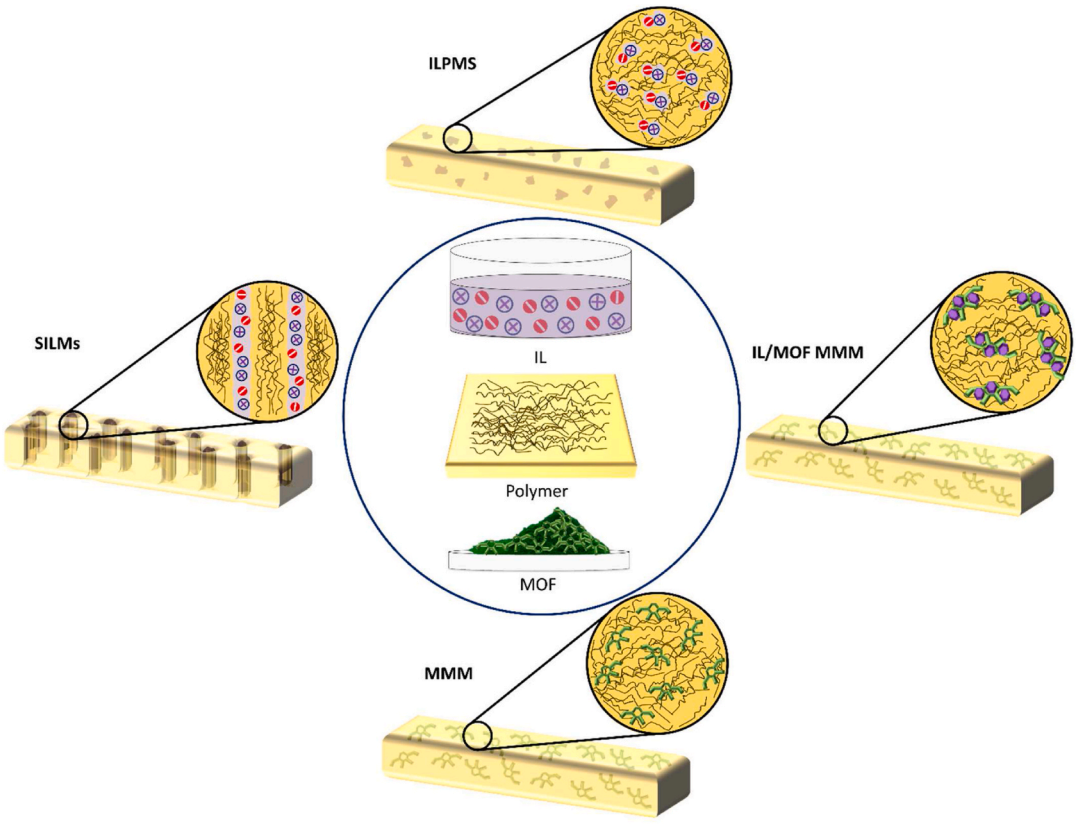


Fig. 7. Schematic representation of supported IL membranes (SILMs), IL polymer membranes (ILPMs), IL/MOF mixed matrix membranes (IL/MOF MMMs), and MOF-based mixed matrix membranes (MMM).

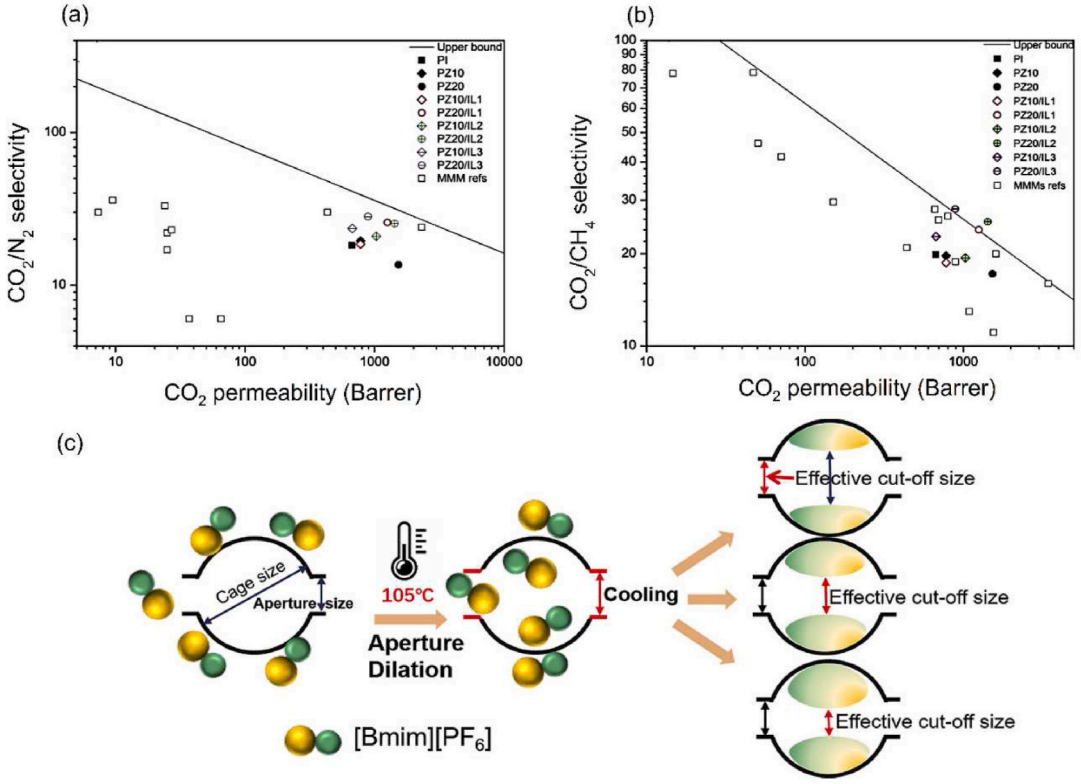


Fig. 8. Robeson's plot for gas separation performance of 6FDA-durene based MMMs comprised of ZIF-67 coated with IL1([Bmim][BF_4]), IL2([Emim][Tf_2N]), IL3 ([Bmim][Tf_2N]), and their comparison with the literature (a) CO_2/N_2 and (b) CO_2/CH_4. Reproduced with permission [22]. Copyright 2019, Elsevier. (c) Schematic illustration of confining IL in ZIF-8 nanocages by adsorption/infiltration method for tuning effective cage size. Reproduced with permission [138]. Copyright 2020, Elsevier.

improvement in the selectivity of CO_2/N_2 from 18.5 to 22.7 was observed for ZSM-5 zeolite particles, which were blended with [BMIM][Tf_2N] and PI. Similarly, to enhance the zeolites' performances as a filler, ILs, such as [BMIM][Tf_2N] [134], [BMIM][BF_4] [135], [EMIM][Tf_2N] [129], [BMIM][Ac] [136], and [APTMS][Ac] [137], have been incorporated. Besides polymer/filler interfacial compatibility in MMM, a recent study focused on achieving fine-tuning of effective cage size of MOF by confining [BMIM][PF_6] into ZIF-8 nanocages through two-step adsorption/infiltration method depicted in Fig. 8(c) to fabricate IL@Pebax/ZIF-8 based MMMs. By following this strategy, the gas pairs with similar sizes can be screened more precisely. The membranes with 8 and 25 wt% IL loadings successfully surpassed the upper bound with CO_2 permeability and CO_2/N_2 selectivity of 117 Barrer and 84.5, respectively [138]. These studies show that IL incorporation in membranes has an incremental effect on gas separation properties. A comparative study was carried out to compare the separation performances of ILPM, IL/MOF MMM, and conventional MMM with ZIF-67/PSf, and [APTMS][Ac]. Results demonstrated that IL/ZIF-67/PSf MMM showed superior selectivity for CO_2/CH_4 and CO_2/N_2 of 72.1 and 74.5, respectively [139].

MMMs comprised of PILs have become an interesting research area due to their high mechanical strength and improved processibility [89]. PIL-based MMMs containing styrene-based poly(IL), [EMIM][Tf_2N] as IL and SAPO-34 zeolite showed an increase in permeability by 63% with 11% increment in the selectivity of CO_2/CH_4 and CO_2/N_2 [25]. To address interfacial defects, PIL-based MMMs were prepared by varying PILs (poly([SMIM][Tf_2N]) or poly([VMIM][Tf_2N])), their degree of polymerization (reducing crosslinker), and the zeolite loadings (25–40 wt%). Mechanically robust membranes with superior CO_2 permeability and CO_2/CH_4 selectivity around 260 Barrer and 90, respectively, outperform the upper bound [140].

This section highlighted the performance of different IL-modified membranes and their potential roles in improving gas separation performances. Generally, ILs enhance the gas separation performance by contributing to the solubility selectivity of the penetrant gases. However, the stability of IL incorporated membranes at high temperatures and pressures are still needed to be addressed. Finally, as there can be unlimited combinations of ILs and polymers, new composites based on ILs can be explored for further advancement in the field.

4.2. *Liquid-phase adsorption and separation*

The scope of application for hybrid composites can be extended to the liquid phase adsorption and separation processes due to rapidly increasing number of wastes from the petrochemical, food, pharmaceutical, steel, and chemical industries [141]. Hence, selective removal of hazardous materials from water must be achieved by adsorptive materials that have tunable structures and high adsorption capabilities, such as IL/porous material composites [38,70,142,143].

After the introduction of IL/porous material composites in the field of liquid-phase adsorption and separation, enhanced diversity of adsorbed molecules is reported due to the ease of task-specific synthesis. Just as selective gas phase adsorption, there are studies present in the literature in which contaminants, such as sulfur [38,144], benzothiophene [70,145], oil [146], hexavalent chromium [28,147], polycyclic aromatic hydrocarbons (PAHs) [64,148], organic contaminants (atrazine (ATZ), diuron, and diclofenac) [149], antibiotics [150–152], drugs [153], organic herbicides [154], pesticides [155], mercury [156–158], auxins [159], fipronil [160], and dyes [8,161], are selectively adsorbed from their solutions. Among these studies, IL/MOF [8,38,144], IL/zeolite [148,152,162,163], IL/AC [157,158], IL/graphene [159,160], or IL/MOF-derived carbon (MDC) [149,164] composites almost always offer higher performance measures compared to those of their pristine counterparts in terms of both maximum adsorption capacity and

adsorption selectivity. The main challenge of this subject can be defined as limiting the use of hydrophobic ILs and water-stable support materials due to water-containing solutions and polar solvents. Therefore, selection of IL/porous material pairing should be conducted elaborately for the integrity of the prepared composite during the adsorption process. Moreover, different strategies can be preferred, such as functionalization of ILs to induce a change in their hydrophilic character or task-specific synthesis of ILs, particularly for liquid-phase usage. In the case of task-specific modification, it is widely known that the chemical nature of IL is mostly controlled by the choice of anion, and hence, choosing water-immiscible or desired solvent-stable anion will provide an IL for enhanced liquid-phase performance [165]. Likewise, the support material should also be selected by considering stability in desired liquid environment, such as water, fuel, etc.

With the appopriate choice of pairing, modification with ILs becomes significant to increase affinity towards desired molecules. Recently, IL/functionalized-MOF (IL/fMOF) concept was introduced by our group to the liquid adsorption field for improved methylene blue (MB) adsorption from an aqueous solution [8]. In this study, MB adsorptions of water-stable MOFs, UiO-66 and its amine-functionalized counterpart NH_2-UiO-66, were investigated upon the impregnation of water stable and hydrophobic IL, [BMIM][PF_6]. IL-impregnated composites reached higher values for maximum adsorption than their pristine counterparts. In another study, adsorption capacities of both methyl orange (MO) and MB were increased upon IL impregnation due to newly formed interactions, namely electrostatic interactions, hydrogen bonding, and π-π stacking interactions [166]. Upon [BMIM][PF_6] impregnation, the adsorption capacity of pristine MIL-53(Al) increased from 84.5 to 44 mg/g to 204.9 and 60 mg/g, respectively, for MB and MO which further promotes the potential of IL-impregnation on liquid adsorption capabilities of porous materials.

Considering these studies, we can infer that selecting the suitable IL and porous material with respect to solid or liquid contaminant and considering the chemical, adsorptive, and electrostatic interactions between contaminant and composite could be the key to an efficient liquid-phase separation process.

4.3. Heterogeneous catalysis

IL/porous material composites have developed a strong interest in the field of heterogeneous catalysis as well. The use of composites as heterogeneous catalysts offers various advantages compared to homogeneous catalysts, such as bulk ILs. Using bulk ILs as homogeneous catalysts makes it challenging to separate and purify the products, which can be hindered by the use of IL/porous material composites as heterogeneous catalysts [167]. Furthermore, the use of composites offers enormous flexibility, as it allows to combine various active sites; those of the porous material in combination with that of the IL [168]. Characteristics of the active sites can be further controlled by performing various functionalization on the porous material. Moreover, by using the high surface area offered by the porous support, the active sites within the ILs can be effectively dispersed, and the concentration of the reactants around the active sites can be enhanced. In the following section, various promising strategies for improving the catalytic performance of IL/porous material composites are discussed.

IL/MOFs and IL/COFs. MOFs have drawn widespread attention in the field of heterogeneous catalysis, thanks to their high porosity, tunable physical/chemical properties, uniform and tunable pore structures allowing the control of product selectivities, and high surface area offering a large number of active sites [169–172]. Besides the utilization of MOFs as catalysts where the framework metal, as well as the organic linker, can participate in the reaction [172], MOFs can be used as supports [173] and as templates to prepare carbon-embedded catalysts [174]. Likewise, COFs are also promising candidates to use in heterogeneous catalysis because of their ordered pores, tunable structure compatible with various modification techniques, and high crystallinity [175]. Another modification strategy is to integrate MOFs [171] or COFs with functional materials, such as ILs [176]. In this context, the use of IL/MOF and IL/COF catalysts in heterogeneous catalysis is a promising approach to obtain high-performance catalysts in various reactions [177,178], including but not limited to the cycloaddition of CO_2 and epoxides [101,168,179–194], biodiesel production [195–200], and oxidative desulfurization [201–203].

For the cycloaddition of CO_2 to epoxides, the presence of the following active sites are crucial: (i) Lewis acid sites, such as metal sites or hydrogen bond donors to polarize the epoxide, (ii) nucleophiles, such as halide anions to accelerate ring-opening, and (iii) Lewis basic sites, such as amino groups of tertiary N moieties to promote the adsorption and activation of CO_2 [168,180]. Various approaches have been reported to obtain such multifunctional IL/MOF composites, consisting of different IL and MOF pairs and using different preparation methods, as summarized in the following section and Table 2.

One of the first examples showing the use of an IL/MOF composite as a catalyst for the cycloaddition of propylene oxide and CO_2 was reported by Ma and coworkers [183]. A quaternary ammonium salt and a phosphorus salt IL were functionalized on MIL-101(Cr) by post-synthetic modification. The resulting composites included $[Br]^-$ anions of the IL, which synergistically worked with Cr^{3+} Lewis acidic sites leading to a higher yield of propylene carbonate compared to various benchmark MOFs, as shown in Fig. 9(a). A composite formed by the grafting of [AmPyl][I] onto ZIF-90 by post-covalent functionalization was another catalyst tested for the solventless cycloaddition of propylene oxide and CO_2 where the composite (IL/ZIF-90) provided approximately two-times higher yield for propylene carbonate compared to the pristine counterpart at identical conditions [184]. Liu et al. stepwise functionalized MIL-101(Cr) with imidazolium-based ILs by post-synthesis method [188]. CO_2-temperature programmed desorption (TPD) results of MIL-101(Cr), and the composite (MIL-101-IMBr) demonstrated that MIL-101 does not provide any basic sites, whereas MIL-101-IMBr shows basic characteristic, as in Fig. 9(b), which was attributed to the presence of N atoms in the imidazolium ring. The prepared MIL-101-IMBr-6 composite showed excellent reusability, as given in Fig. 9(c). In another study, an imidazolium-based-IL with carboxylic acid moieties was grafted on MIL-101(Cr), where the imidazolium part activates CO_2 and the carboxylic acid part activates the C–O bond in the epoxy ring of the epoxide via hydrogen bonding [182]. In addition, the MIL-101(Cr) served as a mesoporous framework increasing the CO_2 concentration around the IL. Thus, the composite exhibited much higher catalytic performance for solventless cycloaddition of styrene oxide with CO_2 compared to the parent MIL-101 without any co-catalyst.

The catalytic performance of MOFs for the cycloaddition of epoxides and CO_2 can be markedly enhanced by introducing Lewis base linkers to the MOF, such as $–NH_2$, –OH, or –S═O [205]. Various composites obtained by the incorporation of ILs into functionalized MOFs have been reported [179,190,192]. For instance, [MAcMIM][Br] and [MAcMBenzIM][Br] were introduced into a functionalized MOF, UiO-66-NH_2, where NH_3-TPD and CO_2-TPD data confirmed the presence of Lewis Zr^{4+} acidic sites, the acidic sites due to IL, and NH_2 strong basic sites for both composites [192]. The composite obtained by introducing [MAcMIM][Br] provided better catalytic performance for the cycloaddition reaction of CO_2 and epichlorohydrin because of the steric hindrance caused by the bulky benzimidazolium group in [MAcMBenzIM][Br]. Thus, the type of IL also has a significant effect on the catalytic performance along with the multifunctional sites [181].

[AeMIM][Br] was grafted on an aldehyde-functionalized ZIF-8 via post-synthetic modification for its utilization for the solvent- and co-catalyst-free cycloaddition of CO_2 and propylene oxide [179]. The coordinatively unsaturated Zn sites acted as Lewis acid sites, whereas the Br^- ions acted as Lewis base sites. The presence of Zn^{2+} and Br^- centers were found to decrease the energy barrier synergistically for propylene oxide ring-opening, resulting in enhanced catalytic performance for the IL-grafted ZIF sample. The proposed mechanism in Fig. 9

Table 2
A summary of recent reports presenting catalytic performance of CO_2 cycloaddition of epoxides catalyzed by IL/MOF and IL/COF composites.

Catalyst name	Epoxide (mmol)	Catalyst amount	Time (h)	CO_2 Pressure (MPa)	Temperature (°C)	Yield (%)
MIL-101-N(n-Bu)$_3$Br [183]	Propylene oxide, 30 mmol	0.27 mmol	8	2.0	80	99
IL-ZIF-90 [184]	Propylene oxide, 18.1 mmol	0.09 mmol	3	1.0	120	95
UiO-67-IL [185]	Epichlorohydrin	0.7 mol %[a]	3	0.1	90	99[b]
UiO-67-IL [185]	Epichlorohydrin	1.5 mol %[a]	8	0.1	90	95
MIL-101-IMBr-6 [188]	Propylene oxide, 18.6 mmol	100 mg	4	0.8	80	93[c]
MIL-101(Cr)-TSIL [182]	Styrene oxide, 15 mmol	100 mg	2	2.0	110	95
ILA@U6N [192]	Epichlorohydrin, 25 mmol	60 mg	4	1.2	80	96
IL-ZIF-8(0.5) [179]	Propylene oxide, 25 mmol	30 mg	3	1.0	110	98
IL/MIL-101-NH$_2$ [190]	Propylene oxide, 29 mmol	0.13 mmol	1	1.3	120	91
MIL-101(Cr)-[(AIm)$_2$][ZnBr$_2$] [168]	Epichlorohydrin, 35.7 mmol	100 mg	1	1.0	120	99
MIL-101(Cr)-[(AIm)$_2$][ZnBr$_2$] [168]	Propylene oxide, 35.7 mmol	100 mg	1	1.0	120	97
Cu$_3$(BTC)$_2$@1.2[BMIM][Cl] [181]	Epichlorohydrin, 3.15 mmol	10 mol %[d]	20	0.7	100	85[e]
polyILs@MIL-101 [101]	Epichlorohydrin, 1 mmol	100 mg	24	0.1	70	94[f]
MIL-IL(B) [193]	Styrene oxide, 15 mmol	100 mg	2	2	110	80
SP@UiO-66-NH$_2$ [180]	Epichlorohydrin, 0.18 mmol	200 mg	8	2.5	95	96
COF-IL [15]	Styrene oxide, 13 mmol	232 mg	48	0.1	80	98
COF-HNU3 [204]	Propylene oxide, 10 mmol	0.002 mol%[g]	48	2	100	99

[a] Catalyst amount was reported as catalyst to epoxide ratio as mol %.
[b] 1 mol % n-Bu$_4$NBr was used as co-catalyst.
[c] 8.7 ml dicholoromethane was used as solvent.
[d] Catalyst amount was reported as catalyst to epoxide ratio as mol % based on Cu.
[e] 0.5 dicholoroethane was used as solvent.
[f] 2 ml acetonitrile was used as solvent.
[g] Catalyst amount was reported as catalyst to epoxide ratio as mol % based on imidazolium salt active site.

(d) showed that the Lewis acidic Zn site activates the epoxide ring, whereupon the ring-opening of the propylene oxide takes place thanks to the nucleophilic attack of Br^-. Thereafter, the oxygen of the opened ring attacks the C of CO_2, forming a carbonate complex, and the ring closes, forming the propylene carbonate product.

The grafting of ILs on MOFs, as presented in the examples mentioned above offers advantages, such as structural stability and proper catalyst recovery, as there is no leaching of the IL. However, many of them need complex functionalization reactions. Thus, impregnation of ILs in the cages of MOFs is a simple and promising process for immobilizing the IL by means of coordination bonds [168]. For instance, a functionalized MOF, NH_2-MIL-101, was used to create a bifunctional catalyst by the immobilization of [C_2COOHmim][Cl] by a simple post-synthetic modification [190]. Likewise, a Zn containing IL, [(AIm)$_2$][ZnBr$_2$], was immobilized on MIL-101(Cr), leading to a combination of various active sites: Zn^{4+} and Cr^{3+} Lewis acid sites, nucleophilic Br, the amino groups, and ternary N sites acting as Lewis bases.

To investigate the effect of various preparation methods, [2-AeMIM][Br] was immobilized on MIL-101(Cr) by two approaches: via covalent bonds and via coordination bonds [193]. Although no significant difference was observed for the catalytic performance of these composites, a great difference was observed in their recyclability. The weak coordination bond between the amine group of the IL with Cr^{3+} sites in the MOF was responsible for the low stability of the composite prepared via coordination bonds. Another example for functionalization of MOFs with ILs by both covalent and coordination interactions was the incorporation of [CBMIM][Br] to UiO-66-NH_2 by amidation and [SPMIM][Br] to UiO-66-NH_2 by –NH_2 and –O_3H_S interaction [180]. The addition of [SPMIM][Br] by –NH_2 and –O_3H_S interaction was found more effective in terms of the catalytic activity for the cycloaddition reaction.

In general, esterification, transesterification, and simultaneous esterification/transesterification reactions are performed for biodiesel production, where transesterification is the most common method [195,198,206]. Several IL/MOF composites exist to obtain heterogeneous catalysts having Lewis/Bronsted acid sites. For example, to obtain a composite with both Bronsted and Lewis acidic sites, sulfonated ILs (acidic ILs (AILs)) were introduced into a Keggin-type polyoxometalate (POM) acid-functionalized MOF to form the MOF-supported POM-based IL catalyst (AILs/POM/UiO-66-2COOH composite) [200]. An increased acidity could be obtained by the formed composite, providing a high performance for the simultaneous transesterification and esterification reaction of low-cost acidic oils. The composite performed markedly higher than the parent MOF (UiO-66-2COOH). By a similar approach, phosphomolybdenum-based sulfonated ILs functionalized MIL-100(Fe) composites (AIL/HPMo@MIL-100(Fe)) were synthesized for their application in transesterification-esterifications of acidic oils [196]. Moreover, Han and coworkers showed that immobilizing 2-mercaptobenzimidazole ILs with electron-rich –SH groups on MIL-101(Cr) via S–Cr coordinate bonds leads to high activity and stability for the esterification of oleic acid with methanol compared to the parent MOF [197].

Besides various examples showing the utilization of IL/MOF composites as efficient catalysts in the cycloaddition reaction of CO_2 and epoxides, these composites are also good-performing catalysts for oxidative desulfurization. [PrSO_3HMIm][HSO_4] was immobilized on MIL-100(Fe) by the wet-impregnation method, which was used for the oxidative desulfurization of dibenzothiophene, thiophene, and benzothiophene using H_2O_2 as the oxidant [203]. The composite provided more sulfur removal compared to the pristine IL. Qi and coworkers prepared an IL-functionalized MOF by post-synthetic ligand exchange between the MOF and monocarboxylic functional IL which they used for the oxidative desulfurization of dibenzothiophene while utilizing H_2O_2 as the oxidant [201]. The dibenzothiophene adsorption capacity results of the pristine UiO-66 and composite showed that the latter provided a much better adsorption capacity, which was attributed to the negative charged sulfur in dibenzothiophene and positively charged imidazole ring. A polyoxometalate-based MOF was prepared by using a carboxyl functionalized IL, [MIM(CH_2)$_3$COOH][Cl], as a bridge between UiO-66 and phosphotungstate which performed markedly better for the oxidative desulfurization of dibenzothiophene using H_2O_2 as the oxidant than pristine UiO-66, phosphotungstic acid, and the physical mixture of UiO-66 and heteropolyanion-based IL [202].

IL/COF composites are promising catalysts, allowing the incorporation and dispersion of various active sites similar to the IL/MOF composites. A recent review article addresses these IL/COF composite catalysts by providing extensive data regarding their catalytic performances for various reactions [102]. Hence, we provide only a summary of several of these IL/COF composites used in catalysis. For instance, incorporating an allyl-imidazolium-based IL into acylhydrazone-linked COF (COF-IL) leads to a highly active composite for the cycloaddition of CO_2 and styrene oxide without any solvent or co-catalyst under mild

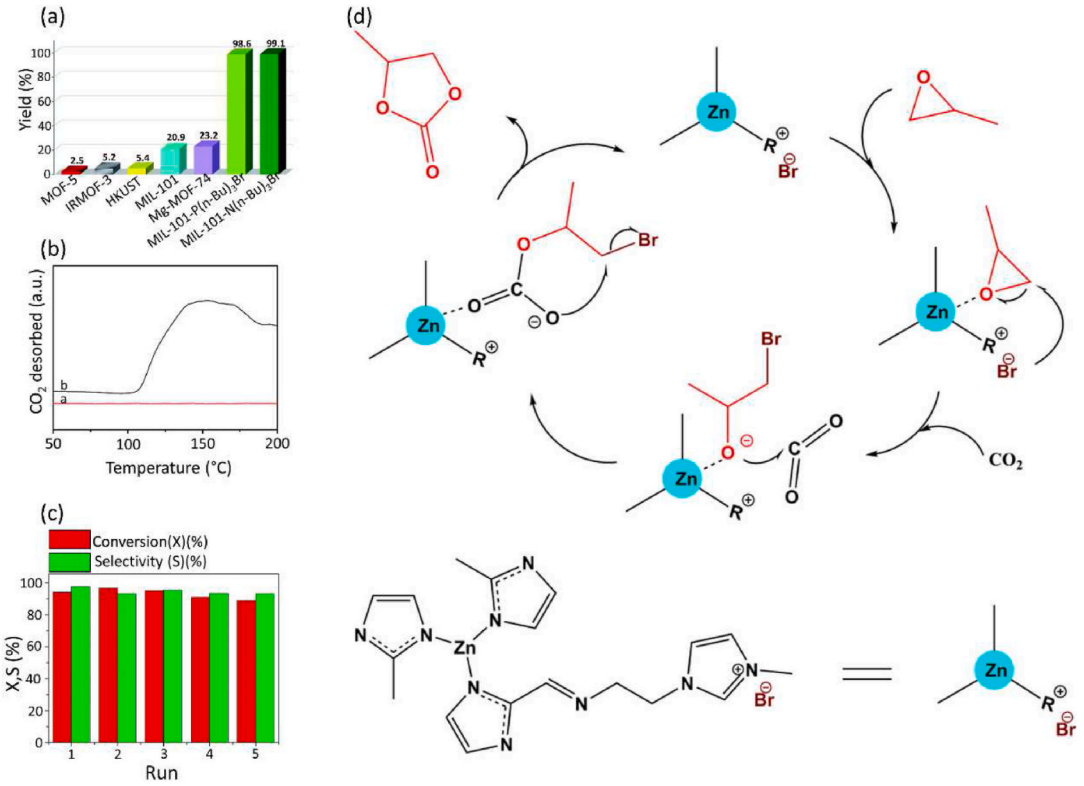


Fig. 9. (a) The yield of propylene carbonate by the cycloaddition of propylene oxide and CO_2 for quaternary ammonium salt (dark green) and phosphorus salt (light green) IL functionalized MIL-101(Cr) composites in comparison with various MOF catalysts. Reaction conditions (solvent-free and co-catalyst-free): Propylene oxide (30 mmol), catalyst (0.27 mmol), CO_2 pressure (2 MPa), reaction temperature (80 °C), and reaction time (8 h). Reproduced with permission [183]. Copyright 2015, The Royal Society of Chemistry. (b) CO_2-TPD profiles of MIL-101(Cr) (red) and IL-functionalized counterpart (black, MIL-101-IMBr-6). Reproduced with permission [188]. Copyright 2018, Elsevier. (c) The recyclability of MIL-101-IMBr-6. Reproduced with permission [188]. Copyright 2018, Elsevier. (d) Proposed mechanism for the cycloaddition of CO_2 and epoxides over [AeMIM][Br] grafted aldehyde-functionalized ZIF-8. Reproduced with permission [179]. Copyright 2021, Elsevier. (For interpretation of the references to colour in this figure legend, the reader is referred to the Web version of this article.)

conditions [15]. The catalytic performance was attributed to the high imidazolium content and the large pore size of the composite. Likewise, an imidazolium salt functionalized COF obtained by the post-synthesis method was used for the solvent-free and co-catalyst-free cycloaddition of CO_2 and propylene oxide [204]. The IL/COF composite provided 50-times higher performance in terms of turnover number compared to the best-performing metal-free COF catalyst for the cycloaddition reaction. The $[Br]^-$ anion of the IL and high concentration of imidazolium cations led to highly dispersed multifunctional active centers in the pores of the COF, resulting in high performance. This imidazolium salt functionalized COF also provided a catalytic activity for the reductive N-formylation of amines with CO_2. Another IL/COF composite tested for the formylation reaction was obtained by grafting [Et_4NBr] on a COF by post-synthetic modification [207]. The resultant composite provided a high CO_2 sorption capacity accompanied by high catalytic performance for the formylation of amines with CO_2 and phenylsilane. An acid-base neutralization reaction was used to graft imidazolium salts on a COF, which provided enhanced catalytic performance for the Knoevenagel condensation reaction and the CO_2 cycloaddition with epoxides [208].

IL/MOF and IL/COF composites are efficient catalysts for various reactions providing enhanced catalytic performance compared to bulk IL and pristine MOFs or COFs. The incorporation of ILs with a variety of MOFs or COFs provides significant flexibility in combining different types of active sites within the composite. Regarding the synthesis of composite catalysts, the immobilization of ILs offers a simple route for synthesis. In contrast, the grafting of ILs is an effective method for hindering the leaching of the IL and offering structural stability. Most of the presented studies focus on incorporating a single IL into MOF or COF for its catalytic performance testing; however, it would be worth investigating the effect of structural factors of the IL on the catalytic performance.

IL/zeolites. Zeolites, another essential crystalline molecular sieve material, are the most successful catalysts in the chemical industry owing to their high stability, strong acid/base properties, and excellent selectivity for many reactions [209]. Hence, based on the unique properties of ILs, combining zeolite and IL as a catalyst can provide better catalytic performance, such as catalytic cyclization of CO_2 with epoxides. Typically, the acidic sites in zeolite are not conducive to CO_2 activation [210], therefore the acid/base groups of ILs may significantly affect the catalytic activity. Guo and coworkers grafted [AeMIM][Zn_2Br_5] on 3-chloropropyltriethoxysilane modified MCM-22 [211]. The amino, Br^- ion, and Lewis acid sites in the catalyst played essential roles in promoting the cycloaddition of CO_2 and propylene oxide to propylene carbonate. On the contrary, the catalyst activity and selectivity of the other two ILs containing hydroxyl and carboxyl groups are significantly reduced. Similarly, Srivastava and coworkers reported that the simultaneous participation of surface silanol groups and high basicity of the Basic-Nano-ZSM-5-PrMIM-OH were accountable for the excellent activity in the cycloaddition of CO_2 and epichlorohydrin [210].

The introduction of ILs can improve the stability of zeolite catalysts. Tangestaninejad and coworkers added [2-AeMIM][Br] to hierarchical ZSM-5 as a catalyst for inserting CO_2 into epoxide where the catalytic activity did not decrease during the 6-cycle experiment, while the activity of the pure hierarchical ZSM-5 decreased by 60% [212]. It is worth noting that the addition of IL did not affect the conversion and selectivity. Although not mentioned in the article, the IL may likely promote the desorption of products or intermediates and improves the stability of

the catalyst. Besides, some reactions can be achieved by using the difference in the affinity of ILs for gas molecules. Li and coworkers analyzed the performance of the CaX zeolite supported [EMIM][BF_4] catalyst in the acetylene hydrochlorination and found that the Ca^{2+} sites in CaX adsorb HCl and [EMIM][BF_4] mainly adsorbs C_2H_2 during the reaction, and the reaction occurs at the interface of the two phases [213]. Based on the excellent solubility of KA oil (a ketone-alcohol oil mixture consisting of cyclohexanol and cyclohexanone) in [C_6MIM][HSO_4], the [C_6MIM][HSO_4]/Co/ZSM-5 catalyst prepared by Shao and coworkers was used for the aerobic oxidation of cyclohexane to KA oil and achieved extremely high selectivity without excessive oxidation [214]. Therefore, it can be considered that combined with the excellent thermal stability and porous characteristics of zeolites, IL/zeolite catalyst can provide the possibility of application in more valuable reactions.

IL/porous carbonaceous-materials. ILs are often used to disperse/anchor active metal components loaded on porous carbonaceous-materials [26,215]. However, based on the unique properties of different carbonaceous-materials and ILs, IL/carbonaceous-material catalysts also show potential for many reactions. IL/carbonaceous-material catalysts are also mainly used for coupling CO_2 and epoxides. Using carbon nanotubes grafted with imidazolium-based ILs for the cycloaddition reaction of allyl glycidyl ether and CO_2 showed that the increase of the anion radius ($I^- > Br^- > Cl^-$) improves the conversion from 50.3 to 56.2%; while the length of the alkyl chain in the imidazole group had little effect on the catalytic activity [76]. Likewise, Li and coworkers analyzed the mechanism of graphene oxide (GO) supported imidazole IL catalysts for similar reactions [216]. The results showed that the propylene oxide molecule was initially activated by the hydroxyl group on the GO surface, and then the halide anion in the IL promoted the ring-opening to accelerate the subsequent reaction, and the radius of the halide ion can promote this process (the conversion increased from 68.3% on GO-[SmIm][Cl] to 96.4% on GO-[SmIm][I]). Besides, Baj and coworkers found that in the quaternary ammonium chloride supported by carbon nanotube catalytic system, the length of the spacer group used for quaternary ammonium salt grafting (long and short spacer groups are more active than the intermediate length) significantly affected the catalytic activity [217].

In addition to the typical reaction types described above, other reactions using IL/carbonaceous-material catalysts have also been reported recently, such as the synthesis of 3,4-dihydro-2H-naphtho[2,3-e][1,3]oxazine-5,10-dione [218], oxidative desulfurization [219,220], and synthesis of 3-amino alkylated indole [221]. In summary, the porous carbonaceous-materials as supports have achieved great success in anchoring precious metals [222–224] and preparing high loading of atomic dispersion catalyst [225], and the introduction of adjustable ILs will provide more abundant applications for porous carbonaceous-materials based catalysts.

4.4. Ionic conductivity

With the increasing attention for the nanoconfined ILs, more studies focus on integrating IL/porous material composites to batteries and electrochemical systems. For instance, in the very first attempt to incorporate ILs into MOFs for ionic conductivity modifications, EMI-TFSA was incorporated into ZIF-8, and especially at low temperatures, IL/MOF composite exhibited a better ionic conductivity compared to that of bulk EMI-TFSA as given in Fig. 10(a). The sudden decrease in the ionic conductivity of bulk ILs due to freezing is a common challenge for IL usage in conductive systems [226,227]. Several studies focused on tackling this problem by increasing the number of contacts between IL molecules and a host material as in the case of loading ILs into ZIF-8 pores [29,228,229]. Subsequently, for mentioned studies, a phase change for Li-doped EMI-TFSA was observed, whereas Li-doped EMI-TFSA/ZIF-8 composites preserved their structure due to the nano-size effect in the micropores arising from the IL addition. Despite its ability to function better at low temperatures, the Li-doped IL/MOF sample showed two orders of magnitude lower conductivity than Li-doped IL above 250 K because of the decrease in self-diffusion coefficients of Li^+ ions in the composite [229].

Although Li doping to IL has some challenges reported in the context of low Li and counterion dissociation rates which result in low diffusion coefficients and low ionic conductivities [229,231], the boosting effect of Li-doped IL on ionic conductivity compared to host material was substantiated with several studies involving different MOF structures such as MOF-525(Cu) [30], HKUST-1 [7,232], UiO-66 [233], MIL-101 [234], and ZIF-90-NH_2 [230]. Li-doped IL addition did not only enhance the Li^+ transport by promoting uniform ion distribution but also improved the operation endurance of composites by allowing them to operate under varying temperatures despite causing a decrease in the thermal decomposition temperature of composites. As most of the lithium-ion batteries suffer from the weak interactions between the electrodes and the electrolyte, it can be deduced from all these studies that the incorporation of Li-IL into MOF structures can make the ion-conducting network stronger, enhance the interaction across the cathode, hence increase the ionic conductivity as it can be seen in Fig. 10 (b–c) with two different materials as mentioned above.

Lithium conduction is a hot topic for research since lithium batteries have a vast application area, but sodium conduction-based electrical storage systems are also being investigated as an alternative. As the pioneering work on IL incorporation into MOFs for Na^+ conduction, five different ILs ([EMIM][BF_4], [EMIM][NTf_2], [BMIM][NTf_2], [BMIM][PF_6], and [C_4Py][BF_4]) with their matching Na^+ salts ($NaBF_4$, $NaNTf_2$,

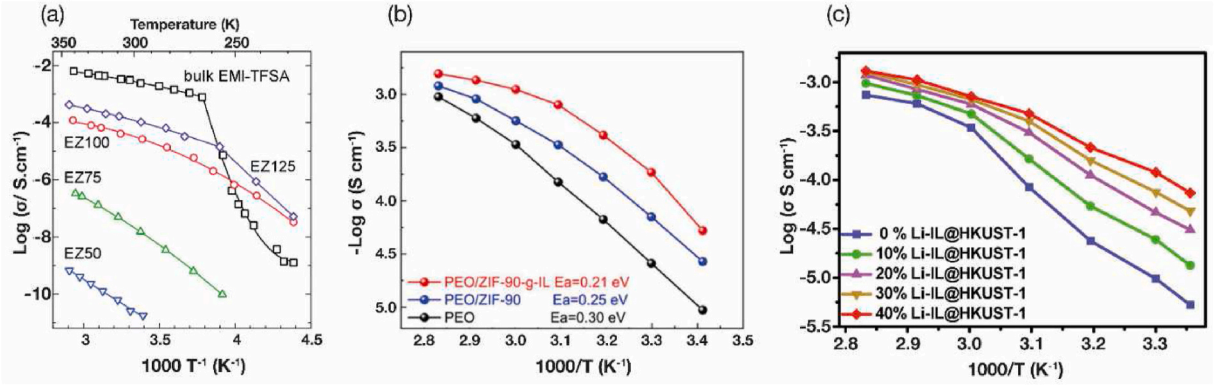


Fig. 10. (a) Ionic conductivities of IL incorporated composites of ZIF-8 upon heating (as 50% IL loading corresponds to EZ50). Reproduced with permission [29]. Copyright 2015, The Royal Society of Chemistry. (b) Ionic conductivities of solid electrolytes with PEO, PEO/ZIF-90, and PEO/ZIF-90-IL. Reprinted with permission [230]. Copyright 2021, Elsevier. (c) Ionic conductivities of composite polymer electrolytes containing IL-loaded HKUST-1 with respect to temperature. Reproduced with permission [7]. Copyright 2020, American Chemical Society.

and $NaPF_6$) were injected into the pores of MIL-101-SO_3Na to synthesize Na^+ conducting composites [235]. It was reported that excessive IL loading could cause IL leakage from the composite, but owing to the addition of appropriate salts, more IL could be loaded to the composite without the risk of leakage, which resulted in improved conductivity. There are other examples of IL-doped composites with compatible salt solutions, which suggest that the ionic conductivity of a composite can be improved by not solely incorporating ILs into MOFs but also by tuning the ILs with suitable salts or ions [236–238]. Also, the optimal amount of IL loading to MOFs is another important parameter to consider since high pore filling might result in decreased ionic conductivity as it was investigated by several groups [239–242]. An excess amount of IL embedded in the MOF structure was found to be inducing density fluctuation of ions, hence causing a blockage in pore openings [239]. Parallel to the IL loading, the cation and anion contribution to ion movement within pores was reported to be crucial via MD simulations. Experimental results combined with MD simulations illustrated the interactions between MOFs and ILs through a nanoscopic viewpoint. When IL loading amount was comparatively low, anion and cation parts of the IL were observed to be sharing the free space of host material independently but for the higher amount of IL loadings, they were found to be sharing overlapping conduction pathways which resulted in an inhomogeneous distribution of IL's components, hence a decrease in the conductivity [239,242].

As the electrochemical sensitivities and ionic conductivities of COFs are limited [40], they are usually combined with conductive materials, such as ILs before integrating the composites into sensors [243], or in some studies they are directly mixed with ILs [244]. Very recently, the enhancing effect of incorporating ILs in COFs on proton conductivity was illustrated for the first time with an imidazolium-based IL, [BMIM][BF_4] impregnated into COFs which later integrated to a membrane. Using IL created an ample amount of proton hopping sites resulting in two-times higher conductive composites compared to composites without IL [245]. Similar to COFs, the ionic conductivity of zeolites is restricted to cases where adsorption of gases or water on zeolite surface is possible [246]. Therefore, in some studies, they were functionalized with ILs to maintain sufficient proton conductivities for proton exchange membrane (PEM) fuel cells, while their addition did not change the proton permeability significantly [247–250].

Apart from MOFs, COFs, and zeolites, graphene, due to its high surface area and high electrical and thermal conductivity, and graphene oxide (GO), due to its strong mechanical properties, high surface area, and high ionic conductivity, attract attention as appealing candidates for supercapacitors and other electrochemical devices [251,252]. ILs can be used as electrolytes inside the graphene electrodes [39,253–255], or they can be used in the preparation of carbon-based electrodes [44,254,256–259]. They are proven to be efficient tools for improving the dispersion in nanocomposites when agglomeration is a problem, such as the cases where graphene sheets or carbon nanotubes (CNTs) are used [39,254,256,259].

Lastly, with the addition of suitable ILs to the host materials for the synthesis of IL/membrane composites, the ionic transport mechanisms of polymer-matrix membranes can be modified, resulting in more conductive membranes [260–264]. Generally, the proton conductivities of existing PEMs tend to decrease with increasing operating temperature. However, the IL incorporation to polymer matrix is found to enhance the thermal stability of the IL/membrane composites and sustain high conductivity values [260,262,264]. Although in most cases conductive path within membrane matrix becomes stronger with increased IL loading [265,266], some cases exemplify that after some IL loading, the ionic conductivity of the composite starts to decrease due to the interference of non-confined IL on composite with the path of proton transfer [201,267,268].

Considering all these studies, we can point that IL incorporation into appropriate hosts is proven to be a promising method in terms of enhancing the ionic transportability of composite materials by unlocking a wide range of opportunities, such as uniform dispersion of conductive ions, increased contact area for the conduction pathway, and advanced operation temperatures. Besides all the enhancements that IL incorporation provides to a composite, several challenges remain to be addressed on IL incorporation, such as leakage in the form of physical vulnerability and the adjustment of enough IL loading. Optimizing these parameters with respect to operation conditions has the potential to further improve the conductive performances of IL-incorporated composites.

5. Computational studies

Several porous materials, such as MOFs, COFs, and zeolites, have been synthesized up to date, and identifying the best candidates for the desired application is crucial to obtain promising results and outperform conventional materials. However, the performance analysis of thousands of porous materials is unrealistic by experimental methods. Computational tools provide valuable assistance in screening a large number of materials to predict the top performing materials for task-specific purposes. Quantum chemical methods are mainly used for the quantitative determination of selective adsorption behaviors of porous materials, such as elucidating the preferential adsorption sites, calculating the binding energies between gases and materials, and calculating the ion pair energy between the anion and the cation of the IL [269]. In addition, electronic structure properties, such as HOMO, LUMO, hardness, softness, ionization potential and electron affinity [270–273], vibrational spectra, dipole moment, volume, and polarizability of ILs and porous materials [11,274,275] can also be obtained via DFT calculations. These properties can offer opportunities for representing IL molecules in deeper analysis of big data through machine learning algorithms. Moreover, one can gain mechanistic insights for the elucidation of decomposition, catalytic conversion, and chemical adsorption mechanisms of ILs, porous materials, and their composites [276–281]. In addition, these calculations can complement the experimental data in the way of identifying the complex spectroscopic features measured experimentally. It would be noteworthy to emphasize that, since these calculations are computationally very expensive, especially for the systems containing many atoms, they cannot be routinely applied to MOF-like structures.

DFT is a widely used method for describing the electronic properties of composite structures due to its computational attractiveness and accuracy. However, the accuracy of the results strongly depends on the choice of the functional used. Medium to long-range dispersion interactions are poorly described in local exchange-correlation functionals such as Perdew-Burke-Ernzerhof (PBE) [282] and the Becke-three-parameter-Lee-Yang-Parr (B3LYP) [283,284]. For example, many porous materials contain aromatic organic linkers that form aromatic-aromatic interactions. This type of non-covalent interactions within the framework has significant contributions to the adsorption dynamics and reactions taking place in the active sites. Therefore, non-bonded interactions should be treated carefully. Recently, the task of functional selection was investigated extensively by Prakash et al. [285]. Well-known DFT methods were tested with and without dispersion corrections by comparing the calculations with the data taken from the experimental crystal structure of the ZIF-8 framework. BLYP and PBE methods, including Grimme's D2 correction [286] predicted the cell parameters with only 0.3% deviation from the crystal structure. Structural changes upon different kinds of IL loadings were further analyzed, and it was shown that BLYP-D2 functional reproduced the experimental findings. The geometric analysis revealed that the nanopores of hydrophobic ZIF-8 stabilize the hydrophobic IL molecules. Thus, ILs and MOFs with similar hydrophobicity (like-like pairs) are suggested to be used together for the design of more stable composites. However, it should be noted that the performance of these functionals is not guaranteed to work similarly well for other materials. Thus, we recommend that several benchmark studies should be performed to find the most

appropriate level of theory for each system.

The choice of the periodic or cluster model to be used is another challenge when performing DFT calculations. The application of periodic boundary conditions is very demanding in terms of computational cost and it is usually used in binding energy calculations [287]. In cases where the phenomena of interest are localized (adsorption, gas separation, catalysis, etc.), using molecular cluster models representing the active part of the porous material appears to be an appropriate choice, since they are computationally less demanding. It is important to note that the cluster should be protonated or deprotonated to obtain charge neutrality to prevent errors arising from localized charge modulations. Abroshan and Kim [288] elucidated the structural stability of isoreticular MOF (IRMOF-1) upon confinement of ILs by modeling the nanoporous cavity of the IRMOF structure. The cluster model was constructed from a zinc oxide core (Zn_4O) coordinated by six formate (HCO_2) anions for DFT calculations. It was shown that the direct interactions of the anion of the IL deformed the structure by coordinating with zinc atoms. Regarding this finding, IRMOFs are not suggested to be used as support systems for ILs. Using the cluster model approach, most likely interaction sites of Cu-BTC were characterized by molecular electrostatic potential (MESP) isosurfaces, and the impact of [EMIM][ETS] on the structure of MOF was shown by the changes that occurred in the Cu–O distances and O–Cu–O angles of the pristine MOF and IL confined MOF [68]. The findings point out that the anions of the IL strongly coordinate with Cu atoms and occupy the open metal sites, which in return avoids the adsorption of water molecules from these sites. Finally, water molecules are directed to the smaller pores, and the extent of the degradation of the Cu-BTC by water adsorption is lessened.

The incorporation of ILs into porous materials changes the gas uptake and adsorption selectivity, and the reasons behind this have been a matter of debate for a long time. To explain the adsorption dynamics of a top performing MOF and IL/MOF composite for CH_4/N_2 separation, we recently performed DFT calculations on cluster models of SAHYAD03 and its [BMIM][SCN] composite [289]. The deep analysis of the pristine and IL complex structures showed that both of the gases prefer primarily to interact with triazole rings on the organic linkers rather than on the metal site, and when the IL is incorporated into the MOF, the adsorption sites for the gases are occupied by the IL molecules.

In cases where the adsorption sites are located on the linker atoms, representative cluster models should be ensured to be constraint to mimic the MOF environment. For this purpose, the atoms in the chemically active part of the model are allowed to be optimized, and the atoms in the rest of the structure are frozen. Using this approach, Mohamed et al. [290] selected CO_2 adsorption sites of ZIF-8 as cluster models for the quantum mechanics study, which were detected from snapshots of Monte Carlo simulations. By calculating the binding energies between CO_2-ILs and CO_2-ZIF-8, it was shown that the affinity of CO_2 for the ZIF-8 increases as the ILs are confined within the ZIF-8 since the number of interactions of CO_2 increases as well. Binding energy calculations indicated that [BMIM][$B(CN)_4$] is the most CO_2 selective IL among the tested ILs, whereas [BMIM][TCM] is the weakest. Most of the cases, the elucidation of the interactions between the IL molecules and the surface of the host material requires precise assignment of the spectroscopic features, which is very challenging. In this regard, DFT calculations can complement the experimental results by offering opportunities to identify the individual spectroscopic features at the atomic level. For instance, Kinik et al. [11] analyzed the interactions of the IL with the atoms of the ZIF-8 cage. The most stable DFT optimized geometry illustrates that the IL molecule lies inside the cage with the cation aligned parallel to the plane of the pore opening of the cage and anion aligned parallel to an imidazolium ring of ZIF-8. With the help of the band assignments done by the DFT calculations, the corresponding shifts in these features could be analyzed in detail. Accordingly, the red shifts on the IR features associated with the $[PF_6]^-$ anion's stretching frequencies indicate the weakening of the P–F bond due to the electron sharing between ZIF-8 atoms and the anion. This weakening in turn leads to weaker interactions with the $[BMIM]^+$ cation in consistence with the blue shifts observed on the IR features associated with the imidazolium ring.

In addition to the structural investigation studies of IL/MOFs, DFT methods can be applied to analyze the chemical properties. Determination of the thermal stability limits of the IL/MOF composites is important since hybrid materials are usually exposed to high temperatures in industrial processes. The stability limits of the bulk ILs or MOFs alone are insufficient to get insights about the composite's thermal behavior since the interactions between the IL molecules and MOF atoms have strong effects on controlling the structural integrity. Therefore, the development of mathematical expressions through Quantum Structure-Property Relationship (QSPR) analysis using the DFT descriptors can provide valuable information about the decomposition temperatures of these types of composites. For instance, Multiple Linear Regression models derived for the prediction of T'_{onset} of IL/CuBTC and IL/ZIF-8 have been shown to be useful and practical; by simply calculating molecular properties of 1,3-dialkylimidazolium based ILs (cation's CPK ovality, anion's HOMO energy, anion's CPK volume, and CPK area for IL/CuBTC; cation's dipole, anion's HOMO and LUMO energies, polarizability, and ZPE for IL/ZIF-8) with the B3LYP/6-31+G* level of theory, one can estimate the thermal decomposition temperatures of corresponding IL/MOFs, and thus, design novel composites thermally stable for any desired application [79].

CO_2 conversion through chemical fixation with epoxides by using MOFs as catalysts has been extensively studied, but the mechanistic conversion details remain mainly unraveled. The cycloaddition mechanism of CO_2 with propylene oxide (PO) in the presence of [TBAB]/MIL-101 [281] and [TBAB]/NTU-180 [291] were investigated by performing DFT calculations to gain insights into the catalytic activity of the IL/MOF binary systems. The high catalytic activity of IL/MOF complexes, which dropped the activation barriers from 48.7 to 14.4 kcal/mol for [TBAB]/MIL-101 and from 62.6 to 21.9 kcal/mol for [TBAB]/NTU-180, is attributed to the Lewis acidic copper sites which facilitate the ring-opening and the stabilization of the intermediates and transition states by the MOF.

Adsorption, selectivity, catalytic activity, and conductivity properties of the ILs and their porous material complexes are driven by specific intermolecular interactions such as hydrogen bonds, halogen bonds, π-π stacking, dipole-dipole, or van der Waals interactions. Therefore, a correct description of these interactions is vital for the rationalization of their behaviors. DFT calculations allow a high level of accuracy in evaluating the physical and chemical information of the materials at the atomistic level. Studies including DFT calculations should be expanded to design more effective IL/porous material complexes for any target application.

Molecular-level approaches are also crucial for investigating intermolecular interactions between ILs, materials, and adsorbates. The bulk ILs have layered surfaces, and the adsorption of the gases occurs by gas transfer through the interface. The solubility of a gas inside the bulk IL is generally calculated by COSMO-RS theory and Molecular Dynamics (MD) simulations. When the ILs are incorporated into porous materials, they disperse in the pores, and the interactions between the ions may be subjected to decrease or increase compared to the bulk phase due to the confinement effect induced by the support material [292]. ILs inside the porous material act as additional adsorption sites, and as a result, the solubility of the gases is different in bulk IL and in porous material than the composite material. In this sense, Grand Canonical Monte Carlo (GCMC) and Molecular Dynamics (MD) simulations provide significant assistance in discovering the most promising IL/porous material systems. The top performing adsorbents can be identified by computing several performance evaluation metrics such as adsorption selectivity and working capacity. Computational studies on IL-incorporated zeolites and carbon-based porous materials, such as zeolite templated carbon (ZTC) [293], carbon nanotube (CNT) [294], and CNT bundles [295,296], have been mainly performed for CO_2/N_2, and CO_2/CH_4 separation

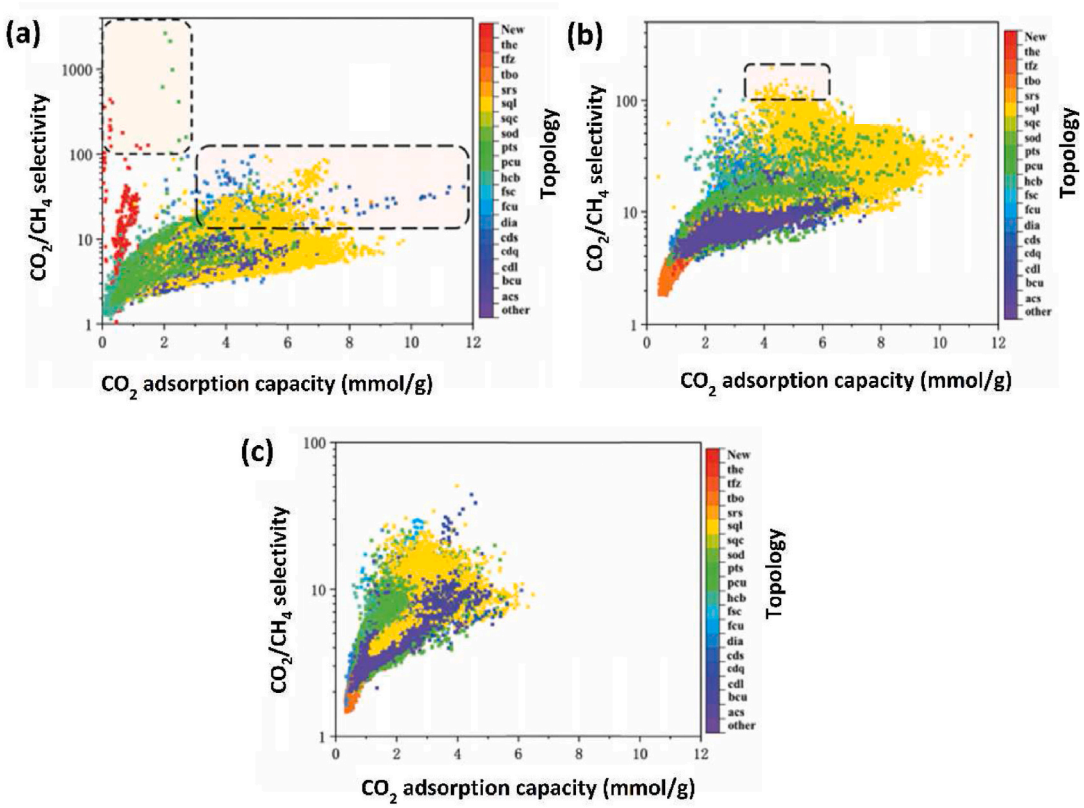


Fig. 11. Relationship between the CO_2/CH_4 separation performance and MOF topologies (a) pristine MOFs, (b) [MMIM][BF_4]/MOFs, and (c) [BMIM][Tf_2N]/MOFs. Reproduced with permission from Ref. [324].

and the adsorption selectivities of the composites are reported to be higher than their corresponding pristine materials. Although ZTCs, CNTs, and CNT bundles have advantages for IL incorporation, such as high surface areas and large pore volumes, their available adsorption sites do not offer strong electrostatic interactions to obtain high gas adsorption capacity and/or selectivity [297]. Therefore, other classes of porous materials, such as MOFs and COFs, were shown to be more suitable for IL incorporation. The majority of the IL/MOF computational studies use ZIFs [11,12,47,298–304], IRMOF-1 [37,298,305,306], Cu-BTC [307,308], and MIL-100(Fe) [309] to focus on the separation of various gas mixtures, including CO_2/N_2, CO_2/CH_4, CH_4/N_2, and H_2S/CH_4. The main reasons behind selecting these MOFs are related to their high surface area, good thermal and chemical stability, high adsorption capacity, and/or water resistance [310–312]. The existence of open metal sites in MOFs is also known to be effective for enhanced gas adsorption and separation [313]. However, all IL/MOF composites are not guaranteed to possess high-performance gas separation. For instance, a computational study demonstrated that incorporation of [BMIM][SCN] into MOF-74(Mg) resulted in a lesser extent of improvement in CO_2/N_2 and CO_2/CH_4 selectivities compared to other IL/MOF and IL/COF composites due to the competitive adsorption between anion of the IL and CO_2 molecules around the coordinatively unsaturated metal sites (CUS) of the MOF in spite of the formation of new adsorption sites created by $[SCN]^-$ anion for CO_2 [298]. Thus, the selection of the appropriate porous material and the IL is vitally important. Like IL/MOF composites, IL/COF composites have been examined in a number of studies [298,302,314] for gas separation applications. In one of these studies, flue gas separation performances of three IL/MOF (InOF-1, UiO-66, and ZIF-8), two IL/COF (COF-108 and COF-300), and one IL/single-wall carbon nanotube (SWCNT) composite were compared [302]. The CO_2/N_2 selectivities of IL/InOF-1 and IL/COF-300 composites were found to be comparable and significantly higher than other composites, indicating the great potential of IL/COF composites for gas separation applications.

When modeling the IL/porous material systems with computational tools, the porous material and the IL molecules are usually treated as perfect and rigid crystalline structures to reduce the computational costs. As a result, their distribution of accessible/inaccessible adsorption sites may differ from the experiments. A scaling factor, which is the ratio of experimental pore volume to theoretical pore volume or a pressure-dependent function, can be used, if needed, to match the gas uptakes obtained from GCMC simulations with those measured experimentally to minimize the differences between real and simulated crystal structures [307,315–317].

The main outcomes of the studies mentioned above reveal the presence of significant improvements in adsorption selectivities, particularly at low pressures upon IL incorporation, and several of them demonstrate the importance of anion selection, which is known to control an IL's gas solubility [318,319] to obtain promising IL/porous material composites. For instance, incorporation of five different ILs (combinations of $[EMIM]^+$ with different anions, $[BF_4]^-$, $[SCN]^-$, $[NO_3]^-$, $[PF_6]^-$, $[Tf_2N]^-$) into CuBTC using GCMC simulations showed that the composites containing $[SCN]^-$ and $[Tf_2N]^-$ have the highest and the lowest heat of adsorption values, respectively [308]. The amount of adsorbed CO_2 decreases as the anion becomes bulkier, proving that the anion type has an effect on CO_2 adsorption. In another computational study [320], the effect of anion type was investigated for [BMIM][X]/Cu-TDPAT composites, where [X] represents any of the following anions: $[BF_4]^-$, $[Tf_2N]^-$, $[Cl]^-$, and $[PF_6]^-$. The highest isosteric heat of adsorption (Q_{st}) value was obtained from the [BMIM][Cl]/Cu-TDPAT composite, which has the smallest anion size. This was attributed to the effect of the size of the anions on the distribution of ILs inside the pores of Cu-TDPAT.

Computational studies have also been performed for examining membrane-based CO_2/N_2 and CO_2/CH_4 separation in IL/MOF and IL/MOF/polymer composites. Incorporation of [BMIM][SCN] into IRMOF-

1 [305], ZIF-71, and Na-rho-ZMOF [321] showed that although CO_2 diffusivities decreased due to the occupation of the free pore volume by ILs, their permeabilities and membrane selectivities were higher than polymeric membranes. In another computational study [299], [BMIM][BF_4] was added as a wetting agent between the polymer and ZIF-8 to avoid interfacial defects, which are known to reduce adsorption capacities and selectivities [22,322]. The composite model system was represented by placing ZIF-8 at the center of the simulation cell, locating two 6FDA-durene polymer layers on the sides, and then filling the IL inside the cell, which describes the interface of the MMM for identifying gas transport mechanisms and interactions between the gases and the composite. The thickness of the ZIF-8 layer in the composite system is close to 6.4 nm, and the polymer region had a thickness around 7–10 Å. The IL incorporation resulted in enhanced selectivity and permeability, which enabled the IL/ZIF-8/6FDA-durene composite membrane to surpass the upper bound.

The success of the aforementioned studies guided the researchers to screen the experimental and hypothetical MOF databases to identify the top-performing IL incorporated MOF composites. An HTCS study [323] for the CO_2/N_2 separation performances of synthesized MOFs and their [BMIM][BF_4]-incorporated composites revealed that the decrease in pore sizes and porosities upon IL incorporation has a more pronounced effect on MOFs which have narrow pores and low porosities, resulting in higher CO_2/N_2 selectivities. In another HTCS study [324], [MMIM][BF_4] and [BMIM][Tf_2N] were incorporated into a set of hypothetical MOFs to examine their CO_2/CH_4 separation performances. In addition to the influence of pore size, the topology of the MOFs was found to be a key factor in determining promising IL/MOF composites, as shown in Fig. 11. CO_2 adsorption capacities and CO_2/CH_4 selectivities of [MMIM][BF_4]/MOF composites were found to be significantly higher than those of [BMIM][Tf_2N], demonstrating the importance of the selection of IL to have promising results. These studies show the importance of computational screening to direct the experimental efforts to highly promising materials and to assist researchers in designing new IL-incorporated materials with exceptional performance for various applications.

6. Summary and outlook

ILs are one of the promising agents to modify the physicochemical properties of a pristine host material. In this review, we highlighted the promising aspects of IL/porous material composites where the structural dynamics of pristine material are tuned by the addition of ILs. We examined the field of IL/porous material composites to an extension of their preparation methodologies, characterization techniques, and application areas. IL incorporation enhances the performance of pristine materials in various applications, including gas adsorption and separation, catalysis, liquid-phase adsorption and separation, and ionic conductivity. These enhanced performances were explained by the interactions between the IL and the porous materials. Both experimental and computational studies were discussed to gain more in-depth insight into the possibilities for different types of IL/porous material composites. There are potential limitations that affect the performance of IL/porous material composites, which were addressed below, together with our suggestions for future directions in the field.

Selecting appropriate preparation technique: There are various *in-situ* and post-synthesis modification techniques to prepare IL/porous material composites. Hence, choosing a task-specific preparation technique is significant. The mechanism and strength of the molecular interactions between IL and porous materials dramatically change with different *in-situ*/post-synthesis techniques, resulting in completely different IL/porous material composites in terms of both characteristic and performance measures. For instance, due to steric hindrance, relatively large ILs may not enter the zeolite cages, which requires an *in-situ* synthesis method, such as ship-in-a-bottle, to encapsulate IL molecules in the cages. Moreover, during ionothermal synthesis of IL-based hybrid MOFs, several studies reported structures with only one constituent of IL while the other constituent remained in the solution to maintain surface neutrality of the resulting hybrid material [33,42,48]. For this synthesis technique, ILs' desired properties cannot be produced within the hybrid material due to the lack of control over the final structural design. Therefore, in the case of MOFs, the usage of post-synthesis techniques to incorporate IL will be more beneficial and flexible in terms of taking advantage of IL's desired properties, such as gas solubility and ion mobility. In contrast, for negatively charged zeolite structures, post-synthesis techniques yield composites containing only the cation part of IL, where the anion part remains in the solution [325]. Thus, the structural integrity of the ILs is generally lost in such materials. Accordingly, a detailed evaluation of the advantages and disadvantages of the preparation techniques is crucial for further research studies.

Rational design of IL-porous material composites: There are limitless combinations for IL/porous material composites owing to the high number of ILs available. In the case of rational design, the determination of newly formed interactions and their effects on the performance should be elucidated in detail. By understanding the effect of the specific functionalization on desired performance measures, appropriate IL and porous material combinations can be made. For example, the selectivity of materials towards a particular molecule can be directly adjusted and enhanced by the rational selection of IL-porous material combination. Many IL/porous material composites have been examined so far, but it is still not quite sufficient compared to the theoretical number of IL-porous material combinations. In this aspect, computational studies can provide opportunities for large-scale screening for IL-containing porous hybrid materials and their performance of desired applications.

Thermal and chemical stability of IL/porous material composites: Another aspect to be considered for future research is the thermal and chemical stability limits of composites at elevated temperatures/pressures. In most cases, IL/porous material composites have new characteristics compared to their parent constituents, resulting in lower thermal stability limits due to newly formed interactions between IL and porous material. However, most industrial processes require moderately high temperature and/or pressure conditions. Hence, developing porous material composites with adequate stability limits is crucial for their usage and should be investigated further by taking different IL/porous material composites into account. Moreover, corresponding recyclability or reusability concept of these materials is mostly overlooked in the literature. It is crucial to understand the effect of the application on structural integrity of the composite as it will be important while evaluating the performances. Therefore, reported performance data on IL-incorporated composites should also include reusability of these materials at least up to multiple cycles.

Fundamental understanding of the structural effects of the individual constituents of the composites on performance: Structural properties of IL containing hybrid materials, such as pore size and shape, porosity, surface area, stability, flexibility, crystallinity, and morphology, are directly related to the those of IL and porous material, which can be altered by functionalization methods. Various studies focused on these structural effects by modifying the porous materials or ILs by functional group addition, thermal treatments, changing the metal nodes or linkers, polarity, and hydrophobicity/hydrophilicity. For each case, the structural change affects the performance measures, either causing a different interaction mechanism between the IL and the porous material or a change in the position of IL in the resulting hybrid material. In gas-phase/liquid-phase adsorption and separation applications, performance efficiencies are changing with newly formed interactions between IL and porous material due to the blockage of the existing adsorption sites or the opening of the new ones. Likewise, for catalysis applications, many studies showed the advantage of combining various active sites from the IL and porous material to obtain multifunctional catalysts, as well as adjusting the reactant or product concentration around the active sites. ILs contribution to ionic conductivity includes maintaining the ion mobility within the host materials and allowing them to operate at a variety of conditions, such as higher/lower

temperatures, due to enhanced thermal and mechanical stability. Hence, to benefit from the IL incorporation, a fundamental level understanding of the interaction mechanism in composites and investigating the resulting effect on the performance measures are of great importance.

Testing IL/porous material composites for other gas separations: Currently, experimental studies of IL-porous material composites mostly focus on flue gas separation and natural gas purification (CO_2/N_2 and CO_2/CH_4) processes. However, it would be of great interest to explore the potential of these versatile materials in industrially important gas separation processes such as hydrocarbon separation (C_2H_2/C_2H_4, C_2H_2/CO_2, C_2H_4/C_2C_6), hydrogen separation (H_2/CO_2, H_2/CH_4, H_2/O_2, H_2/N_2, H_2/CH_4, H_2/CO), sulfur separation (H_2S/CH_4), and most importantly oxygen separation due to ongoing COVID-19 pandemic (O_2/N_2).

Applicability into real-life processes: The behavior of IL/porous material composites should be evaluated under various temperature, pressure, and humidity conditions with the exposure of different chemical environments mimicking the realistic application conditions to assess their applicability. Lack of investigations on different process conditions generates an important drawback for their real-life usage. Going from lab-scale to industrial pilot-scale is also required to assess the real-life efficiency of the process parameters. Therefore, the number of studies on the applicability, especially for the best-performing IL/porous material composites, should be extended for future usage. For instance, in the case of gas-phase adsorption and separation, most of the research in the field focuses on single-component gas adsorption experiments rather than mixture gas. However, in real-life processes, almost all process streams consist of gas mixtures having impurities. Therefore, the focus should be on mixture-gas experiments under industrial conditions. Accordingly, more research on potential adsorption processes, such as PSA, PVSA and TSA systems, is needed to widen the scope of investigation related with the applicability of composite materials. Moreover, from an operational cost perspective, the superior selectivity performance of IL-incorporated adsorbents can provide opportunities for lowering the cost. Currently, there are several case studies available on the operation costs of CO_2 and H_2 separation processes, which highlight the benefits of using highly selective "ideal" adsorbents, where "ideal" refers to the materials with high gas recovery, selectivity, energy penalty and productivity [326]. The lowest possible CO_2 avoided costs are reported for the adsorbents with superior CO_2 selectivity over specified gasses which further demonstrates the promising process implementation aspect of IL-incorporated composites [326,327]. For instance, in a case study, the cost of CO_2 capture was shown to reduce from US$49 per ton CO_2 avoided to US$30 with a hypothetical adsorbent which provides 3-times higher CO_2/N_2 selectivity compared to the conventional adsorbent [328]. Consequently, the improved selectivity offered by IL-incorporated composites provides opportunities for decreasing the operation cost. Likewise, IL-incorporated composite membranes have shown rapid development for CO_2 separation in the past few years. However, the applicability of these membranes at an industrial scale is still scarce due to their short lifetime. Industrial requirements can be achieved by utilizing different synthesis methods to fabricate thin-film composite membranes consisting of thin IL layer and by investigating their long-period life span under real conditions. In addition to these, the subject of material cost is highly overlooked in IL/porous material composites and should be carefully evaluated. Performance increase with increasing IL loadings for most applications, such as gas-phase and liquid-phase separation. However, the cost of ILs and porous materials, especially for the conventionally expensive MOFs, creates a significant limitation for future large-scale industrial usage. Thereby, further investigation on loading effect and task-specific modifications for IL and porous material is extremely important to obtain best-performing IL/porous material composites with lower IL loadings and lower material costs.

Combining experiments and simulations: Porous materials and ILs are simulated as rigid structures in computational studies. It would be useful to simulate a set of composites considering framework flexibility to reveal its effect on performance. Several force fields and charge assignment methods are used to describe the intermolecular interactions between porous materials, ILs, and guests. Comparing simulation results that utilize different force fields and charge assignment methods with the experimental data would be important to examine their impact on the outcome. We note that several performance evaluation metrics (i.e., selectivity, working capacity, regenerability, and permeability) obtained from the molecular simulations in addition to the structural properties (i.e., pore size, surface area, and porosity) are crucial to identify promising IL/porous material adsorbents and membranes among thousands of materials. In addition, quantum chemical methods provide insight into the interactions between the identified host material, IL, and adsorbates. Our literature review highlighted that only a few ILs had been incorporated into MOFs in large-scale computational screening studies [323,324], which indicates that the potential of IL/MOF composites has not been fully examined. In addition, experimental synthesis of identified promising real and hypothetical IL/MOF composites from the screening studies has not been achieved, and potential limitations include stability issues, non-applicability to real process conditions, and deviations between experimental and simulation results. Therefore, synthesis and testing of both real and hypothetical promising composites obtained from molecular simulations are important in directing research efforts and assessing their applicability to industry.

Combining various computational tools: Understanding the electronic structures and structure-function relationships of ILs and porous materials, and the interactions between the IL and the porous material by quantum mechanical and molecular-level approaches will enable researchers to incorporate different functionalities into the ILs and porous materials. Implementation of machine learning strategies by correlating chemical or physical descriptors (such as charge, HOMO/LUMO, hardness/softness, pore size, porosity, crystal structure, molecular weight, etc.) with the performance outputs create great opportunities for the generation of new composites [329,330]. Accordingly, data repositories for porous materials and ILs should be increased to build accurate and consistent machine learning models. Thus, besides structural information, gas adsorption, and diffusion data gathered from GCMC and MD simulations, the usage of DFT-derived representative and informative descriptors for defining the ILs and the porous materials would be very beneficial for predicting the distinct properties of these systems, which in turn offer a broad potential towards rational design.

Future advances in experimental and computational methodologies will provide a more in-depth insight into the great potential of IL-containing hybrid materials, and with time, we believe that these promising hybrid materials will evolve as alternative materials for various applications than their conventional counterparts.

CRediT authorship contribution statement

Ozce Durak: Writing – review & editing, Writing – original draft, Conceptualization. **Muhammad Zeeshan:** Conceptualization, Writing – original draft, Writing – review & editing. **Nitasha Habib:** Writing – review & editing, Writing – original draft, Conceptualization. **Hasan Can Gulbalkan:** Conceptualization, Writing – original draft, Writing – review & editing. **Ala Abdulalem Abdo Moqbel Alsuhile:** Writing – review & editing, Writing – original draft, Conceptualization. **Hatice Pelin Caglayan:** Conceptualization, Writing – original draft, Writing – review & editing. **Samira F. Kurtoğlu-Öztulum:** Writing – review & editing, Writing – original draft, Conceptualization. **Yuxin Zhao:** Conceptualization, Writing – original draft, Writing – review & editing. **Zeynep Pinar Haslak:** Writing – review & editing, Writing – original draft, Conceptualization. **Alper Uzun:** Writing – review & editing, Conceptualization, Writing – original draft, Supervision, Methodology. **Seda Keskin:** Writing – review & editing, Writing – original draft, Supervision, Methodology, Conceptualization.

Declaration of competing interest

The authors declare that they have no known competing financial interests or personal relationships that could have appeared to influence the work reported in this paper.

Acknowledgements

This study was funded by the Scientific and Technological Research Council of Turkey (TUBITAK) under 1001-Scientific and Technological Research Projects Funding Program (Project Number 114R093) and Koç University Seed Fund Program. S.K. acknowledges ERC-2017-Starting Grant. This study was also funded by the European Research Council (ERC) under the European Union's Horizon 2020 research and innovation programme (ERC-2017-Starting Grant, grant agreement no. 756489-COSMOS). The authors thank to the support of Koç University TÜPRAŞ Energy Center (KUTEM) and Koç University Surface Science and Technology Center (KUYTAM). The authors also acknowledge TARLA for the support in cooperative research.

Abbreviations

[APTMS][Ac] 3-(trimethoxysilyl)propan-1-aminium acetate
[$(Aim)_2$][$ZnBr_2$] bis 1-(3-aminopropyl)-imidazolium zinc bromide
[AeMIM][Br] 1-aminoethyl-3-methylimidazolium bromide
[AmPyl][I] 1-aminopyridinium iodide
[BMIM][Br] 1-butyl-3-methylimidazolium bromide
[BMIM][BF_4] 1-butyl-3-methylimidazolium tetrafluoroborate
[BMIM][NTf_2] 1-butyl-3-methylimidazolium bis (trifluoromethylsulfonyl)imide
[BMIM][PF_6] 1-butyl-3-methylimidazolium hexafluorophosphate
[BMMIM][PF_6] 1-butyl-2,3-dimethylimidazolium hexafluorophosphate
[BMIM][Ac] 1-butyl-3-methylimidazolium acetate
[BMIM][SCN] 1-butyl-3-methylimidazolium thiocyanate
[BMIM][CF_3SO_3] 1-butyl-3-methylimidazolium trifluoromethanesulfonate
[BMIM][$MeSO_3$] 1-butyl-3-methylimidazolium methanesulfonate
[BMIM][$MeSO_4$] 1-butyl-3-methylimidazolium methyl sulfate
[BMIM][$B(CN)_4$] 1-butyl-3-methylimidazolium tetracyanoborate
[BMIM][TCM] 1-butyl-3-methylimidazolium tricyanomethanide
[BMIM][$OcSO_4$] 1-butyl-3-methylimidazolium octyl sulfate
[BMIM][DCA] 1-butyl-3-methylimidazolium dicyanamide
[BMIM][DBP] 1-butyl-3-methylimidazolium dibutylphosphate
[Benz][Ac] benzimidazolium-1-acetate
[BSPy][HSO_4] 1-(4-sulfonic acid)-butylpyridinium hydrogen sulfate
[C_2MIM][NTf_2] 1-ethyl-3-methylimidazolium bis (trifluoromethylsulfonyl)imide
[C_2OHMIM][NTf_2] 1-(2-hydroxyethyl)-methylimidazolium bis (trifluoromethylsulfonyl)imide
[C_2COOHmim][Cl] 1-carboxyethyl-3-methylimidazolium chloride
[C_2COOHMIM][Cl] 1-carboxyethyl-3-methylimidazolium chloride
[C_4Py][BF_4] N-butyl-pyridinium tetrafluoroborate
[C_6MIM][Tf_2N] 1-hexyl-3-methylimidazolium bis (trifluoromethylsulfonyl)imide
[C_6mim][HSO_4] 1-hexyl-3-methylimidazolium hydrogen sulfate
[CBMIM][Br] 1-(4-carboxybutyl)-3-methylimidazolium bromide
[EMIM][Ac] 1-ethyl-3-methylimidazolium acetate
[EMIM][DEP] 1-ethyl-3-methylimidazolium diethylphosphate
[EMIM][CF_3SO_3] 1-ethyl-3-methylimidazolium trifluoromethanesulfonate
[EMIM][Tf_2N] or EMI-TFSA 1-ethyl-3-methylimidazolium bis (trifluoromethylsulfonyl)imide
[EMIM][BF_4] 1-ethyl-3-methylimidazolium tetrafluoroborate
[EMIM][SCN] 1-ethyl-3-methylimidazolium thiocyanate
[EMIM][Gly] 1-ethyl-3-methylimidazolium glycol
[Et_4NBr] (2-bromoethyl)-triethylammonium bromide
[HEMIM][DCA] 1-(2-hydroxyethyl)-3-methylimidazolium dicyanamide
[HMIM][BF_4] 1-hexyl-3-methylimidazolium tetrafluoroborate
[HOOCEMIM][Cl] 1-carboxyethyl-3-methylimidazolium chloride
IL[OH] basic ionic liquid
[MAcMIM][Br] 1-methylacetamido-3-methylimidazolium bromide
[MAcMBenzIM][Br] 1-methylacetamido-3-methylbenzimidazolium bromide
[MIM$(CH_2)_3$COOH][Cl] 1-carboxypropyl-3-methyl imidazole chlorine salt
[MMIM][BF_4] 1,3-dimethylimidazolium tetrafluoroborate
[MPIm][Br] 1-methyl-3-propylimidazolium bromide
[$PrSO_3$HMIm][HSO_4] 1-sulfopropyl-3-methyl-imidazolium hydrosulphate
[PrMIM][OH] chloropropyl-silylated imidazolium hydroxide
[$P_{6,6,6,14}$][NTf_2] trihexyl(tetradecyl)phosphonium bis (trifluoromethylsulfonyl)imide
[SPMIM][Br] 1-(3-sulfopropyl)-3-methylimidazolium bromide
[SmIm][I] 1-(trimethoxysilyl)propyl-3-methylimidazolium iodide
[SmIm][Cl] 1-(trimethoxysilyl)propyl-3-methylimidazolium chloride
[TETA][L] triethylenetetramine lactate
[VEIM][Br] 1-vinyl-3-ethylimidazolium bromide
[2-AeMIM][Br] 1-(2-aminoethyl)-3-methyl-imidazolium bromide

References

[1] K.N. Marsh, J.A. Boxall, R. Lichtenthaler, Room temperature ionic liquids and their mixtures—a review, Fluid Phase Equil. 219 (1) (2004) 93–98, https://doi.org/10.1016/j.fluid.2004.02.003.
[2] M. Zeeshan, V. Nozari, M.B. Yagci, T. Isık, U. Unal, V. Ortalan, S. Keskin, A. Uzun, Core–shell type ionic liquid/metal organic framework composite: an exceptionally high CO_2/CH_4 selectivity, J. Am. Chem. Soc. 140 (32) (2018) 10113–10116, https://doi.org/10.1021/jacs.8b05802.
[3] N.Y.M. Yusuf, M.S. Masdar, W.N.R.W. Isahak, D. Nordin, T. Husaini, E.H. Majlan, S.Y. Wu, S.A.M. Rejab, C.C. Lye, Impregnated carbon–ionic liquid as innovative adsorbent for H_2/CO_2. separation from biohydrogen, Int. J. Hydrogen Energy 44 (6) (2019) 3414–3424, https://doi.org/10.1016/j.ijhydene.2018.06.155.
[4] M. Zeeshan, K. Yalcin, F.E. Sarac Oztuna, U. Unal, S. Keskin, A. Uzun, A new class of porous materials for efficient CO_2. separation: ionic liquid/graphene aerogel composites, Carbon 171 (2021) 79–87, https://doi.org/10.1016/j.carbon.2020.08.079.
[5] K.B. Sezginel, S. Keskin, A. Uzun, Tuning the gas separation performance of CuBTC by ionic liquid incorporation, Langmuir 32 (4) (2016) 1139–1147, https://doi.org/10.1021/acs.langmuir.5b04123.
[6] K.M. Gupta, Y. Chen, Z. Hu, J. Jiang, Metal–organic framework supported ionic liquid membranes for CO_2 capture: anion effects, Phys. Chem. Chem. Phys. 14 (16) (2012) 5785–5794, https://doi.org/10.1039/C2CP23972H.
[7] Z. Wang, H. Zhou, C. Meng, W. Xiong, Y. Cai, P. Hu, H. Pang, A. Yuan, Enhancing ion transport: function of ionic liquid decorated MOFs in polymer electrolytes for all-solid-state lithium batteries, ACS Appl. Energy Mater. 3 (5) (2020) 4265–4274, https://doi.org/10.1021/acsaem.9b02543.
[8] S. Kavak, H. Kulak, H.M. Polat, S. Keskin, A. Uzun, Fast and selective adsorption of methylene blue from water using [BMIM][PF_6]-incorporated UiO-66 and NH_2-UiO-66, Cryst. Growth Des. 20 (6) (2020) 3590–3595, https://doi.org/10.1021/acs.cgd.0c00309.
[9] Q.-x. Luo, B.-w. An, M. Ji, J. Zhang, Hybridization of metal–organic frameworks and task-specific ionic liquids: fundamentals and challenges, Mater. Chem. Front. 2 (2) (2018) 219–234, https://doi.org/10.1039/C7QM00416H.
[10] F.W.M.d. Silva, G.M. Magalhães, E.O. Jardim, J. Silvestre-Albero, A. Sepúlveda-Escribano, D.C.S. de Azevedo, S.M.P. de Lucena, CO_2 adsorption on ionic liquid—modified Cu-BTC: experimental and simulation study, Adsorpt. Sci. Technol. 33 (2) (2015) 223–242, https://doi.org/10.1260/0263-6174.33.2.223.
[11] F.P. Kinik, C. Altintas, V. Balci, B. Koyuturk, A. Uzun, S. Keskin, [BMIM][PF_6] incorporation doubles CO_2 selectivity of ZIF-8: elucidation of interactions and their consequences on performance, ACS Appl. Mater. Interfaces 8 (45) (2016) 30992–31005, https://doi.org/10.1021/acsami.6b11087.
[12] B. Koyuturk, C. Altintas, F.P. Kinik, S. Keskin, A. Uzun, Improving gas separation performance of ZIF-8 by [BMIM][BF_4] incorporation: interactions and their consequences on performance, J. Phys. Chem. C 121 (19) (2017) 10370–10381, https://doi.org/10.1021/acs.jpcc.7b00848.
[13] H. Kulak, H.M. Polat, S. Kavak, S. Keskin, A. Uzun, Improving CO_2 separation performance of MIL-53(Al) by incorporating 1-n-Butyl-3-Methylimidazolium methyl sulfate, Energy Technol. 7 (7) (2019) 1900157, https://doi.org/10.1002/ente.201900157.
[14] Y. Xin, C. Wang, Y. Wang, J. Sun, Y. Gao, Encapsulation of an ionic liquid into the nanopores of a 3D covalent organic framework, RSC Adv. 7 (3) (2017) 1697–1700, https://doi.org/10.1039/C6RA27213D.

[15] L.-G. Ding, B.-J. Yao, F. Li, S.-C. Shi, N. Huang, H.-B. Yin, Q. Guan, Y.-B. Dong, Ionic liquid-decorated COF and its covalent composite aerogel for selective CO_2 adsorption and catalytic conversion, J. Mater. Chem. A 7 (9) (2019) 4689–4698, https://doi.org/10.1039/C8TA12046C.

[16] Y. Yu, J. Mai, L. Wang, X. Li, Z. Jiang, F. Wang, Ship-in-a-bottle synthesis of amine-functionalized ionic liquids in NaY zeolite for CO_2 capture, Sci. Rep. 4 (1) (2014) 5997, https://doi.org/10.1038/srep05997.

[17] H. Li, T. Zhang, S. Yuan, S. Tang, MCM-36 zeolites tailored with acidic ionic liquid to regulate adsorption properties of isobutane and 1-butene, Chin. J. Chem. Eng. 24 (12) (2016) 1703–1711, https://doi.org/10.1016/j.cjche.2016.05.033.

[18] P. Tamilarasan, S. Ramaprabhu, Integration of polymerized ionic liquid with graphene for enhanced CO_2 adsorption, J. Mater. Chem. A 3 (1) (2015) 101–108, https://doi.org/10.1039/C4TA04808C.

[19] C.X. Guo, Z.S. Lu, Y. Lei, C.M. Li, Ionic liquid–graphene composite for ultratrace explosive trinitrotoluene detection, Electrochem. Commun. 12 (9) (2010) 1237–1240, https://doi.org/10.1016/j.elecom.2010.06.028.

[20] M. Althuluth, J.P. Overbeek, H.J. Van Wees, L.F. Zubeir, W.G. Haije, A. Berrouk, C.J. Peters, M.C. Kroon, Natural gas purification using supported ionic liquid membrane, J. Membr. Sci. 484 (2015) 80–86, https://doi.org/10.1016/j.memsci.2015.02.033.

[21] K. Halder, M.M. Khan, J. Grünauer, S. Shishatskiy, C. Abetz, V. Filiz, V. Abetz, Blend membranes of ionic liquid and polymers of intrinsic microporosity with improved gas separation characteristics, J. Membr. Sci. 539 (2017) 368–382, https://doi.org/10.1016/j.memsci.2017.06.022.

[22] M.-T. Vu, R. Lin, H. Diao, Z. Zhu, S.K. Bhatia, S. Smart, Effect of ionic liquids (ILs) on MOFs/polymer interfacial enhancement in mixed matrix membranes, J. Membr. Sci. 587 (2019) 117157, https://doi.org/10.1016/j.memsci.2019.05.081.

[23] Y. Ban, Z. Li, Y. Li, Y. Peng, H. Jin, W. Jiao, A. Guo, P. Wang, Q. Yang, C. Zhong, W. Yang, Confinement of ionic liquids in nanocages: tailoring the molecular sieving properties of ZIF-8 for membrane-based CO_2 capture, Angew. Chem. Int. Ed. Engl. 54 (51) (2015) 15483–15487, https://doi.org/10.1002/anie.201505508.

[24] J. Ma, Y. Ying, X. Guo, H. Huang, D. Liu, C. Zhong, Fabrication of mixed-matrix membrane containing metal–organic framework composite with task-specific ionic liquid for efficient CO_2 separation, J. Mater. Chem. A 4 (19) (2016) 7281–7288, https://doi.org/10.1039/C6TA02611G.

[25] Y.C. Hudiono, T.K. Carlisle, A.L. LaFrate, D.L. Gin, R.D. Noble, Novel mixed matrix membranes based on polymerizable room-temperature ionic liquids and SAPO-34 particles to improve CO_2 separation, J. Membr. Sci. 370 (1–2) (2011) 141–148, https://doi.org/10.1016/j.memsci.2011.01.012.

[26] L. Rodriguez-Perez, E. Teuma, A. Falqui, M. Gomez, P. Serp, Supported ionic liquid phase catalysis on functionalized carbon nanotubes, Chem. Commun 35 (2008) 4201–4203, https://doi.org/10.1039/B804969F.

[27] Q.-x. Luo, M. Ji, M.-h. Lu, C. Hao, J.-s. Qiu, Y.-q. Li, Organic electron-rich N-heterocyclic compound as a chemical bridge: building a Brönsted acidic ionic liquid confined in MIL-101 nanocages, J. Mater. Chem. A 1 (22) (2013) 6530–6534, https://doi.org/10.1039/C3TA10975E.

[28] A. Nasrollahpour, S.E. Moradi, Hexavalent chromium removal from water by ionic liquid modified metal-organic frameworks adsorbent, Microporous Mesoporous Mater. 243 (2017) 47–55, https://doi.org/10.1016/j.micromeso.2017.02.006.

[29] K. Fujie, K. Otsubo, R. Ikeda, T. Yamada, H. Kitagawa, Low temperature ionic conductor: ionic liquid incorporated within a metal–organic framework, Chem. Sci. 6 (7) (2015) 4306–4310, https://doi.org/10.1039/C5SC01398D.

[30] Z. Wang, R. Tan, H. Wang, L. Yang, J. Hu, H. Chen, F. Pan, A metal–organic-framework-based electrolyte with nanowetted interfaces for high-energy-density solid-state lithium battery, Adv. Mater. 30 (2) (2018) 1704436, https://doi.org/10.1002/adma.201704436.

[31] F.P. Kinik, A. Uzun, S. Keskin, Ionic liquid/metal-organic framework composites: from synthesis to applications, ChemSusChem 10 (14) (2017) 2842–2863, https://doi.org/10.1002/cssc.201700716.

[32] J. Fuller, A.C. Breda, R.T. Carlin, Ionic liquid-polymer gel electrolytes, J. Electrochem. Soc. 144 (4) (1997) L67–L70, https://doi.org/10.1149/1.1837555.

[33] K. Jin, X. Huang, L. Pang, J. Li, A. Appel, S. Wherland, $[Cu(i)(bpp)]BF_4$: the first extended coordination network prepared solvothermally in an ionic liquid solvent, Chem. Commun 23 (2002) 2872–2873, https://doi.org/10.1039/B209937N.

[34] R.E. Morris, Ionothermal synthesis—ionic liquids as functional solvents in the preparation of crystalline materials, Chem. Commun. 21 (2009) 2990–2998, https://doi.org/10.1039/B902611H.

[35] Q. Ji, I. Honma, S.-M. Paek, M. Akada, J.P. Hill, A. Vinu, K. Ariga, Layer-by-Layer films of graphene and ionic liquids for highly selective gas sensing, Angew. Chem. Int. Ed. 49 (50) (2010) 9737–9739, https://doi.org/10.1002/anie.201004929.

[36] E.R. Cooper, C.D. Andrews, P.S. Wheatley, P.B. Webb, P. Wormald, R.E. Morris, Ionic liquids and eutectic mixtures as solvent and template in synthesis of zeolite analogues, Nature 430 (2004) 1012–1016, https://doi.org/10.1038/nature02860, 7003.

[37] Y. Chen, Z. Hu, K.M. Gupta, J. Jiang, Ionic liquid/metal–organic framework composite for CO_2 capture: a computational investigation, J. Phys. Chem. C 115 (44) (2011) 21736–21742, https://doi.org/10.1021/jp208361p.

[38] N.A. Khan, Z. Hasan, S.H. Jhung, Ionic liquids supported on metal-organic frameworks: remarkable adsorbents for adsorptive desulfurization, Chem. Eur J. 20 (2) (2014) 376–380, https://doi.org/10.1002/chem.201304291.

[39] Z. Hu, X. Zhang, S. Chen, A graphene oxide and ionic liquid assisted anion-immobilized polymer electrolyte with high ionic conductivity for dendrite-free lithium metal batteries, J. Power Sources 477 (2020) 228754, https://doi.org/10.1016/j.jpowsour.2020.228754.

[40] S. Chen, B. Yuan, G. Liu, D. Zhang, Electrochemical sensors based on covalent organic frameworks: a critical review, Front. Chem. 8 (2020), https://doi.org/10.3389/fchem.2020.601044, 1082.

[41] M. Zeeshan, H. Kulak, S. Kavak, H.M. Polat, O. Durak, S. Keskin, A. Uzun, Influence of anion size and electronic structure on the gas separation performance of ionic liquid/ZIF-8 composites, Microporous Mesoporous Mater. 306 (2020) 110446, https://doi.org/10.1016/j.micromeso.2020.110446.

[42] E.R. Parnham, R.E. Morris, Ionothermal synthesis of zeolites, metal–organic frameworks, and inorganic–organic hybrids, Acc. Chem. Res. 40 (10) (2007) 1005–1013, https://doi.org/10.1021/ar700025k.

[43] X. Guan, Y. Ma, H. Li, Y. Yusran, M. Xue, Q. Fang, Y. Yan, V. Valtchev, S. Qiu, Fast, ambient temperature and pressure ionothermal synthesis of three-dimensional covalent organic frameworks, J. Am. Chem. Soc. 140 (13) (2018) 4494–4498, https://doi.org/10.1021/jacs.8b01320.

[44] N. Zdolšek, R.P. Rocha, J. Krstić, T. Trtić-Petrović, B. Šljukić, J.L. Figueiredo, M. J. Vujković, Electrochemical investigation of ionic liquid-derived porous carbon materials for supercapacitors: pseudocapacitance versus electrical double layer, Electrochim. Acta 298 (2019) 541–551, https://doi.org/10.1016/j.electacta.2018.12.129.

[45] M. Antonietti, D. Kuang, B. Smarsly, Y. Zhou, Ionic liquids for the convenient synthesis of functional nanoparticles and other inorganic nanostructures, Angew. Chem. Int. Ed. Engl. 43 (38) (2004) 4988–4992, https://doi.org/10.1002/anie.200460091.

[46] A. Taubert, Z. Li, Inorganic materials from ionic liquids, Dalton Trans. 7 (2007) 723–727, https://doi.org/10.1039/B616593A.

[47] A. Thomas, R. Ahamed, M. Prakash, Selection of a suitable ZIF-8/ionic liquid (IL) based composite for selective CO_2 capture: the role of anions at the interface, RSC Adv. 10 (64) (2020) 39160–39170, https://doi.org/10.1039/D0RA07927H.

[48] D.N. Dybtsev, H. Chun, K. Kim, Three-dimensional metal–organic framework with (3,4)-connected net, synthesized from an ionic liquid medium, Chem. Commun. 14 (2004) 1594–1595, https://doi.org/10.1039/B403001J.

[49] J. Zhang, S. Chen, X. Bu, Multiple functions of ionic liquids in the synthesis of three-dimensional low-connectivity homochiral and achiral frameworks, Angew. Chem. 47 (29) (2008) 5434–5437, https://doi.org/10.1002/anie.200801838.

[50] W. Xiao, Z. Sun, S. Chen, H. Zhang, Y. Zhao, C. Huang, Z. Liu, Ionic liquid-stabilized graphene and its use in immobilizing a metal nanocatalyst, RSC Adv. 2 (21) (2012) 8189–8193, https://doi.org/10.1039/C2RA20774E.

[51] K. Zawada Donato, L. Matějka, R. Mauler, R. Donato, Recent applications of ionic liquids in the sol-gel process for polymer–silica nanocomposites with ionic interfaces, Colloids Interfaces 1 (2017) 5, https://doi.org/10.3390/colloids1010005.

[52] A. Vioux, L. Viau, S. Volland, J. Le Bideau, Use of ionic liquids in sol-gel; ionogels and applications, Compt. Rendus Chem. 13 (1) (2010) 242–255, https://doi.org/10.1016/j.crci.2009.07.002.

[53] Ö. Durak, H. Kulak, S. Kavak, H.M. Polat, S. Keskin, A. Uzun, Towards complete elucidation of structural factors controlling thermal stability of IL/MOF composites: effects of ligand functionalization on MOFs, J. Phys. Condens. Matter 32 (48) (2020) 484001, https://doi.org/10.1088/1361-648x/aba06c.

[54] M. Li, P.J. Pham, C.U. Pittman Jr., T. Li, Selective solid-phase extraction of α-tocopherol by functionalized ionic liquid-modified mesoporous SBA-15 adsorbent, Anal. Sci. 24 (10) (2008) 1245–1250, https://doi.org/10.2116/analsci.24.1245.

[55] O.C. Vangeli, G.E. Romanos, K.G. Beltsios, D. Fokas, E.P. Kouvelos, K. L. Stefanopoulos, N.K. Kanellopoulos, Grafting of imidazolium based ionic liquid on the pore surface of nanoporous materials—study of physicochemical and thermodynamic properties, J. Phys. Chem. B 114 (19) (2010) 6480–6491, https://doi.org/10.1021/jp912205y.

[56] M. Han, Z. Gu, C. Chen, Z. Wu, Y. Que, Q. Wang, H. Wan, G. Guan, Efficient confinement of ionic liquids in MIL-100(Fe) frameworks by the "impregnation-reaction-encapsulation" strategy for biodiesel production, RSC Adv. 6 (43) (2016) 37110–37117, https://doi.org/10.1039/C6RA00579A.

[57] H. Li, L. Tuo, K. Yang, H.-K. Jeong, Y. Dai, G. He, W. Zhao, Simultaneous enhancement of mechanical properties and CO_2 selectivity of ZIF-8 mixed matrix membranes: interfacial toughening effect of ionic liquid, J. Membr. Sci. 511 (2016) 130–142, https://doi.org/10.1016/j.memsci.2016.03.050.

[58] C. Chen, Z. Wu, Y. Que, B. Li, Q. Guo, Z. Li, L. Wang, H. Wan, G. Guan, Immobilization of a thiol-functionalized ionic liquid onto HKUST-1 through thiol compounds as the chemical bridge, RSC Adv. 6 (59) (2016) 54119–54128, https://doi.org/10.1039/C6RA03317B.

[59] H.M.A. Hassan, M.A. Betiha, S.K. Mohamed, E.A. El-Sharkawy, E.A. Ahmed, Stable and recyclable MIL-101(Cr)–Ionic liquid based hybrid nanomaterials as heterogeneous catalyst, J. Mol. Liq. 236 (2017) 385–394, https://doi.org/10.1016/j.molliq.2017.04.034.

[60] S. Abednatanzi, A. Abbasi, M. Masteri-Farahani, Immobilization of catalytically active polyoxotungstate into ionic liquid-modified MIL-100(Fe): a recyclable catalyst for selective oxidation of benzyl alcohol, Catal. Commun. 96 (2017) 6–10, https://doi.org/10.1016/j.catcom.2017.03.011.

[61] J. Wu, Y. Gao, W. Zhang, Y. Tan, A. Tang, Y. Men, B. Tang, Deep desulfurization by oxidation using an active ionic liquid-supported Zr metal–organic framework as catalyst, Appl. Organomet. Chem. 29 (2) (2015) 96–100, https://doi.org/10.1002/aoc.3251.

[62] Q. Luo, X. Song, M. Ji, S. Park, C. Hao, Y. Li, Molecular size- and shape-selective Knoevenagel condensation over microporous $Cu_3(BTC)_2$ immobilized amino-functionalized basic ionic liquid catalyst, Appl. Catal., A 478 (2014) 81–90, https://doi.org/10.1016/j.apcata.2014.03.041.

[63] H. Wan, C. Chen, Z. Wu, Y. Que, Y. Feng, W. Wang, L. Wang, G. Guan, X. Liu, Encapsulation of heteropolyanion-based ionic liquid within the metal–organic framework MIL-100(Fe) for biodiesel production, ChemCatChem 7 (3) (2015) 441–449, https://doi.org/10.1002/cctc.201402800.

[64] A. Nasrollahpour, S.E. Moradi, M.J. Baniamerian, Vortex-Assisted dispersive solid-phase microextraction using ionic liquid-modified metal-organic frameworks of PAHs from environmental water, vegetable, and fruit juice samples, Food Anal. Methods 10 (8) (2017) 2815–2826, https://doi.org/10.1007/s12161-017-0843-0.

[65] S. Abednatanzi, K. Leus, P.G. Derakhshandeh, F. Nahra, K. De Keukeleere, K. Van Hecke, I. Van Driessche, A. Abbasi, S.P. Nolan, P.V. Der Voort, POM@IL-MOFs – inclusion of POMs in ionic liquid modified MOFs to produce recyclable oxidation catalysts, Catal. Sci. Technol. 7 (7) (2017) 1478–1487, https://doi.org/10.1039/C6CY02662A.

[66] K. Fujie, T. Yamada, R. Ikeda, H. Kitagawa, Introduction of an ionic liquid into the micropores of a metal–organic framework and its anomalous phase behavior, Angew. Chem. Int. Ed. 53 (42) (2014) 11302–11305, https://doi.org/10.1002/anie.201406011.

[67] M. Li, P.J. Pham, T. Wang, T. Li, Synthesis of Ionic Liquids Immobilized Mesoporous Adsorbents with Silver Salts and Applications in Concentration of Polyunsaturated Fatty Acid Methyl Esters, ACS National Meeting Book of Abstracts, 2007.

[68] N.R. Dhumal, M.P. Singh, J.A. Anderson, J. Kiefer, H.J. Kim, Molecular interactions of a Cu-based metal–organic framework with a confined imidazolium-based ionic liquid: a combined density functional theory and experimental vibrational spectroscopy study, J. Phys. Chem. C 120 (6) (2016) 3295–3304, https://doi.org/10.1021/acs.jpcc.5b10123.

[69] X.-L. Sun, W.-H. Deng, H. Chen, H.-L. Han, J.M. Taylor, C.-Q. Wan, G. Xu, A metal–organic framework impregnated with a binary ionic liquid for safe proton conduction above 100°C, Chem. Eur J. 23 (6) (2017) 1248–1252, https://doi.org/10.1002/chem.201605215.

[70] N.A. Khan, Z. Hasan, S.H. Jhung, Ionic liquid@MIL-101 prepared via the ship-in-bottle technique: remarkable adsorbents for the removal of benzothiophene from liquid fuel, Chem. Commun 52 (12) (2016) 2561–2564, https://doi.org/10.1039/C5CC08896H.

[71] S. Park, H.-K. Jeong, Highly H_2O permeable ionic liquid encapsulated metal–organic framework membranes for energy-efficient air-dehumidification, J. Mater. Chem. A 8 (44) (2020) 23645–23653, https://doi.org/10.1039/D0TA07780A.

[72] Z. Li, W. Wang, Y. Chen, C. Xiong, G. He, Y. Cao, H. Wu, M.D. Guiver, Z. Jiang, Constructing efficient ion nanochannels in alkaline anion exchange membranes by the in situ assembly of a poly(ionic liquid) in metal–organic frameworks, J. Mater. Chem. A 4 (6) (2016) 2340–2348, https://doi.org/10.1039/C5TA10452A.

[73] M.A. Macchione, C. Biglione, M. Strumia, Design, synthesis and architectures of hybrid nanomaterials for therapy and diagnosis applications, Polymers 10 (5) (2018), https://doi.org/10.3390/polym10050527.

[74] M.A. Pizzoccaro-Zilamy, S.M. Piña, B. Rebiere, C. Daniel, D. Farrusseng, M. Drobek, G. Silly, A. Julbe, G. Guerrero, Controlled grafting of dialkylphosphonate-based ionic liquids on γ-alumina: design of hybrid materials with high potential for CO_2 separation applications, RSC Adv. 9 (35) (2019) 19882–19894, https://doi.org/10.1039/C9RA01265F.

[75] P. Tamilarasan, S. Ramaprabhu, Amine-rich ionic liquid grafted graphene for sub-ambient carbon dioxide adsorption, RSC Adv. 6 (4) (2016) 3032–3040, https://doi.org/10.1039/C5RA22029G.

[76] L. Han, H. Li, S.-J. Choi, M.-S. Park, S.-M. Lee, Y.-J. Kim, D.-W. Park, Ionic liquids grafted on carbon nanotubes as highly efficient heterogeneous catalysts for the synthesis of cyclic carbonates, Appl. Catal., A 429–430 (2012) 67–72, https://doi.org/10.1016/j.apcata.2012.04.008.

[77] C.M.Q. Le, X.T. Cao, L.G. Bach, W.-K. Lee, I. Kang, K.T. Lim, Direct grafting imidazolium-based poly(ionic liquid) onto multiwalled carbon nanotubes via Diels-Alder "click" reaction, Mol. Cryst. Liq. Cryst. 660 (1) (2018) 143–149, https://doi.org/10.1080/15421406.2018.1456136.

[78] R. Soengas, Y. Navarro, M.J. Iglesias, F. López-Ortiz, Immobilized gold nanoparticles prepared from gold(III)-Containing ionic liquids on silica: application to the sustainable synthesis of propargylamines, Molecules 23 (11) (2018), https://doi.org/10.3390/molecules23112975.

[79] M. Zeeshan, V. Nozari, S. Keskin, A. Uzun, Structural factors determining thermal stability limits of ionic liquid/MOF composites: imidazolium ionic liquids combined with CuBTC and ZIF-8, Ind. Eng. Chem. Res. 58 (31) (2019) 14124–14138, https://doi.org/10.1021/acs.iecr.9b02415.

[80] C. Bowers, Matrix effect corrections in X-ray fluorescence spectrometry, J. Chem. Educ. 96 (11) (2019) 2597–2599, https://doi.org/10.1021/acs.jchemed.9b00630.

[81] T.J. Ferreira, R.P. Ribeiro, J.P. Mota, L.P. Rebelo, J.M. Esperança, I.A. Esteves, Ionic liquid-impregnated metal–organic frameworks for CO_2/CH_4 separation, ACS Appl. Nano Mater. 2 (12) (2019) 7933–7950, https://doi.org/10.1021/acsanm.9b01936.

[82] E. Torralba-Calleja, J. Skinner, D. Gutiérrez-Tauste, CO_2 capture in ionic liquids: a review of solubilities and experimental methods, J. Chem. (2013) 473584, https://doi.org/10.1155/2013/473584, 2013.

[83] Z. Lei, C. Dai, B. Chen, Gas solubility in ionic liquids, Chem. Rev. 114 (2) (2014) 1289–1326, https://doi.org/10.1021/cr300497a.

[84] M.I. Cabaço, M. Besnard, Y. Danten, J.A.P. Coutinho, Carbon dioxide in 1-Butyl-3-methylimidazolium acetate. I. Unusual solubility investigated by Raman spectroscopy and DFT calculations, J. Phys. Chem. 116 (6) (2012) 1605–1620, https://doi.org/10.1021/jp211211n.

[85] K. Jin, T. Zhang, S. Yuan, S. Tang, Regulation of isobutane/1-butene adsorption behaviors on the acidic ionic liquids-functionalized MCM-22 zeolite, Chin. J. Chem. Eng. 26 (1) (2018) 127–136, https://doi.org/10.1016/j.cjche.2017.05.023.

[86] Y. Li, T. Zhang, S. Tang, Adsorption/desorption of 2,2,4-trimethylpentane on MCM-36 zeolite functionalized by acidic ionic liquid, Adsorption 24 (2) (2018) 179–190, https://doi.org/10.1007/s10450-018-9935-4.

[87] F.J. Hernández-Fernández, A.P. de los Ríos, F. Tomás-Alonso, J.M. Palacios, G. Víllora, Preparation of supported ionic liquid membranes: influence of the ionic liquid immobilization method on their operational stability, J. Membr. Sci. 341 (1) (2009) 172–177, https://doi.org/10.1016/j.memsci.2009.06.003.

[88] H.Z. Chen, P. Li, T.-S. Chung, PVDF/ionic liquid polymer blends with superior separation performance for removing CO_2 from hydrogen and flue gas, Int. J. Hydrogen Energy 37 (16) (2012) 11796–11804, https://doi.org/10.1016/j.ijhydene.2012.05.111.

[89] C.A. Dunn, Z. Shi, R. Zhou, D.L. Gin, R.D. Noble, (Cross-linked poly (ionic liquid)–ionic liquid–zeolite) mixed-matrix membranes for CO_2/CH_4 gas separations based on curable ionic liquid prepolymers, Ind. Eng. Chem. Res. 58 (11) (2019) 4704–4708, https://doi.org/10.1021/acs.iecr.8b06464.

[90] A. Khan, M.A. Qyyum, H. Saulat, R. Ahmad, X. Peng, M. Lee, Metal–organic frameworks for biogas upgrading: recent advancements, challenges, and future recommendations, Appl. Mater. Today 22 (2021) 100925, https://doi.org/10.1016/j.apmt.2020.100925.

[91] M. Mohamedali, H. Ibrahim, A.J.C.E.J. Henni, Incorporation of acetate-based ionic liquids into a zeolitic imidazolate framework (ZIF-8) as efficient sorbents for carbon dioxide capture, Chem. Eng. J. 334 (2018) 817–828, https://doi.org/10.1016/j.cej.2017.10.104.

[92] M. Zeeshan, S. Keskin, A. Uzun, Enhancing CO_2/CH_4 and CO_2/N_2 separation performances of ZIF-8 by post-synthesis modification with [BMIM][SCN], Polyhedron 155 (2018) 485–492, https://doi.org/10.1016/j.poly.2018.08.073.

[93] V. Nozari, M. Zeeshan, S. Keskin, A. Uzun, Effect of methylation of ionic liquids on the gas separation performance of ionic liquid/metal–organic framework composites, CrystEngComm 20 (44) (2018) 7137–7143, https://doi.org/10.1039/C8CE01364K.

[94] V. Nozari, S. Keskin, A. Uzun, Toward rational design of ionic liquid/metal–organic framework composites: effects of interionic interaction energy, ACS Omega 2 (10) (2017) 6613–6618, https://doi.org/10.1021/acsomega.7b01074.

[95] X. Wei, N. Li, Y. Wang, Z. Xie, H. Huang, G. Yang, T. Li, X. Qin, S. Li, H. Yang, J. Zhu, F. You, C. Wu, Y. Liu, Zeolitic imidazolate frameworks-based nanomaterials for biosensing, cancer imaging and phototheranostics, Appl. Mater. Today 23 (2021) 100995, https://doi.org/10.1016/j.apmt.2021.100995.

[96] P.J. Carvalho, V.H. Álvarez, B. Schröder, A.M. Gil, I.M. Marrucho, M. Aznar, L.M. N.B.F. Santos, J.A.P. Coutinho, Specific solvation interactions of CO_2 on acetate and trifluoroacetate imidazolium based ionic liquids at high pressures, J. Phys. Chem. B 113 (19) (2009) 6803–6812, https://doi.org/10.1021/jp901275b.

[97] W. Shi, R.L. Thompson, E. Albenze, J.A. Steckel, H.B. Nulwala, D.R. Luebke, Contribution of the acetate anion to CO_2 solubility in ionic liquids: theoretical method development and experimental study, J. Phys. Chem. B 118 (26) (2014) 7383–7394, https://doi.org/10.1021/jp502425a.

[98] S. Kavak, H.M. Polat, H. Kulak, S. Keskin, A. Uzun, MIL-53(Al) as a versatile platform for ionic-liquid/MOF composites to enhance CO_2 selectivity over CH_4 and N_2, Chem. Asian J. 14 (20) (2019) 3655–3667, https://doi.org/10.1002/asia.201900634.

[99] N. Al-Janabi, P. Hill, L. Torrente-Murciano, A. Garforth, P. Gorgojo, F. Siperstein, X. Fan, Mapping the Cu-BTC metal–organic framework (HKUST-1) stability envelope in the presence of water vapour for CO_2 adsorption from flue gases, Chem. Eng. J. 281 (2015) 669–677, https://doi.org/10.1016/j.cej.2015.07.020.

[100] A. Alam, R. Bera, M. Ansari, A. Hassan, N. Das, Triptycene-based and amine-linked nanoporous networks for efficient CO_2 capture and separation, Front. Energy Res. 7 (2019) 141, https://doi.org/10.3389/fenrg.2019.00141.

[101] M. Ding, H.-L. Jiang, Incorporation of imidazolium-based poly(ionic liquid)s into a metal–organic framework for CO_2 capture and conversion, ACS Catal. 8 (4) (2018) 3194–3201, https://doi.org/10.1021/acscatal.7b03404.

[102] Y. Zhang, M.-X. Wu, G. Zhou, X.-H. Wang, X. Liu, A rising star from two worlds: collaboration of COFs and ILs, Adv. Funct. Mater. (2021) 2104996, https://doi.org/10.1002/adfm.202104996, n/a(n/a).

[103] J.-Y. Wang, E. Mangano, S. Brandani, D.M. Ruthven, A review of common practices in gravimetric and volumetric adsorption kinetic experiments, Adsorption 27 (3) (2021) 295–318, https://doi.org/10.1007/s10450-020-00276-7.

[104] Y. Belmabkhout, M. Frère, G.D. Weireld, High-pressure adsorption measurements. A comparative study of the volumetric and gravimetric methods, Meas. Sci. Technol. 15 (5) (2004) 848–858, https://doi.org/10.1088/0957-0233/15/5/010.

[105] S. Sircar, C.-Y. Wang, A.D. Lueking, Design of high pressure differential volumetric adsorption measurements with increased accuracy, Adsorption 19 (6) (2013) 1211–1234, https://doi.org/10.1007/s10450-013-9558-8.

[106] D.E. Demirocak, S.S. Srinivasan, M.K. Ram, D.Y. Goswami, E.K. Stefanakos, Volumetric hydrogen sorption measurements – uncertainty error analysis and the

importance of thermal equilibration time, Int. J. Hydrogen Energy 38 (3) (2013) 1469–1477, https://doi.org/10.1016/j.ijhydene.2012.11.013.
[107] J. Burress, D. Bethea, B. Troub, Combination volumetric and gravimetric sorption instrument for high accuracy measurements of methane adsorption, Rev. Sci. Instrum. 88 (5) (2017), 053902, https://doi.org/10.1063/1.4982889.
[108] M. Nakashima, S. Shimada, M. Inagaki, T.A. Centeno, On the adsorption of CO_2 by molecular sieve carbons—volumetric and gravimetric studies, Carbon 33 (9) (1995) 1301–1306, https://doi.org/10.1016/0008-6223(95)00077-Q.
[109] M. Zeeshan, H.C. Gulbalkan, Z.P. Haslak, S. Keskin, A. Uzun, Doubling CO_2/N_2 separation performance of CuBTC by incorporation of 1-n-ethyl-3-methylimidazolium diethyl phosphate, Microporous Mesoporous Mater. 316 (2021) 110947, https://doi.org/10.1016/j.micromeso.2021.110947.
[110] N. Ahmad, A. Vijaya Bhaskar Reddy, B.B. Saha, Nasruddin, M. Moniruzzaman, Synthesis and characterization of ionic liquid polymer composite with zeolite and its application for carbon dioxide capture, IOP Conf. Ser. Mater. Sci. Eng. 458 (2018), 012009, https://doi.org/10.1088/1757-899x/458/1/012009.
[111] Y. Yu, J. Mai, L. Huang, L. Wang, X. Li, Ship in a bottle synthesis of ionic liquids in NaY supercages for CO_2 capture, RSC Adv. 4 (25) (2014) 12756–12762, https://doi.org/10.1039/C3RA46971A.
[112] Y. Ma, J. Mao, C. Xiao, T. Zhao, L. Zang, Zeolite supported ionic liquid improved by cyclodextrins for efficient removal capacity of H_2S, Chem. Lett. 48 (2018), https://doi.org/10.1246/cl.180812.
[113] K. Jin, T. Zhang, J. Ji, M. Zhang, Y. Zhang, S. Tang, Functionalization of MCM-22 by dual acidic ionic liquid and its paraffin absorption modulation properties, Ind. Eng. Chem. Res. 54 (1) (2015) 164–170, https://doi.org/10.1021/ie504327t.
[114] A. Erto, A. Silvestre-Albero, J. Silvestre-Albero, F. Rodríguez-Reinoso, M. Balsamo, A. Lancia, F. Montagnaro, Carbon-supported ionic liquids as innovative adsorbents for CO_2 separation from synthetic flue-gas, J. Colloid Interface Sci. 448 (2015) 41–50, https://doi.org/10.1016/j.jcis.2015.01.089.
[115] M.S. Raja Shahrom, A.R. Nordin, C.D. Wilfred, The improvement of activated carbon as CO_2 adsorbent with supported amine functionalized ionic liquids, J. Environ. Eng. Technol. 7 (5) (2019) 103319, https://doi.org/10.1016/j.jece.2019.103319.
[116] X. He, J. Zhu, H. Wang, M. Zhou, S. Zhang, Surface functionalization of activated carbon with phosphonium ionic liquid for CO_2 adsorption, Coatings 9 (9) (2019), https://doi.org/10.3390/coatings9090590.
[117] T. Abbas, G. Gonfa, K.C. Lethesh, M.I.A. Mutalib, M.b. Abai, K.Y. Cheun, E. Khan, Mercury capture from natural gas by carbon supported ionic liquids: synthesis, evaluation and molecular mechanism, Fuel 177 (2016) 296–303, https://doi.org/10.1016/j.fuel.2016.03.032.
[118] G. Severa, K. Bethune, R. Rocheleau, S. Higgins, SO_2 sorption by activated carbon supported ionic liquids under simulated atmospheric conditions, Chem. Eng. J. 265 (2015) 249–258, https://doi.org/10.1016/j.cej.2014.12.051.
[119] P. Tamilarasan, S. Ramaprabhu, Ionic liquid functionalization – an effective way to tune carbon dioxide adsorption properties of carbon nanotubes, RSC Adv. 5 (44) (2015) 35098–35106, https://doi.org/10.1039/C5RA02159F.
[120] S. Ghosh, S. Ramaprabhu, High-pressure investigation of ionic functionalized graphitic carbon nitride nanostructures for CO_2 capture, J. CO2 Util. 21 (2017) 89–99, https://doi.org/10.1016/j.jcou.2017.06.022.
[121] L.M. Robeson, The upper bound revisited, J. Membr. Sci. 320 (1–2) (2008) 390–400, https://doi.org/10.1016/j.memsci.2008.04.030.
[122] P. Scovazzo, D. Havard, M. McShea, S. Mixon, D. Morgan, Long-term, continuous mixed-gas dry fed CO_2/CH_4 and CO_2/N_2 separation performance and selectivities for room temperature ionic liquid membranes, J. Membr. Sci. 327 (1–2) (2009) 41–48, https://doi.org/10.1016/j.memsci.2008.10.056.
[123] I. Kopczynska, M. Joskowska, R. Aranowski, Wetting processes in supported ionic liquid membranes technology, Fizykochemiczne Problemy Mineralurgii - Physicochem. Probl. Min. Process. 50 (2014) 373–386, https://doi.org/10.5277/ppmp140131.
[124] P. Izák, Š. Hovorka, T. Bartovský, L. Bartovská, J.G. Crespo, Swelling of polymeric membranes in room temperature ionic liquids, J. Membr. Sci. 296 (1) (2007) 131–138, https://doi.org/10.1016/j.memsci.2007.03.022.
[125] A. Kumar, M.S. Manna, A.K. Ghoshal, P. Saha, Study of the supported liquid membrane for the estimation of the synergistic effects of influential parameters on its stability, J. Environ. Eng. Technol. 4 (1) (2016) 943–949, https://doi.org/10.1016/j.jece.2015.12.024.
[126] Z. Shamair, N. Habib, M.A. Gilani, A.L. Khan, Theoretical and experimental investigation of CO_2 separation from CH_4 and N_2 through supported ionic liquid membranes, Appl. Energy 268 (2020) 115016, https://doi.org/10.1016/j.apenergy.2020.115016.
[127] L. Lozano, C. Godínez, A. De Los Rios, F. Hernández-Fernández, S. Sánchez-Segado, F.J. Alguacil, Recent advances in supported ionic liquid membrane technology, J. Membr. Sci. 376 (1–2) (2011) 1–14, https://doi.org/10.1016/j.memsci.2011.03.036.
[128] S. Kanehashi, M. Kishida, T. Kidesaki, R. Shindo, S. Sato, T. Miyakoshi, K. Nagai, CO_2 separation properties of a glassy aromatic polyimide composite membranes containing high-content 1-butyl-3-methylimidazolium bis (trifluoromethylsulfonyl) imide ionic liquid, J. Membr. Sci. 430 (2013) 211–222, https://doi.org/10.1016/j.memsci.2012.12.003.
[129] D.F. Mohshim, H. Mukhtar, Z. Man, The effect of incorporating ionic liquid into polyethersulfone-SAPO34 based mixed matrix membrane on CO_2 gas separation performance, Separ. Purif. Technol. 135 (2014) 252–258, https://doi.org/10.1016/j.seppur.2014.08.019.
[130] Y.C. Hudiono, T.K. Carlisle, J.E. Bara, Y. Zhang, D.L. Gin, R.D. Noble, A three-component mixed-matrix membrane with enhanced CO_2 separation properties based on zeolites and ionic liquid materials, J. Membr. Sci. 350 (1–2) (2010) 117–123, https://doi.org/10.1016/j.memsci.2009.12.018.
[131] R. Nasir, N.N.R. Ahmad, H. Mukhtar, D.F. Mohshim, Effect of ionic liquid inclusion and amino–functionalized SAPO-34 on the performance of mixed matrix membranes for CO_2/CH_4 separation, J. Environ. Eng. Technol. 6 (2) (2018) 2363–2368, https://doi.org/10.1016/j.jece.2018.03.032.
[132] M. Li, X. Zhang, S. Zeng, L. bai, H. Gao, J. Deng, Q. Yang, S. Zhang, Pebax-based composite membranes with high gas transport properties enhanced by ionic liquids for CO_2 separation, RSC Adv. 7 (11) (2017) 6422–6431, https://doi.org/10.1039/C6RA27221E.
[133] C.A. Dunn, S. Denning, J.M. Crawford, R. Zhou, G.E. Dwulet, M.A. Carreon, D. L. Gin, R.D. Noble, CO_2/CH_4 separation characteristics of poly (RTIL)-RTIL-zeolite mixed-matrix membranes evaluated under binary feeds up to 40 bar and 50 °C, J. Membr. Sci. 621 (2021), https://doi.org/10.1016/j.memsci.2020.118979, 118979.
[134] R. Shindo, M. Kishida, H. Sawa, T. Kidesaki, S. Sato, S. Kanehashi, K. Nagai, Characterization and gas permeation properties of polyimide/ZSM-5 zeolite composite membranes containing ionic liquid, J. Membr. Sci. 454 (2014) 330–338, https://doi.org/10.1016/j.memsci.2013.12.031.
[135] N. Ahmad, C. Leo, A. Ahmad, Effects of solvent and ionic liquid properties on ionic liquid enhanced polysulfone/SAPO-34 mixed matrix membrane for CO_2 removal, Microporous Mesoporous Mater. 283 (2019) 64–72, https://doi.org/10.1016/j.micromeso.2019.04.001.
[136] N. Ahmad, C. Leo, A. Mohammad, A. Ahmad, Interfacial sealing and functionalization of polysulfone/SAPO-34 mixed matrix membrane using acetate-based ionic liquid in post-impregnation for CO_2 capture, Separ. Purif. Technol. 197 (2018) 439–448, https://doi.org/10.1016/j.seppur.2017.12.054.
[137] A. Ilyas, N. Muhammad, M.A. Gilani, I.F. Vankelecom, A.L. Khan, Effect of zeolite surface modification with ionic liquid [APTMS][Ac] on gas separation performance of mixed matrix membranes, Separ. Purif. Technol. 205 (2018) 176–183, https://doi.org/10.1016/j.seppur.2018.05.040.
[138] Z. Guo, W. Zheng, X. Yan, Y. Dai, X. Ruan, X. Yang, X. Li, N. Zhang, G. He, Ionic liquid tuning nanocage size of MOFs through a two-step adsorption/infiltration strategy for enhanced gas screening of mixed-matrix membranes, J. Membr. Sci. (2020) 118101, https://doi.org/10.1016/j.memsci.2020.118101.
[139] I. Yasmeen, A. Ilyas, Z. Shamair, M.A. Gilani, S. Rafiq, M.R. Bilad, A.L. Khan, Synergistic effects of highly selective ionic liquid confined in nanocages: exploiting the three component mixed matrix membranes for CO_2 capture, Chem. Eng. Res. Des. 155 (2020) 123–132, https://doi.org/10.1016/j.cherd.2020.01.006.
[140] Z.V. Singh, M.G. Cowan, W.M. McDanel, Y. Luo, R. Zhou, D.L. Gin, R.D. Noble, Determination and optimization of factors affecting CO_2/CH_4 separation performance in poly (ionic liquid)-ionic liquid-zeolite mixed-matrix membranes, J. Membr. Sci. 509 (2016) 149–155, https://doi.org/10.1016/j.memsci.2016.02.034.
[141] A.Z. Aris, Z.A. Mohd Hir, M.R. Razak, Metal-organic frameworks (MOFs) for the adsorptive removal of selected endocrine disrupting compounds (EDCs) from aqueous solution: a review, Appl. Mater. Today 21 (2020) 100796, https://doi.org/10.1016/j.apmt.2020.100796.
[142] F. Wang, Z. Zhang, J. Yang, L. Wang, Y. Lin, Y. Wei, Immobilization of room temperature ionic liquid (RTIL) on silica gel for adsorption removal of thiophenic sulfur compounds from fuel, Fuel 107 (2013) 394–399, https://doi.org/10.1016/j.fuel.2012.11.033.
[143] H. Lyu, J. Fan, Y. Ling, Y. Yu, Z. Xie, Functionalized cross-linked chitosan with ionic liquid and highly efficient removal of azo dyes from aqueous solution, Int. J. Biol. Macromol. 126 (2019) 1023–1029, https://doi.org/10.1016/j.ijbiomac.2018.12.117.
[144] N.A. Khan, B.N. Bhadra, S.H. Jhung, Heteropoly acid-loaded ionic liquid@metal-organic frameworks: effective and reusable adsorbents for the desulfurization of a liquid model fuel, Chem. Eng. J. 334 (2018) 2215–2221, https://doi.org/10.1016/j.cej.2017.11.159.
[145] A. Khodadadi Dizaji, H.R. Mortaheb, B. Mokhtarani, Noncovalently functionalized graphene oxide/graphene with imidazolium-based ionic liquids for adsorptive removal of dibenzothiophene from model fuel, J. Mater. Sci. 51 (22) (2016) 10092–10103, https://doi.org/10.1007/s10853-016-0237-5.
[146] X. Ou, Y. Ren, J. Guo, Y. Zhou, Y. Yuan, Q. Liu, F. Yan, ZIF-8@Poly(ionic liquid)-grafted cotton cloth for switchable water/oil emulsion separation, ACS Appl. Polym. Mater. 2 (8) (2020) 3433–3439, https://doi.org/10.1021/acsapm.0c00495.
[147] R.S. Zambare, P.R. Nemade, Ionic liquid-modified graphene oxide sponge for hexavalent chromium removal from water, Colloids Surf., A 609 (2021) 125657, https://doi.org/10.1016/j.colsurfa.2020.125657.
[148] C. Chen, Z. Fu, W. Zhou, Q. Chen, C. Wang, L. Xu, Z. Wang, H. Zhang, Ionic liquid-immobilized NaY zeolite-based matrix solid phase dispersion for the extraction of active constituents in Rheum palmatum L, Microchem. J. 152 (2020) 104245, https://doi.org/10.1016/j.microc.2019.104245.
[149] I. Ahmed, T. Panja, N.A. Khan, M. Sarker, J.-S. Yu, S.H. Jhung, Nitrogen-doped porous carbons from ionic liquids@MOF: remarkable adsorbents for both aqueous and nonaqueous media, ACS Appl. Mater. Interfaces 9 (11) (2017) 10276–10285, https://doi.org/10.1021/acsami.7b00859.
[150] A. Yohannes, J. Li, S. Yao, Various metal organic frameworks combined with imidazolium, quinolinum and benzothiazolium ionic liquids for removal of three antibiotics from water, J. Mol. Liq. 318 (2020) 114304, https://doi.org/10.1016/j.molliq.2020.114304.
[151] D. Lu, C. Liu, M. Qin, J. Deng, G. Shi, T. Zhou, Functionalized ionic liquids-supported metal organic frameworks for dispersive solid phase extraction of

sulfonamide antibiotics in water samples, Anal. Chim. Acta 1133 (2020) 88–98, https://doi.org/10.1016/j.aca.2020.07.074.
[152] K. Sun, Y. Shi, W. Xu, N. Potter, Z. Li, J. Zhu, Modification of clays and zeolites by ionic liquids for the uptake of chloramphenicol from water, Chem. Eng. J. 313 (2017) 336–344, https://doi.org/10.1016/j.cej.2016.12.083.
[153] A. Yohannes, X. Feng, S. Yao, Dispersive solid-phase extraction of racemic drugs using chiral ionic liquid-metal-organic framework composite sorbent, J. Chromatogr. A 1627 (2020) 461395, https://doi.org/10.1016/j.chroma.2020.461395.
[154] X. Huang, S. Feng, G. Zhu, W. Zheng, C. Shao, N. Zhou, Q. Meng, Removal of organic herbicides from aqueous solution by ionic liquid modified chitosan/metal-organic framework composite, Int. J. Biol. Macromol. 149 (2020) 882–892, https://doi.org/10.1016/j.ijbiomac.2020.01.165.
[155] J. Ben Attig, L. Latrous, M. Zougagh, Á. Ríos, Ionic liquid and magnetic multiwalled carbon nanotubes for extraction of N-methylcarbamate pesticides from water samples prior their determination by capillary electrophoresis, Talanta 226 (2021) 122106, https://doi.org/10.1016/j.talanta.2021.122106.
[156] A.C. Sotolongo, M.M. Messina, F.J. Ibañez, R.G. Wuilloud, Hybrid ionic liquid-3D graphene-Ni foam for on-line preconcentration and separation of Hg species in water with atomic fluorescence spectrometry detection, Talanta 210 (2020) 120614, https://doi.org/10.1016/j.talanta.2019.120614.
[157] L. Sun, M. Wang, W. Li, S. Luo, Y. Wu, C. Ma, S. Liu, Carbon material–immobilized ionic liquids were applied on absorption of Hg^{2+} from water phase, Environ. Sci. Pollut. Res. 27 (21) (2020) 26882–26904, https://doi.org/10.1007/s11356-020-09054-y.
[158] M.A. Habila, Z.A. AlOthman, A.A. Ghfar, M.I.M. Al-Zaben, A.A.S. Alothman, A. A. Abdeltawab, A. El-Marghany, M. Sheikh, Phosphonium-based ionic liquid modified activated carbon from mixed recyclable waste for mercury(II) uptake, Molecules 24 (3) (2019), https://doi.org/10.3390/molecules24030570.
[159] H. Zhang, X. Wu, Y. Yuan, D. Han, F. Qiao, H. Yan, An ionic liquid functionalized graphene adsorbent with multiple adsorption mechanisms for pipette-tip solid-phase extraction of auxins in soybean sprouts, Food Chem. 265 (2018) 290–297, https://doi.org/10.1016/j.foodchem.2018.05.090.
[160] M. Li, C. Yang, H. Yan, Y. Han, D. Han, An integrated solid phase extraction with ionic liquid-thiol-graphene oxide as adsorbent for rapid isolation of fipronil residual in chicken eggs, J. Chromatogr. A 1631 (2020) 461568, https://doi.org/10.1016/j.chroma.2020.461568.
[161] Y. Xiao, F. Chen, X. Zhu, H. Qin, H. Huang, Y. Zhang, D. Yin, X. He, K. Wang, Ionic liquid-assisted formation of lanthanide metal-organic framework nano/microrods for superefficient removal of Congo red, Chem. Res. Chin. Univ. 31 (6) (2015) 899–903, https://doi.org/10.1007/s40242-015-5237-5.
[162] X. Xing, P.-H. Chang, G. Lv, W.-T. Jiang, J.-S. Jean, L. Liao, Z. Li, Ionic-liquid-crafted zeolite for the removal of anionic dye methyl orange, J. Taiwan Inst. Chem. Eng. 59 (2016) 237–243, https://doi.org/10.1016/j.jtice.2015.07.026.
[163] M. Shirani, A. Semnani, S. Habibollahi, H. Haddadi, M. Narimani, Synthesis and application of magnetic NaY zeolite composite immobilized with ionic liquid for adsorption desulfurization of fuel using response surface methodology, J. Porous Mater. 23 (3) (2016) 701–712, https://doi.org/10.1007/s10934-016-0125-z.
[164] M. Sarker, H.J. An, D.K. Yoo, S.H. Jhung, Nitrogen-doped porous carbon from ionic liquid@Al-metal-organic framework: a prominent adsorbent for purification of both aqueous and non-aqueous solutions, Chem. Eng. J. 338 (2018) 107–116, https://doi.org/10.1016/j.cej.2017.12.157.
[165] J.G. Huddleston, A.E. Visser, W.M. Reichert, H.D. Willauer, G.A. Broker, R. D. Rogers, Characterization and comparison of hydrophilic and hydrophobic room temperature ionic liquids incorporating the imidazolium cation, Green Chem. 3 (4) (2001) 156–164, https://doi.org/10.1039/B103275P.
[166] S. Kavak, Ö. Durak, H. Kulak, H.M. Polat, S. Keskin, A. Uzun, Enhanced water purification performance of ionic liquid impregnated metal-organic framework: dye removal by [BMIM][PF_6]/MIL-53(Al) composite, Front. Chem. 8 (2021), https://doi.org/10.3389/fchem.2020.622567, 622567-622567.
[167] S. Lian, C. Song, Q. Liu, E. Duan, H. Ren, Y. Kitamura, Recent advances in ionic liquids-based hybrid processes for CO_2 capture and utilization, J. Environ. Sci. (China) 99 (2021) 281–295, https://doi.org/10.1016/j.jes.2020.06.034.
[168] M. Zou, W. Dai, P. Mao, B. Li, J. Mao, S. Zhang, L. Yang, S. Luo, X. Luo, J. Zou, Integration of multifunctionalities on ionic liquid-anchored MIL-101(Cr): a robust and efficient heterogeneous catalyst for conversion of CO_2 into cyclic carbonates, Microporous Mesoporous Mater. 312 (2021) 110750, https://doi.org/10.1016/j.micromeso.2020.110750.
[169] J. Lee, O.K. Farha, J. Roberts, K.A. Scheidt, S.T. Nguyen, J.T. Hupp, Metal-organic framework materials as catalysts, Chem. Soc. Rev. 38 (5) (2009) 1450–1459, https://doi.org/10.1039/b807080f.
[170] U. Kokcam-Demir, A. Goldman, L. Esrafili, M. Gharib, A. Morsali, O. Weingart, C. Janiak, Coordinatively unsaturated metal sites (open metal sites) in metal-organic frameworks: design and applications, Chem. Soc. Rev. 49 (9) (2020) 2751–2798, https://doi.org/10.1039/c9cs00609e.
[171] L. Chen, Q. Xu, Metal-organic framework composites for catalysis, Matter 1 (1) (2019) 57–89, https://doi.org/10.1016/j.matt.2019.05.018.
[172] S.T. Meek, J.A. Greathouse, M.D. Allendorf, Metal-organic frameworks: a rapidly growing class of versatile nanoporous materials, Adv. Mater. 23 (2) (2011) 249–267, https://doi.org/10.1002/adma.201002854.
[173] D. Yang, C.A. Gaggioli, E. Conley, M. Babucci, L. Gagliardi, B.C. Gates, Synthesis and characterization of tetrairidium clusters in the metal organic framework UiO-67: catalyst for ethylene hydrogenation, J. Catal. 382 (2020) 165–172, https://doi.org/10.1016/j.jcat.2019.11.031.
[174] Ö. Akarçay, S.F. Kurtoğlu, A. Uzun, Ammonia decomposition on a highly-dispersed carbon-embedded iron catalyst derived from Fe-BTC: stable and high performance at relatively low temperatures, Int. J. Hydrogen Energy 45 (53) (2020) 28664–28681, https://doi.org/10.1016/j.ijhydene.2020.07.188.
[175] Y. Yusran, H. Li, X. Guan, Q. Fang, S. Qiu, Covalent organic frameworks for catalysis, EnergyChem 2 (3) (2020) 100035, https://doi.org/10.1016/j.enchem.2020.100035.
[176] G.S. Deiko, V.I. Isaeva, L.M. Kustov, New molecular sieve materials: composites based on metal–organic frameworks and ionic liquids, Petrol. Chem. 59 (8) (2019) 770–787, https://doi.org/10.1134/s096554411908005x.
[177] S.Y. Chong, T.T. Wang, L.C. Cheng, H.Y. Lv, M. Ji, Metal-organic framework MIL-101-NH_2-supported acetate-based butylimidazolium ionic liquid as a highly efficient heterogeneous catalyst for the synthesis of 3-Aryl-2-oxazolidinones, Langmuir 35 (2) (2019) 495–503, https://doi.org/10.1021/acs.langmuir.8b03153.
[178] S. Askari, M. Jafarzadeh, D.B. Christensen, S. Kegnæs, A synergic activity of urea/butyl imidazolium ionic liquid supported on UiO-66-NH_2 metal–organic framework for synthesis of oximes, Catal. Lett. 150 (11) (2020) 3159–3173, https://doi.org/10.1007/s10562-020-03203-1.
[179] W. Xiang, C. Shen, Z. Lu, S. Chen, X. Li, R. Zou, Y. Zhang, C.-j. Liu, CO_2 cycloaddition over ionic liquid immobilized hybrid zeolitic imidazolate frameworks: effect of Lewis acid/base sites, Chem. Eng. Sci. 233 (2021) 116429, https://doi.org/10.1016/j.ces.2020.116429.
[180] Y. Wu, Y. Xiao, H. Yuan, Z. Zhang, S. Shi, R. Wei, L. Gao, G. Xiao, Imidazolium ionic liquid functionalized UiO-66-NH_2 as highly efficient catalysts for chemical fixation of CO_2 into cyclic carbonates, Microporous Mesoporous Mater. 310 (2021) 110578, https://doi.org/10.1016/j.micromeso.2020.110578.
[181] E.S. Larrea, R. Fernández de Luis, A. Fidalgo-Marijuan, E.M. Maya, M. Iglesias, M. I. Arriortua, Study of the versatility of CuBTC@IL-derived materials for heterogeneous catalysis, CrystEngComm 22 (17) (2020) 2904–2913, https://doi.org/10.1039/c9ce01157a.
[182] M. Bahadori, S. Tangestaninejad, M. Bertmer, M. Moghadam, V. Mirkhani, I. Mohammadpoor−Baltork, R. Kardanpour, F. Zadehahmadi, Task-specific ionic liquid functionalized–MIL–101(Cr) as a heterogeneous and efficient catalyst for the cycloaddition of CO_2 with epoxides under solvent free conditions, ACS Sustain. Chem. Eng. 7 (4) (2019) 3962–3973, https://doi.org/10.1021/acssuschemeng.8b05226.
[183] D. Ma, B. Li, K. Liu, X. Zhang, W. Zou, Y. Yang, G. Li, Z. Shi, S. Feng, Bifunctional MOF heterogeneous catalysts based on the synergy of dual functional sites for efficient conversion of CO_2 under mild and co-catalyst free conditions, J. Mater. Chem. A 3 (46) (2015) 23136–23142, https://doi.org/10.1039/C5TA07026K.
[184] J. Tharun, K.-M. Bhin, R. Roshan, D.W. Kim, A.C. Kathalikkattil, R. Babu, H. Y. Ahn, Y.S. Won, D.-W. Park, Ionic liquid tethered post functionalized ZIF-90 framework for the cycloaddition of propylene oxide and CO_2, Green Chem. 18 (8) (2016) 2479–2487, https://doi.org/10.1039/C5GC02153G.
[185] L.G. Ding, B.J. Yao, W.L. Jiang, J.T. Li, Q.J. Fu, Y.A. Li, Z.H. Liu, J.P. Ma, Y. B. Dong, Bifunctional imidazolium-based ionic liquid decorated UiO-67 type MOF for selective CO_2 adsorption and catalytic property for CO_2 cycloaddition with epoxides, Inorg. Chem. 56 (4) (2017) 2337–2344, https://doi.org/10.1021/acs.inorgchem.6b03169.
[186] J. Liang, R.P. Chen, X.Y. Wang, T.T. Liu, X.S. Wang, Y.B. Huang, R. Cao, Postsynthetic ionization of an imidazole-containing metal-organic framework for the cycloaddition of carbon dioxide and epoxides, Chem. Sci. 8 (2) (2017) 1570–1575, https://doi.org/10.1039/c6sc04357g.
[187] Y.L. Hu, R.L. Zhang, D. Fang, Quaternary phosphonium cationic ionic liquid/porous metal–organic framework as an efficient catalytic system for cycloaddition of carbon dioxide into cyclic carbonates, Environ. Chem. Lett. 17 (1) (2018) 501–508, https://doi.org/10.1007/s10311-018-0793-9.
[188] D. Liu, G. Li, H. Liu, Functionalized MIL-101 with imidazolium-based ionic liquids for the cycloaddition of CO_2 and epoxides under mild condition, Appl. Surf. Sci. 428 (2018) 218–225, https://doi.org/10.1016/j.apsusc.2017.09.040.
[189] Y. Sun, H. Huang, H. Vardhan, B. Aguila, C. Zhong, J.A. Perman, A.M. Al-Enizi, A. Nafady, S. Ma, Facile approach to graft ionic liquid into MOF for improving the efficiency of CO_2 chemical fixation, ACS Appl. Mater. Interfaces 10 (32) (2018) 27124–27130, https://doi.org/10.1021/acsami.8b08914.
[190] T. Wang, X. Song, Q. Luo, X. Yang, S. Chong, J. Zhang, M. Ji, Acid-base bifunctional catalyst: carboxyl ionic liquid immobilized on MIL-101-NH_2 for rapid synthesis of propylene carbonate from CO_2 and propylene oxide under facile solvent-free conditions, Microporous Mesoporous Mater. 267 (2018) 84–92, https://doi.org/10.1016/j.micromeso.2018.03.011.
[191] J. Cao, W. Shan, Q. Wang, X. Ling, G. Li, Y. Lyu, Y. Zhou, J. Wang, Ordered porous poly(ionic liquid) crystallines: spacing confined ionic surface enhancing selective CO_2 capture and fixation, ACS Appl. Mater. Interfaces 11 (6) (2019) 6031–6041, https://doi.org/10.1021/acsami.8b19420.
[192] J.F. Kurisingal, Y. Rachuri, R.S. Pillai, Y. Gu, Y. Choe, D.W. Park, Ionic-liquid-functionalized UiO-66 framework: an experimental and theoretical study on the cycloaddition of CO_2 and epoxides, ChemSusChem 12 (5) (2019) 1033–1042, https://doi.org/10.1002/cssc.201802838.
[193] M. Bahadori, A. Marandi, S. Tangestaninejad, M. Moghadam, V. Mirkhani, I. Mohammadpoor-Baltork, Ionic liquid-decorated MIL-101(Cr) via covalent and coordination bonds for efficient solvent-free CO_2 conversion and CO_2 capture at low pressure, J. Phys. Chem. C 124 (16) (2020) 8716–8725, https://doi.org/10.1021/acs.jpcc.9b11668.
[194] H. Yuan, Y. Wu, X. Pan, L. Gao, G. Xiao, Pyridyl ionic liquid functionalized ZIF-90 for catalytic conversion of CO_2 into cyclic carbonates, Catal. Lett. 150 (12) (2020) 3561–3571, https://doi.org/10.1007/s10562-020-03259-z.
[195] H. Shi, Z. Gu, M. Han, C. Chen, Z. Chen, J. Ding, Q. Wang, H. Wan, G. Guan, Preparation of heterogeneous interfacial catalyst benzimidazole-based acid ILs@

MIL-100(Fe) and its application in esterification, Colloids Surf., A 608 (2021) 125585, https://doi.org/10.1016/j.colsurfa.2020.125585.
[196] W. Xie, F. Wan, Biodiesel production from acidic oils using polyoxometalate-based sulfonated ionic liquids functionalized metal–organic frameworks, Catal. Lett. 149 (10) (2019) 2916–2929, https://doi.org/10.1007/s10562-019-02800-z.
[197] M. Han, Y. Li, Z. Gu, H. Shi, C. Chen, Q. Wang, H. Wan, G. Guan, Immobilization of thiol-functionalized ionic liquids onto the surface of MIL-101(Cr) frameworks by S Cr coordination bond for biodiesel production, Colloids Surf., A 553 (2018) 593–600, https://doi.org/10.1016/j.colsurfa.2018.05.085.
[198] Z. Xu, G. Zhao, L. Ullah, M. Wang, A. Wang, Y. Zhang, S. Zhang, Acidic ionic liquid based UiO-67 type MOFs: a stable and efficient heterogeneous catalyst for esterification, RSC Adv. 8 (18) (2018) 10009–10016, https://doi.org/10.1039/c8ra01119b.
[199] C. Ye, Z. Qi, D. Cai, T. Qiu, Design and synthesis of ionic liquid supported hierarchically porous Zr metal–organic framework as a novel Brønsted–Lewis acidic catalyst in biodiesel synthesis, Ind. Eng. Chem. Res. 58 (3) (2018) 1123–1132, https://doi.org/10.1021/acs.iecr.8b04107.
[200] W. Xie, F. Wan, Immobilization of polyoxometalate-based sulfonated ionic liquids on UiO-66-2COOH metal-organic frameworks for biodiesel production via one-pot transesterification-esterification of acidic vegetable oils, Chem. Eng. J. 365 (2019) 40–50, https://doi.org/10.1016/j.cej.2019.02.016.
[201] Z. Qi, T. Qiu, H. Wang, C. Ye, Synthesis of ionic-liquid-functionalized UiO-66 framework by post-synthetic ligand exchange for the ultra-deep desulfurization, Fuel 268 (2020) 117336, https://doi.org/10.1016/j.fuel.2020.117336.
[202] Z. Qi, Z. Huang, H. Wang, L. Li, C. Ye, T. Qiu, In situ bridging encapsulation of a carboxyl-functionalized phosphotungstic acid ionic liquid in UiO-66: a remarkable catalyst for oxidative desulfurization, Chem. Eng. Sci. 225 (2020) 115818, https://doi.org/10.1016/j.ces.2020.115818.
[203] W. Yang, G. Guo, Z. Mei, Y. Yu, Deep oxidative desulfurization of model fuels catalysed by immobilized ionic liquid on MIL-100(Fe), RSC Adv. 9 (38) (2019) 21804–21809, https://doi.org/10.1039/c9ra03035b.
[204] J. Qiu, Y. Zhao, Z. Li, H. Wang, Y. Shi, J. Wang, Imidazolium-salt-functionalized covalent organic frameworks for highly efficient catalysis of CO_2 conversion, ChemSusChem 12 (11) (2019) 2421–2427, https://doi.org/10.1002/cssc.201900570.
[205] W.-G. Cui, G.-Y. Zhang, T.-L. Hu, X.-H. Bu, Metal-organic framework-based heterogeneous catalysts for the conversion of C1 chemistry: CO, CO_2 and CH_4, Coord. Chem. Rev. 387 (2019) 79–120, https://doi.org/10.1016/j.ccr.2019.02.001.
[206] M.E. Borges, L. Díaz, Recent developments on heterogeneous catalysts for biodiesel production by oil esterification and transesterification reactions: a review, Renew. Sustain. Energy Rev. 16 (5) (2012) 2839–2849, https://doi.org/10.1016/j.rser.2012.01.071.
[207] B. Dong, L. Wang, S. Zhao, R. Ge, X. Song, Y. Wang, Y. Gao, Immobilization of ionic liquids to covalent organic frameworks for catalyzing the formylation of amines with CO_2 and phenylsilane, Chem. Commun. 52 (44) (2016) 7082–7085, https://doi.org/10.1039/c6cc03058k.
[208] Y. Zhao, Y. Zhao, J. Qiu, Z. Li, H. Wang, J. Wang, Facile grafting of imidazolium salt in covalent organic frameworks with enhanced catalytic activity for CO_2 fixation and the Knoevenagel reaction, ACS Sustain. Chem. Eng. 8 (50) (2020) 18413–18419, https://doi.org/10.1021/acssuschemeng.0c05294.
[209] S. Bhatia, Zeolite Catalysts: Principles and Applications, CRC press, 2020.
[210] B. Sarmah, R. Srivastava, Activation and utilization of CO_2 using ionic liquid or amine-functionalized basic nanocrystalline zeolites for the synthesis of cyclic carbonates and quinazoline-2,4(1H,3H)-dione, Ind. Eng. Chem. Res. 56 (29) (2017) 8202–8215, https://doi.org/10.1021/acs.iecr.7b01406.
[211] L. Guo, L. Deng, X. Jin, Y. Wang, H. Wang, Catalytic conversion of CO_2 into propylene carbonate in a continuous fixed bed reactor by immobilized ionic liquids, RSC Adv. 8 (47) (2018) 26554–26562, https://doi.org/10.1039/c8ra03952f.
[212] N. Nokhodiyan Isfahani, M. Bahadori, A. Marandi, S. Tangestaninejad, M. Moghadam, V. Mirkhani, M. Beheshti, N. Afzali, Ionic liquid modification of hierarchical ZSM-5 for solvent-free insertion of CO_2 to epoxides, Ind. Eng. Chem. Res. 59 (26) (2020) 11970–11978, https://doi.org/10.1021/acs.iecr.0c01173.
[213] B. Wang, H. Lai, Y. Yue, G. Sheng, Y. Deng, H. He, L. Guo, J. Zhao, X. Li, Zeolite supported ionic liquid catalysts for the hydrochlorination of acetylene, Catalysts 8 (9) (2018), https://doi.org/10.3390/catal8090351.
[214] Y. Hong, Y. Fang, X. Zhou, G. Du, J. Mai, D. Sun, Z. Shao, Ionic liquid-modified Co/ZSM-5 catalyzed the aerobic oxidation of cyclohexane: toward improving the activity and selectivity, Ind. Eng. Chem. Res. 58 (43) (2019) 19832–19838, https://doi.org/10.1021/acs.iecr.9b04100.
[215] M. Tunckol, J. Durand, P. Serp, Carbon nanomaterial–ionic liquid hybrids, Carbon 50 (12) (2012) 4303–4334, https://doi.org/10.1016/j.carbon.2012.05.017.
[216] J. Xu, M. Xu, J. Wu, H. Wu, W.-H. Zhang, Y.-X. Li, Graphene oxide immobilized with ionic liquids: facile preparation and efficient catalysis for solvent-free cycloaddition of CO_2 to propylene carbonate, RSC Adv. 5 (88) (2015) 72361–72368, https://doi.org/10.1039/c5ra13533h.
[217] S. Baj, T. Krawczyk, K. Jasiak, A. Siewniak, M. Pawlyta, Catalytic coupling of epoxides and CO_2 to cyclic carbonates by carbon nanotube-supported quaternary ammonium salts, Appl. Catal., A 488 (2014) 96–102, https://doi.org/10.1016/j.apcata.2014.09.034.
[218] S. Gajare, A. Patil, D. Kale, P. Bansode, P. Patil, G. Rashinkar, Graphene oxide-supported ionic liquid phase catalyzed synthesis of 3,4-dihydro-2H-naphtho[2,3-e][1,3]oxazine-5,10-diones, Catal. Lett. 150 (1) (2019) 243–255, https://doi.org/10.1007/s10562-019-02934-0.
[219] H. Zhang, Q. Zhang, L. Zhang, T. Pei, L. Dong, P. Zhou, C. Li, L. Xia, Acidic polymeric ionic liquids based reduced graphene oxide: an efficient and rewriteable catalyst for oxidative desulfurization, Chem. Eng. J. 334 (2018) 285–295, https://doi.org/10.1016/j.cej.2017.10.042.
[220] Z. Yu, X. Huang, S. Xun, M. He, L. Zhu, L. Wu, M. Yuan, W. Zhu, H. Li, Synthesis of carbon nitride supported amphiphilic phosphotungstic acid based ionic liquid for deep oxidative desulfurization of fuels, J. Mol. Liq. 308 (2020), https://doi.org/10.1016/j.molliq.2020.113059.
[221] C. Garkoti, J. Shabir, S. Mozumdar, Amine-terminated ionic liquid modified magnetic graphene oxide (MGO-IL-NH_2): a highly efficient and reusable nanocatalyst for the synthesis of 3-amino alkylated indoles, ChemistrySelect 5 (14) (2020) 4337–4346, https://doi.org/10.1002/slct.202000336.
[222] Z. Zhang, Y. Chen, L. Zhou, C. Chen, Z. Han, B. Zhang, Q. Wu, L. Yang, L. Du, Y. Bu, The simplest construction of single-site catalysts by the synergism of micropore trapping and nitrogen anchoring, Nat. Commun. 10 (1) (2019) 1–7, https://doi.org/10.1038/s41467-019-09596-x.
[223] L. Zhang, X. Liu, X. Zhou, S. Gao, N. Shang, C. Feng, C. Wang, Ultrafine Pd nanoparticles anchored on nitrogen-doping carbon for boosting catalytic transfer hydrogenation of nitroarenes, ACS Omega 3 (9) (2018) 10843–10850, https://doi.org/10.1021/acsomega.8b01141.
[224] X. Duan, L. Ning, Y. Yin, Y. Huang, J. Gao, H. Lin, K. Tan, H. Fang, L. Ye, X. Lu, Y. Yuan, Sulfur moiety as a double-edged sword for realizing ultrafine supported metal nanoclusters with a cationic nature, ACS Appl. Mater. Interfaces 11 (12) (2019) 11317–11326, https://doi.org/10.1021/acsami.8b18952.
[225] M. Babucci, F.E. Sarac Oztuna, L.M. Debefve, A. Boubnov, S.R. Bare, B.C. Gates, U. Unal, A. Uzun, Atomically dispersed reduced graphene aerogel-supported iridium catalyst with an iridium loading of 14.8 wt %, ACS Catal. 9 (11) (2019) 9905–9913, https://doi.org/10.1021/acscatal.9b02231.
[226] R. Göbel, P. Hesemann, J. Weber, E. Möller, A. Friedrich, S. Beuermann, A. Taubert, Surprisingly high, bulk liquid-like mobility of silica-confined ionic liquids, Phys. Chem. Chem. Phys. 11 (19) (2009) 3653–3662, https://doi.org/10.1039/B821833A.
[227] M. Kanakubo, Y. Hiejima, K. Minami, T. Aizawa, H. Nanjo, Melting point depression of ionic liquids confined in nanospaces, Chem. Commun. 17 (2006) 1828–1830, https://doi.org/10.1039/B600074F.
[228] Z. Lei, J. Shen, W. Zhang, Q. Wang, J. Wang, Y. Deng, C. Wang, Exploring porous zeolitic imidazolate frame work-8 (ZIF-8) as an efficient filler for high-performance poly(ethyleneoxide)-based solid polymer electrolytes, Nano Res. 13 (8) (2020) 2259–2267, https://doi.org/10.1007/s12274-020-2845-2.
[229] K. Fujie, R. Ikeda, K. Otsubo, T. Yamada, H. Kitagawa, Lithium ion diffusion in a metal–organic framework mediated by an ionic liquid, Chem. Mater. 27 (21) (2015) 7355–7361, https://doi.org/10.1021/acs.chemmater.5b02986.
[230] Z. Lei, J. Shen, J. Wang, Q. Qiu, G. Zhang, S.-S. Chi, H. Xu, S. Li, W. Zhang, Y. Zhao, Y. Deng, C. Wang, Composite polymer electrolytes with uniform distribution of ionic liquid-grafted ZIF-90 nanofillers for high-performance solid-state Li batteries, Chem. Eng. J. 412 (2021) 128733, https://doi.org/10.1016/j.cej.2021.128733.
[231] F. Castiglione, E. Ragg, A. Mele, G.B. Appetecchi, M. Montanino, S. Passerini, Molecular environment and enhanced diffusivity of Li^+ ions in lithium-salt-doped ionic liquid electrolytes, J. Phys. Chem. Lett. 2 (3) (2011) 153–157, https://doi.org/10.1021/jz101516c.
[232] M. Li, T. Chen, S. Song, Y. Li, J. Bae, HKUST-1@IL-Li solid-state electrolyte with 3D ionic channels and enhanced fast Li+ transport for lithium metal batteries at high temperature, Nanomaterials 11 (3) (2021), https://doi.org/10.3390/nano11030736.
[233] J.-F. Wu, X. Guo, Nanostructured metal–organic framework (MOF)-Derived solid electrolytes realizing fast lithium ion transportation kinetics in solid-state batteries, Small 15 (5) (2019) 1804413, https://doi.org/10.1002/smll.201804413.
[234] Q. Xu, X. Zhang, S. Zeng, L. Bai, S. Zhang, Ionic liquid incorporated metal organic framework for high ionic conductivity over extended temperature range, ACS Sustain. Chem. Eng. 7 (8) (2019) 7892–7899, https://doi.org/10.1021/acssuschemeng.9b00543.
[235] Q. Xu, F. Yang, X. Zhang, J.R. Li, J.F. Chen, S. Zhang, Combining ionic liquids and sodium salts into metal-organic framework for high-performance ionic conduction, Chemelectrochem 7 (1) (2020) 183–190, https://doi.org/10.1002/celc.201901753.
[236] V. Nozari, C. Calahoo, J.M. Tuffnell, P. Adelhelm, K. Wondraczek, S.E. Dutton, T. D. Bennett, L. Wondraczek, Sodium ion conductivity in superionic IL-impregnated metal-organic frameworks: enhancing stability through structural disorder, Sci. Rep. 10 (1) (2020) 3532, https://doi.org/10.1038/s41598-020-60198-w.
[237] W.L. Xue, W.H. Deng, H. Chen, R.H. Liu, J.M. Taylor, Y.K. Li, L. Wang, Y.H. Deng, W.H. Li, Y.Y. Wen, G.E. Wang, C.Q. Wan, G. Xu, MOF-Directed synthesis of crystalline ionic liquids with enhanced proton conduction, Angew. Chem. Int. Ed. (2020), https://doi.org/10.1002/anie.202010783.
[238] J.M. Tuffnell, J.K. Morzy, N.D. Kelly, R. Tan, Q. Song, C. Ducati, T.D. Bennett, S. E. Dutton, Comparison of the ionic conductivity properties of microporous and mesoporous MOFs infiltrated with a Na-ion containing IL mixture, Dalton Trans. 49 (44) (2020) 15914–15924, https://doi.org/10.1039/D0DT02576C.
[239] A.B. Kanj, R. Verma, M. Liu, J. Helfferich, W. Wenzel, L. Heinke, Bunching and immobilization of ionic liquids in nanoporous metal–organic framework, Nano Lett. 19 (3) (2019) 2114–2120, https://doi.org/10.1021/acs.nanolett.8b04694.
[240] S. Shalini, T.P. Vaid, A.J. Matzger, Salt nanoconfinement in zirconium-based metal–organic frameworks leads to pore-size and loading-dependent ionic conductivity enhancement, Chem. Commun. 56 (53) (2020) 7245–7248, https://doi.org/10.1039/D0CC03147J.

[241] Z. Zhang, C. Li, A. Chandresh, L. Heinke, Conductivity measurement of ionic liquids confined in the nanopores of metal–organic frameworks: a case study for [BMIM][TFSI] in HKUST-1, Ionics. https://doi.org/10.1007/s11581-021-04249-w, 2021.
[242] M. Vazquez, M. Liu, Z. Zhang, A. Chandresh, A.B. Kanj, W. Wenzel, L. Heinke, Structural and dynamic insights into the conduction of lithium-ionic-liquid mixtures in nanoporous metal–organic frameworks as solid-state electrolytes, ACS Appl. Mater. Interfaces 13 (18) (2021) 21166–21174, https://doi.org/10.1021/acsami.1c00366.
[243] Z. Li, Z.-W. Liu, Z.-J. Mu, C. Cao, Z. Li, T.-X. Wang, Y. Li, X. Ding, B.-H. Han, W. Feng, Cationic covalent organic framework based all-solid-state electrolytes, Mater. Chem. Front. 4 (4) (2020) 1164–1173, https://doi.org/10.1039/C9QM00781D.
[244] Y. Xin, N. Wang, C. Wang, W. Gao, M. Chen, N. Liu, J. Duan, B. Hou, Electrochemical detection of hydroquinone and catechol with covalent organic framework modified carbon paste electrode, J. Electroanal. Chem. 877 (2020), https://doi.org/10.1016/j.jelechem.2020.114530, 114530-114530.
[245] P. Li, J. Chen, S. Tang, Ionic liquid-impregnated covalent organic framework/silk nanofibril composite membrane for efficient proton conduction, Chem. Eng. J. (2021) 129021, https://doi.org/10.1016/j.cej.2021.129021.
[246] D.N. Stamires, Effect of adsorbed phases on the electrical conductivity of synthetic crystalline zeolites, J. Chem. Phys. 36 (12) (1962) 3174–3181, https://doi.org/10.1063/1.1732446.
[247] S. Ntais, A.M. Moschovi, F. Paloukis, S. Neophytides, V.N. Burganos, V. Dracopoulos, V. Nikolakis, Preparation and ion transport properties of NaY zeolite–ionic liquid composites, J. Power Sources 196 (4) (2011) 2202–2210, https://doi.org/10.1016/j.jpowsour.2010.09.061.
[248] A. Eguizábal, J. Lemus, M. Urbiztondo, A.M. Moschovi, S. Ntais, J. Soler, M. P. Pina, Ammonium based ionic liquids immobilized in large pore zeolites: encapsulation procedures and proton conduction performance, J. Power Sources 196 (9) (2011) 4314–4323, https://doi.org/10.1016/j.jpowsour.2010.12.019.
[249] A. Eguizábal, J. Lemus, M.P. Pina, On the incorporation of protic ionic liquids imbibed in large pore zeolites to polybenzimidazole membranes for high temperature proton exchange membrane fuel cells, J. Power Sources 222 (2013) 483–492, https://doi.org/10.1016/j.jpowsour.2012.07.094.
[250] L.G. da Trindade, E.C. Pereira, SPEEK/Zeolite/Ionic-Liquid anhydrous polymer membranes for fuel-cell applications, Eur. J. Inorg. Chem. 17 (2017) 2369–2376, https://doi.org/10.1002/ejic.201601559, 2017.
[251] M.D. Stoller, S. Park, Z. Yanwu, J. An, R.S. Ruoff, Graphene-Based ultracapacitors, Nano Lett. 8 (10) (2008) 3498–3502, https://doi.org/10.1021/nl802558y.
[252] X. Fu, D. Yu, J. Zhou, S. Li, X. Gao, Y. Han, P. Qi, X. Feng, B. Wang, Inorganic and Organic Hybrid Solid Electrolytes for Lithium-Ion Batteries, CrystEngComm 18 (2016) 4236–4258, https://doi.org/10.1039/C6CE00171H.
[253] Y. Sun, Y. Wang, C. Zhang, S. Chen, H. Chang, N. Guo, J. Liu, Y. Jia, L. Wang, Y. Weng, W. Zhao, K. Jiang, L. Xiao, Flexible mid-infrared radiation modulator with multilayer graphene thin film by ionic liquid gating, ACS Appl. Mater. Interfaces 11 (14) (2019) 13538–13544, https://doi.org/10.1021/acsami.8b21900.
[254] T.Y. Kim, H.W. Lee, M. Stoller, D.R. Dreyer, C.W. Bielawski, R.S. Ruoff, K.S. Suh, High-performance supercapacitors based on poly(ionic liquid)-modified graphene electrodes, ACS Nano 5 (1) (2011) 436–442, https://doi.org/10.1021/nn101968p.
[255] M.P. Down, C.E. Banks, Freestanding three-dimensional graphene macroporous supercapacitor, ACS Appl. Energy Mater. 1 (2) (2018) 891–899, https://doi.org/10.1021/acsaem.7b00338.
[256] A.P. Saxena, M. Deepa, A.G. Joshi, S. Bhandari, A.K. Srivastava, Poly(3,4-ethylenedioxythiophene)-Ionic liquid functionalized graphene/reduced graphene oxide nanostructures: improved conduction and electrochromism, ACS Appl. Mater. Interfaces 3 (4) (2011) 1115–1126, https://doi.org/10.1021/am101255a.
[257] M. Chen, Y. Wang, W. Ma, Y. Huang, Z. Zhao, Ionic liquid gating enhanced photothermoelectric conversion in three-dimensional microporous graphene, ACS Appl. Mater. Interfaces 12 (25) (2020) 28510–28519, https://doi.org/10.1021/acsami.0c05833.
[258] D.J. Bozym, S. Korkut, M.A. Pope, I.A. Aksay, Dehydrated sucrose nanoparticles as spacers for graphene-ionic liquid supercapacitor electrodes, ACS Sustain. Chem. Eng. 4 (12) (2016) 7167–7174, https://doi.org/10.1021/acssuschemeng.6b02050.
[259] Y. Liu, Y. Wang, Y. Nie, C. Wang, X. Ji, L. Zhou, F. Pan, S. Zhang, Preparation of MWCNTs-graphene-cellulose fiber with ionic liquids, ACS Sustain. Chem. Eng. 7 (24) (2019) 20013–20021, https://doi.org/10.1021/acssuschemeng.9b05489.
[260] M. Martinez, Y. Molmeret, L. Cointeaux, C. Iojoiu, J.C. Leprêtre, N. El Kissi, P. Judeinstein, J.Y. Sanchez, Proton-conducting ionic liquid-based Proton Exchange Membrane Fuel Cell membranes: the key role of ionomer-ionic liquid interaction, J. Power Sources 195 (18) (2010) 5829–5839, https://doi.org/10.1016/j.jpowsour.2010.01.036.
[261] V. Compañ, J. Escorihuela, J. Olvera, A. García-Bernabé, A. Andrio, Influence of the anion on diffusivity and mobility of ionic liquids composite polybenzimidazol membranes, Electrochim. Acta 354 (2020), https://doi.org/10.1016/j.electacta.2020.136666, 136666-136666.
[262] A. Al-Othman, P. Nancarrow, M. Tawalbeh, A. Ka'Ki, K. El-Ahwal, B. El Taher, M. Alkasrawi, Novel composite membrane based on zirconium phosphate-ionic liquids for high temperature PEM fuel cells, Int. J. Hydrogen Energy (2020), https://doi.org/10.1016/j.ijhydene.2020.02.112.
[263] B. Niu, S. Luo, C. Lu, W. Yi, J. Liang, S. Guo, D. Wang, F. Zeng, S. Duan, Y. Liu, L. Zhang, B. Xu, Polybenzimidazole and ionic liquid composite membranes for high temperature polymer electrolyte fuel cells, Solid State Ionics 361 (2021) 115569, https://doi.org/10.1016/j.ssi.2021.115569.
[264] T. Zhang, G. Yu, X. Liang, N. Zhao, F. Zhang, F. Qu, Development of anion conducting zeolitic imidazolate framework bottle around ship incorporated with ionic liquids, Int. J. Hydrogen Energy 44 (29) (2019) 14481–14492, https://doi.org/10.1016/j.ijhydene.2019.04.044.
[265] A. Wang, H. Xu, F. Liu, X. Liu, S. Wang, Q. Zhou, J. Chen, S. Yang, L. Zhang, Polyimide-based self-standing polymer electrolyte membrane for lithium-ion batteries, Energy Technol. 6 (2) (2018) 326–332, https://doi.org/10.1002/ente.201700477.
[266] J.C. Barbosa, D.M. Correia, R. Gonçalves, V. de Zea Bermudez, M.M. Silva, S. Lanceros-Mendez, C.M. Costa, Enhanced ionic conductivity in poly(vinylidene fluoride) electrospun separator membranes blended with different ionic liquids for lithium ion batteries, J. Colloid Interface Sci. 582 (2021) 376–386, https://doi.org/10.1016/j.jcis.2020.08.046.
[267] A. Ka'ki, A. Alraeesi, A. Al-Othman, M. Tawalbeh, Proton conduction of novel calcium phosphate nanocomposite membranes for high temperature PEM fuel cells applications, Int. J. Hydrogen Energy (2021), https://doi.org/10.1016/j.ijhydene.2021.01.013.
[268] H. Mohammed, A. Al-Othman, P. Nancarrow, Y. Elsayed, M. Tawalbeh, Enhanced proton conduction in zirconium phosphate/ionic liquids materials for high-temperature fuel cells, Int. J. Hydrogen Energy 46 (6) (2021) 4857–4869, https://doi.org/10.1016/j.ijhydene.2019.09.118.
[269] X. Hu, X. Jia, K. Su, X. Gu, Electronic structural properties of amino/hydroxyl functionalized imidazolium-based bromide ionic liquids, Open Chemistry 18 (1) (2020) 576–583, https://doi.org/10.1515/chem-2020-0068.
[270] N.V. Ilawe, J. Fu, S. Ramanathan, B.M. Wong, J. Wu, Chemical and radiation stability of ionic liquids: a computational screening study, J. Phys. Chem. C 120 (49) (2016) 27757–27767, https://doi.org/10.1021/acs.jpcc.6b08138.
[271] R. Vijayalakshmi, R.A.-O. Anantharaj, A. Brinda Lakshmi, Evaluation of chemical reactivity and stability of ionic liquids using ab initio and COSMO-RS model, (1096-987X (electronic)). https://doi.org/10.1002/jcc.26136, 2020.
[272] M. Souto, K. Strutyński, M. Melle-Franco, J. Rocha, Electroactive organic building blocks for the chemical design of functional porous frameworks (MOFs and COFs) in electronics, Chem. Eur J. 26 (48) (2020) 10912–10935, https://doi.org/10.1002/chem.202001211.
[273] R. Zou, P.-Z. Li, Y.-F. Zeng, J. Liu, R. Zhao, H. Duan, Z. Luo, J.-G. Wang, R. Zou, Y. Zhao, Bimetallic metal-organic frameworks: probing the Lewis acid site for CO_2 conversion, Small 12 (17) (2016) 2334–2343, https://doi.org/10.1002/smll.201503741.
[274] M. Arjmandi, M. Peyravi, M. Pourafshari Chenar, M. Jahanshahi, A. Arjmandi, Study of adsorption of H_2 and CO_2 on distorted structure of MOF-5 framework; A comprehensive DFT study, J. Water Environ. Nanotechnol. 3 (1) (2018) 70–80, https://doi.org/10.22090/jwent.2018.01.007.
[275] C.D. Rodríguez-Fernández, E. López Lago, C. Schröder, L.M. Varela, Non-additive electronic polarizabilities of ionic liquids: charge delocalization effects, J. Mol. Liq. (2021) 117099, https://doi.org/10.1016/j.molliq.2021.117099.
[276] V. Bernales, M.A. Ortuño, D.G. Truhlar, C.J. Cramer, L. Gagliardi, Computational design of functionalized metal–organic framework nodes for catalysis, ACS Cent. Sci. 4 (1) (2018) 5–19, https://doi.org/10.1021/acscentsci.7b00500.
[277] T. Maihom, S. Choomwattana, S. Wannakao, M. Probst, J. Limtrakul, Ethylene epoxidation with nitrous oxide over Fe–BTC metal–organic frameworks: a DFT study, ChemPhysChem 17 (21) (2016) 3416–3422, https://doi.org/10.1002/cphc.201600836.
[278] P. Valvekens, M. Vandichel, M. Waroquier, V. Van Speybroeck, D. De Vos, Metal-dioxidoterephthalate MOFs of the MOF-74 type: microporous basic catalysts with well-defined active sites, J. Catal. 317 (2014) 1–10, https://doi.org/10.1016/j.jcat.2014.06.006.
[279] A. Cândido, T. Rozada, A. Rozada, J. Souza, E. Pilau, F. Rosa, E. Basso, G. Gauze, Mechanistic investigation of DBU-based ionic liquids for aza-michael reaction: mass spectrometry and DFT studies of catalyst role, J. Braz. Chem. Soc. 31 (2020), https://doi.org/10.21577/0103-5053.20200066.
[280] X. Li, CO_2 cycloaddition with propylene oxide to form propylene carbonate on a copper metal-organic framework: a density functional theory study, Mol. Catal. 463 (2018), https://doi.org/10.1016/j.mcat.2018.11.015.
[281] T.-D. Hu, Y.-W. Sun, Y.-H. Ding, A quantum-chemical insight on chemical fixation carbon dioxide with epoxides co-catalyzed by MIL-101 and tetrabutylammonium bromide, J. CO_2 Util. 28 (2018) 200–206, https://doi.org/10.1016/j.jcou.2018.09.027.
[282] J.P. Perdew, K. Burke, M. Ernzerhof, Generalized gradient approximation made simple, Phys. Rev. Lett. 77 (18) (1996) 3865–3868, https://doi.org/10.1103/PhysRevLett.77.3865.
[283] A.D. Becke, A new mixing of Hartree–Fock and local density-functional theories, J. Chem. Phys. 98 (2) (1993) 1372–1377, https://doi.org/10.1063/1.464304.
[284] C. Lee, W. Yang, R.G. Parr, Development of the Colle-Salvetti correlation-energy formula into a functional of the electron density, Phys. Rev. B 37 (2) (1988) 785–789, https://doi.org/10.1103/PhysRevB.37.785.
[285] A. Thomas, K.R. Maiyelvaganan, S. Kamalakannan, M. Prakash, Density functional theory studies on zeolitic imidazolate framework-8 and ionic liquid-based composite materials, ACS Omega 4 (27) (2019) 22655–22666, https://doi.org/10.1021/acsomega.9b03759.
[286] S. Grimme, J. Antony, S. Ehrlich, H. Krieg, A consistent and accurate ab initio parametrization of density functional dispersion correction (DFT-D) for the 94 elements H-Pu, J. Chem. Phys. 132 (15) (2010) 154104, https://doi.org/10.1063/1.3382344.

[287] Z. Zhang, X. Jia, Y. Sun, X. Guo, H. Huang, C. Zhong, Pore engineering of ZIF-8 with ionic liquids for membrane-based CO_2 separation: bearing functional group effect, Green Chem. Eng. 2 (1) (2021) 104–110, https://doi.org/10.1016/j.gce.2020.10.007.
[288] H. Abroshan, H.J. Kim, On the structural stability of ionic liquid–IRMOF composites: a computational study, Phys. Chem. Chem. Phys. 17 (9) (2015) 6248–6254, https://doi.org/10.1039/C4CP02428A.
[289] H. Can Gulbalkan, Z. Pınar Haslak, C. Altintas, A. Uzun, S. Keskin, Assessing CH_4/N_2 separation potential of MOFs, COFs, IL/MOF, MOF/polymer, and COF/polymer composites, Chem. Eng. J. (2021) 131239, https://doi.org/10.1016/j.cej.2021.131239.
[290] A.M.O. Mohamed, S. Moncho, P. Krokidas, K. Kakosimos, E.N. Brothers, I. G. Economou, Computational investigation of the performance of ZIF-8 with encapsulated ionic liquids towards CO_2 capture, Mol. Phys. 117 (23–24) (2019) 3791–3805, https://doi.org/10.1080/00268976.2019.1666170.
[291] X. Li, A.K. Cheetham, J. Jiang, CO_2 cycloaddition with propylene oxide to form propylene carbonate on a copper metal-organic framework: a density functional theory study, Mol. Catal. 463 (2019) 37–44, https://doi.org/10.1016/j.mcat.2018.11.015.
[292] M.A. Ishak, M.F. Taha, M.D. Wirzal, M.N. Nordin, M. Abdurrahman, K. Jumbri, Choline-based ionic liquids-incorporated IRMOF-1 for H_2S/CH_4 capture: insight from molecular dynamics simulation, Processes 8 (4) (2020), https://doi.org/10.3390/pr8040412.
[293] J. Cui, K. Zhang, X. Zhang, Y. Lee, A computational study to design zeolite-templated carbon materials with high performance for CO_2/N_2 separation, Microporous Mesoporous Mater. 295 (2020), https://doi.org/10.1016/j.micromeso.2019.109947, 109947.
[294] I. Skarmoutsos, E.N. Koukaras, E. Klontzas, The impact of ionic liquid loading in three-dimensional carbon nanotube networks on the separation of CO_2/CH_4 fluid mixtures: insights from molecular simulations, J. Phys. Chem. C 125 (24) (2021) 13508–13522, https://doi.org/10.1021/acs.jpcc.1c00346.
[295] Y. Zeng, K. Li, Q. Zhu, J. Wang, Y. Cao, S. Lu, Capture of CO_2 in carbon nanotube bundles supported with room-temperature ionic liquids: a molecular simulation study, Chem. Eng. Sci. 192 (2018) 94–102, https://doi.org/10.1016/j.ces.2018.07.025.
[296] B. Barzegar, F. Feyzi, Effect of ionic liquids in carbon nanotube bundles on CO_2, H_2S, and N_2 separation from CH_4: a computational study, J. Chem. Phys. 154 (19) (2021), https://doi.org/10.1063/5.0050230, 194504.
[297] L. Liu, D. Nicholson, S.K. Bhatia, Exceptionally high performance of charged carbon nanotube arrays for CO_2 separation from flue gas, Carbon 125 (2017) 245–257, https://doi.org/10.1016/j.carbon.2017.09.050.
[298] W. Xue, Z. Li, H. Huang, Q. Yang, D. Liu, Q. Xu, C. Zhong, Effects of ionic liquid dispersion in metal-organic frameworks and covalent organic frameworks on CO_2 capture: a computational study, Chem. Eng. Sci. 140 (2016) 1–9, https://doi.org/10.1016/j.ces.2015.10.003.
[299] R.C. Dutta, S.K. Bhatia, Interfacial engineering of MOF-based mixed matrix membrane through atomistic simulations, J. Phys. Chem. C 124 (1) (2019) 594–604, https://doi.org/10.1021/acs.jpcc.9b09384.
[300] A.M. Mohamed, P. Krokidas, I.G. Economou, Encapsulation of [$bmim^+$][Tf_2N^-] in different ZIF-8 metal analogues and evaluation of their CO_2 selectivity over CH_4 and N_2 using molecular simulation, Mol. Syst. Des. Eng. 5 (7) (2020) 1230–1238, https://doi.org/10.1039/D0ME00021C.
[301] A. Thomas, M. Prakash, The role of binary mixtures of ionic liquids in ZIF-8 for selective gas storage and separation: a perspective from computational approaches, J. Phys. Chem. C 124 (48) (2020) 26203–26213, https://doi.org/10.1021/acs.jpcc.0c07090.
[302] M. Maurya, J.K. Singh, Effect of ionic liquid impregnation in highly water-stable metal–organic frameworks, covalent organic frameworks, and carbon-based adsorbents for post-combustion flue gas treatment, Energy Fuels 33 (4) (2019) 3421–3428, https://doi.org/10.1021/acs.energyfuels.9b00179.
[303] A. Thomas, M. Prakash, Ionic liquid incorporation in zeolitic imidazolate framework-3 for improved CO_2 separation: a computational approach, Appl. Surf. Sci. (2021) 150173, https://doi.org/10.1016/j.apsusc.2021.150173.
[304] A.M. Mohamed, S. Moncho, P. Krokidas, K. Kakosimos, E.N. Brothers, I. G. Economou, Computational investigation of the performance of ZIF-8 with encapsulated ionic liquids towards CO_2 capture, Mol. Phys. 117 (23–24) (2019) 3791–3805, https://doi.org/10.1080/00268976.2019.1666170.
[305] K.M. Gupta, Y. Chen, Z. Hu, J. Jiang, Metal–organic framework supported ionic liquid membranes for CO_2 capture: anion effects, Phys. Chem. Chem. Phys. 14 (16) (2012) 5785–5794, https://doi.org/10.1039/C2CP23972H.
[306] J.M. Vicent-Luna, J.J. Gutiérrez-Sevillano, S. Hamad, J. Anta, S. Calero, Role of ionic liquid [$EMIM]^+$[$SCN]^-$ in the adsorption and diffusion of gases in metal–organic frameworks, ACS Appl. Mater. Interfaces 10 (35) (2018) 29694–29704, https://doi.org/10.1021/acsami.8b11842.
[307] H.M. Polat, M. Zeeshan, A. Uzun, S. Keskin, Unlocking CO_2 separation performance of ionic liquid/CuBTC composites: combining experiments with molecular simulations, Chem. Eng. J. 373 (2019) 1179–1189, https://doi.org/10.1016/j.cej.2019.05.113.
[308] J.M. Vicent-Luna, J.J. Gutiérrez-Sevillano, J.A. Anta, S. Calero, Effect of room-temperature ionic liquids on CO_2 separation by a Cu-BTC metal–organic framework, J. Phys. Chem. C 117 (40) (2013) 20762–20768, https://doi.org/10.1021/jp407176j.
[309] L.T. Oliveira, R.V. Gonçalves, D.V. Gonçalves, D.C.S. de Azevedo, S.M. Pereira de Lucena, Superior performance of mesoporous MOF MIL-100 (Fe) impregnated with ionic liquids for CO_2 adsorption, J. Chem. Eng. Data 64 (5) (2019) 2221–2228, https://doi.org/10.1021/acs.jced.8b01177.
[310] S.R. Venna, M.A. Carreon, Highly permeable zeolite imidazolate framework-8 membranes for CO_2/CH_4 separation, J. Am. Chem. Soc. 132 (1) (2010) 76–78, https://doi.org/10.1021/ja909263x.
[311] R. Babarao, Z. Hu, J. Jiang, S. Chempath, S.I. Sandler, Storage and separation of CO_2 and CH_4 in silicalite, C168 schwarzite, and IRMOF-1: a comparative study from Monte Carlo simulation, Langmuir 23 (2) (2007) 659–666, https://doi.org/10.1021/la062289p.
[312] Z. Liang, M. Marshall, A.L. Chaffee, Comparison of Cu-BTC and zeolite 13X for adsorbent based CO_2 separation, Energy Proc. 1 (1) (2009) 1265–1271, https://doi.org/10.1016/j.egypro.2009.01.166.
[313] Ü. Kökçam-Demir, A. Goldman, L. Esrafili, M. Gharib, A. Morsali, O. Weingart, C. Janiak, Coordinatively unsaturated metal sites (open metal sites) in metal–organic frameworks: design and applications, Chem. Soc. Rev. 49 (9) (2020) 2751–2798, https://doi.org/10.1039/C9CS00609E.
[314] J. Vicent-Luna, A. Luna-Triguero, S. Calero, Storage and separation of carbon dioxide and methane in hydrated covalent organic frameworks, J. Phys. Chem. C 120 (41) (2016) 23756–23762, https://doi.org/10.1021/acs.jpcc.6b05233.
[315] S. Surblé, F. Millange, C. Serre, T. Düren, M. Latroche, S. Bourrelly, P. L. Llewellyn, G. Férey, Synthesis of MIL-102, a chromium carboxylate metal–organic framework, with gas sorption analysis, J. Am. Chem. Soc. 128 (46) (2006) 14889–14896, https://doi.org/10.1021/ja064343u.
[316] Y.-S. Bae, K.L. Mulfort, H. Frost, P. Ryan, S. Punnathanam, L.J. Broadbelt, J. T. Hupp, R.Q. Snurr, Separation of CO_2 from CH_4 using mixed-ligand metal–organic frameworks, Langmuir 24 (16) (2008) 8592–8598, https://doi.org/10.1021/la800555x.
[317] J. Pérez-Pellitero, H. Amrouche, F.R. Siperstein, G. Pirngruber, C. Nieto-Draghi, G. Chaplais, A. Simon-Masseron, D. Bazer-Bachi, D. Peralta, N. Bats, Adsorption of CO_2, CH_4, and N_2 on zeolitic imidazolate frameworks: experiments and simulations, Chem. Eur J. 16 (5) (2010) 1560–1571, https://doi.org/10.1002/chem.200902144.
[318] C. Cadena, J.L. Anthony, J.K. Shah, T.I. Morrow, J.F. Brennecke, E.J. Maginn, Why is CO_2 so soluble in imidazolium-based ionic liquids? J. Am. Chem. Soc. 126 (16) (2004) 5300–5308, https://doi.org/10.1021/ja039615x.
[319] J.L. Anthony, J.L. Anderson, E.J. Maginn, J.F. Brennecke, Anion effects on gas solubility in ionic liquids, J. Phys. Chem. B 109 (13) (2005) 6366–6374, https://doi.org/10.1021/jp046404l.
[320] Z. Li, Y. Xiao, W. Xue, Q. Yang, C. Zhong, Ionic liquid/metal–organic framework composites for H_2S removal from natural gas: a computational exploration, J. Phys. Chem. C 119 (7) (2015) 3674–3683, https://doi.org/10.1021/acs.jpcc.5b00019.
[321] K.M. Gupta, Y. Chen, J. Jiang, Ionic liquid membranes supported by hydrophobic and hydrophilic metal–organic frameworks for CO_2 capture, J. Phys. Chem. C 117 (11) (2013) 5792–5799, https://doi.org/10.1021/jp312404k.
[322] W.S. Chi, B.J. Sundell, K. Zhang, D.J. Harrigan, S.C. Hayden, Z.P. Smith, Mixed-matrix membranes formed from multi-dimensional metal-organic frameworks for enhanced gas transport and plasticization resistance, ChemSusChem 12 (11) (2019) 2355–2360, https://doi.org/10.1002/cssc.201900623.
[323] H.M. Polat, S. Kavak, H. Kulak, A. Uzun, S. Keskin, CO_2 separation from flue gas mixture using [BMIM][BF_4]/MOF composites: linking high-throughput computational screening with experiments, Chem. Eng. J. (2020) 124916, https://doi.org/10.1016/j.cej.2020.124916.
[324] Y. Lan, T. Yan, M. Tong, C. Zhong, Large-scale computational assembly of ionic liquid/MOF composites: synergistic effect in the wire-tube conformation for efficient CO_2/CH_4 separation, J. Mater. Chem. A 7 (20) (2019) 12556–12564, https://doi.org/10.1039/C9TA01752F.
[325] G. Lv, Z. Li, W.-T. Jiang, S. Xu, T.E. Larson, Ionic liquid modification of zeolite and its removal of chromate from water, Green Chem. Lett. Rev. 7 (2) (2014) 191–198, https://doi.org/10.1080/17518253.2014.923518.
[326] S.G. Subraveti, S. Roussanaly, R. Anantharaman, L. Riboldi, A. Rajendran, How much can novel solid sorbents reduce the cost of post-combustion CO_2 capture? A techno-economic investigation on the cost limits of pressure–vacuum swing adsorption, Appl. Energy 306 (2022) 117955, https://doi.org/10.1016/j.apenergy.2021.117955.
[327] M. Nordio, S.A. Wassie, M. Van Sint Annaland, D.A. Pacheco Tanaka, J.L. Viviente Sole, F. Gallucci, Techno-economic evaluation on a hybrid technology for low hydrogen concentration separation and purification from natural gas grid, Int. J. Hydrogen Energy 46 (45) (2021) 23417–23435, https://doi.org/10.1016/j.ijhydene.2020.05.009.
[328] M.T. Ho, G.W. Allinson, D.E. Wiley, Reducing the cost of CO_2 capture from flue gases using pressure swing adsorption, Ind. Eng. Chem. Res. 47 (14) (2008) 4883–4890, https://doi.org/10.1021/ie070831e.
[329] A. Jalal, E. Can, S. Keskin, R. Yildirim, A. Uzun, Selection rules for estimating the solubility of C4-hydrocarbons in imidazolium ionic liquids determined by machine-learning tools, J. Mol. Liq. 284 (2019) 511–521, https://doi.org/10.1016/j.molliq.2019.03.182.
[330] E. Can, A. Jalal, I.G. Zirhlioglu, A. Uzun, R. Yildirim, Predicting water solubility in ionic liquids using machine learning towards design of hydro-philic/phobic ionic liquids, J. Mol. Liq. 332 (2021) 115848, https://doi.org/10.1016/j.molliq.2021.115848.